A MOUSE MODEL OF DVT STABILITY

A MOUSE MODEL OF DEEP VEIN THROMBOSIS STABILITY:

THE EFFECT OF DIRECT THROMBIN INHIBITION

By

LISA JEAN SALDANHA, B.H.Sc. (H)

A Thesis

Submitted to the School of Graduate Studies

In Partial Fulfillment of the Requirements

For the Degree

Masters of Science

McMaster University

MASTER OF SCIENCE (2012)   McMaster University

(Medical Sciences: Blood & Vasculature)   Hamilton, Ontario

TITLE: A Mouse Model of Deep Vein Thrombosis Stability: The Effect of Direct

               Thrombin Inhibition

AUTHOR: Lisa J. Saldanha, B.H.Sc. (H) (McMaster University)

SUPERVISOR: Peter L. Gross, M.D., M.Sc., FRCPC (C).

NUMBER OF PAGES: xiv, 126

ABSTRACT

The effect of direction thrombin inhibition on acute deep vein thrombosis (DVT) stability has not been defined and could contribute to pulmonary embolism (PE) risk. Direct thrombin inhibitors (DTIs) effectively inhibit free and clot-bound thrombin, which could potentiate thrombus instability through disruption of platelet, fibrin, and FXIIIa stabilizing mechanisms. This could manifest as increased thrombus embolization. A clinically relevant mouse model of DVT stability could further our understanding of venous thrombosis pathophysiology and define the effect of direct thrombin inhibition on PE. We hypothesized that acute DTI administration would decrease acute DVT stability and potentially increase PE risk. Platelets were labeled *in vivo*, femoral vein thrombosis was induced using $FeCl_3$, and lepirudin (8U/g) was administered *after* clot formation. Using intravital videomicroscopy (IVM), real time embolization was quantified as a measurement of thrombus stability. Thrombus stability increased in the control group and decreased in the lepirudin-treated group over two hours. The decrease in α_2-antiplasmin (α_2-AP) content within lepirudin-treated thrombi, compared to control thrombi, could possibly contribute to the observed decrease in thrombus stability. Continued growth and embolization established the dynamic nature of formed thrombi. In both groups, emboli were detected in the pulmonary artery circulation. Therefore, we successfully developed a mouse model of venous thrombus stability, which imitated the clinical progression of DVT to PE. DTI administration in the acute DVT setting could decrease thrombus stability, demonstrated through increased embolization and PE. This model could be useful in examining the effect of other antithrombotics and risk factors settings on DVT stability.

ACKNOWLEDGEMENTS

First and foremost, I would like to thank my supervisor, Dr. Peter Gross. I am indebted to you for your continuous support, wonderful mentorship and for welcoming me into your lab. You were never too busy and were always patient and understanding. In short, you have been an awesome PI.

Thank you to my supervisory committee, Dr. Jeff Weitz and Dr. Patricia Liaw, for challenging my abilities and pushing me to make this project better. Your advice and expertise has been invaluable.

Thank you to the rest of my lab: Ran, Nima, Shengjun and Paul. Ran and Nima – I will miss our random hangouts in the intravital room; bonding over failed mouse surgeries is for life.

To Les: thank you for the continual support and guidance in both my labs, old and new. Your mentorship has meant more than you can know, and I am truly happy to call you a friend.

To Ji: all those hours you spent sectioning and embedding tissues will never be forgotten. You are the sweetest. Thank you for your kindness and patience. I will make sure to pass it on.

To Linda and Deanna: you welcomed me into the center and took me on as a 'lab orphan'. Without both of you I probably still wouldn't know how to pipette. Thank you for answering my never-ending questions and never making me feel 'stupid'.

To Mo: you helped me overcome my fear of the mice; your 'lies' kept me on my toes; and simply put, you are the best.

To everyone else at TaARI: thank you for making my three years an enjoyable experience! I would especially like to thank Dr. Anthony Chan (you certainly know how

TABLE OF CONTENTS

FIGURES AND TABLES

2nd hour in control and lepirudin groups

LIST OF ABBREVIATIONS

a	activated
AF	Alexa Fluor
ANOVA	Analysis of Variance
APC	Activated Protein C
AT	Antithrombin
ATH	Antithrombin-Heparin Covalent Complex
AU	Arbitrary Units
AUC	Area Under the Curve
CaCl2	Calcium Chloride
CT	Computed Tomography
DTI	Direct Thrombin Inhibitor
DVT	Deep Vein Thrombosis
EC	Endothelial Cell
EE	Average number of embolic events per minute
EPCR	Endothelial Protein C Receptor
F	Factor
Fab	Fragment antigen binding
FeCl$_3$	Ferric Chloride
FITC	Fluorescein Isothiocyanate
Fluorescent Intensity of EE	Average Fluorescent Intensity of Embolic Events
Fp	Fibrinopeptide
FVL	FV Leiden
GP	Glycoprotein
H & E	Hematoxylin and Eosin
HAT	Heparin-Associated Thrombocytopenia
HCII	Heparin Cofactor II
HIT	Heparin-Induced Thrombocytopenia

HS	Heparan Sulfate
IHC	Immunohistochemstry
IV	Intravenous
IVC	Inferior Vena Cava
IVM	Intravital Microscopy
Large EE	Average number of large embolic events per minute
LMWH	Low Molecular Weight Heparin
mbw	mouse body weight
ms	millisecond
N/A	Not Applicable
nm	nanometer
OCT	Optimal Cutting Temperature
PAR	Protease Activated Receptor
PBS	Phosphate Buffered Saline
PCI	Percutaneous Coronary Intervention
PE	Pulmonary Embolism
PRP	Platelet Rich Plasma
PCI	Percutaneous Coronary Intervention
PS	Phosphatidylserine
PTS	Post-Thrombotic Syndrome
RBC	Red Blood Cell
r-hirudin	Recombinant Hirudin
SD	Standard Deviation
TAFI	Thrombin Activatable Fibrinolysis Inhibitor
TF	Tissue Factor
TFPI	Tissue Factor Pathway Inhibitor
TM	Thrombomodulin
tPA	Tissue Plasminogen Activator
UFH	Unfractionated Heparin
uL	microliter

uPA	Urokinase Plasminogen Activator
VK	Vitamin K
VTE	Venous Thromboembolism
vWF	von Willebrand Factor
α_2-AP	alpha2-antiplasmin
α_2-MG	alpha2-macroglobulin

1.0 INTRODUCTION

1.1. Overview of Hemostasis

Hemostasis is a complex physiological process that maintains the integrity of the vascular system (1). Following vessel wall damage, localized platelet thrombus formation and fibrin generation occur simultaneously to seal the injury site (1,2).

TF initiates coagulation *in vivo* resulting in thrombin generation (3). TF-bearing cells are exposed following vessel wall injury. TF is a high-affinity receptor for factor (F) VII and activated FVII (FVIIa), which circulate in the plasma (2). The TF-FVIIa complex, or extrinsic tenase, activates both FX and FIX. Thrombin activates FV (5) and FXa complexes with FVa, on the TF-bearing cell surface, to form the prothrombinase complex. Other cellular proteases can also activate FV (6). FXa is rapidly inhibited by TF pathway inhibitor (TFPI) and antithrombin (AT) and so remains localized to the TF-bearing cell surface (2). The prothrombinase complex generates trace amounts of thrombin, which amplifies the initial procoagulant signal.

Thrombin activates platelets by cleaving protease-activated receptors (PARs) (3), and is localized to the platelet surface through association with GPIb (7). Thrombin also activates coagulation cofactors V and VIII, as well as FXI (2). Activated platelets release partially activated FV. FVIII is bound to von Willebrand factor (vWF) in the plasma. It is cleaved by thrombin to FVIIIa and then dissociates from vWF (8).

Factor IXa diffuses from the TF-bearing cell and complexes with its cofactor, FVIIIa, on the activated platelet surface to form the intrinsic tenase complex. Factor IXa

can move through the fluid phase to the activated platelet surface, as it is not inhibited by TFPI and is slowly inhibited by AT (9). Activation of FXIa, by thrombin, also generates additional FIXa on the platelet surface and acts as a booster mechanism. The intrinsic tenase complex activates FX. FXa rapidly binds to FVa, and is subsequently protected from inhibition by TFPI and AT (9). The prothrombinase complex, on the activated platelet surface, generates a burst of thrombin that cleaves fibrinogen to form a fibrin clot (2) (Fig. 1).

1.2. Thrombin

Thrombin is a serine protease and consists of two polypeptide chains linked by a disulfide bond (10). Thrombin contains a centrally located active site, and two exosites: exosite 1 facilitates thrombin's interactions with various substrates, while exosite 2 acts as a cofactor-binding site (10).

As the central effector of the coagulation cascade, thrombin has procoagulant, anti-fibrinolytic and anticoagulant roles (11). In its procoagulant and anti-fibrinolytic role, thrombin cleaves fibrinogen to fibrin; activates FXIII to stabilize the thrombus; activates cofactors FV and FVIII; activates thrombin activated fibrinolysis inhibitor (TAFI); activates platelets; and is adsorbed onto the fibrin clot (12).

Fibrinogen consists of three pairs of polypeptide chains - Aα, Bβ, and γ - linked by three disulfide bonds. Thrombin cleaves fibrinopeptide A (FpA) from the Aα-chain and FpB from the Bβ-chain (12). Cleavage of FpA is rapid and results in spontaneous formation of protofibrils from fibrin monomers (12); cleavage of FpB is slower, and

allows for further polymerization and fibrin fibers to form (12). Exosite 1 facilitates the interaction of fibrinogen with thrombin (10). The concentration of thrombin influences thrombus formation, structure and stability (13). Low thrombin concentrations result in thick fibrin fibers and highly permeable clots, which are less dense and stable; high thrombin concentrations produce impermeable clots consisting of thin fibrin fibers.

FXIII is activated by thrombin in the presence of Ca^{2+} to FXIIIa, an activate transglutaminase. Fibrin enhances activation of FXIII by 80–100 fold (14). FXIIIa forms covalent bonds between γ-chains, α-chains and α- and γ-chains of fibrin (15). This stabilizes the formed fibrin clot, enhances its elasticity, and decreases binding of plasminogen to fibrin and subsequent activation to plasmin by tissue-type plasminogen activator (tPA) (14). FXIIIa rapidly cross-links $α_2$-AP to fibrin α-chains, thereby localizing the main physiological inhibitor of plasmin (15,16) and enhancing the antifibrinolytic properties of the clot (14). The effect of FXIIIa-mediated fibrin cross-linking on clot stability is debatable. While it has been shown that both $α_2$-AP cross-linking and α-chain polymerization are involved in fibrinolysis regulation, Fraser et al. have conversely concluded that the antifibrinolytic function of FXIIIa is expressed principally through $α_2$-AP cross-linking (17). In addition, cross-linking of fibrin by FXIIIa *in vitro* has been shown to down-regulate platelet accumulation on the fibrin surface (18). Therefore, FXIIIa could also have an antithrombotic role in thrombus formation.

To activate platelets, thrombin cleaves PAR-1 and PAR-4 in humans and PAR-4 and PAR-3 in mice (19). PARs are G-protein coupled receptors, and have an atypical

3

signaling mechanism. Cleavage at the N-terminal extracellular domain by thrombin exposes the receptor's ligand (20). This tethered ligand binds intramolecularly to the receptor and activates the coupled G proteins, which initiate intracellular signaling (21). PAR activation is irreversible. Activated receptors are internalized, while new ones are translocated to the plasma membrane (21). At low thrombin concentrations, platelets are activated through human PAR-1; at high protease concentrations PAR-4 is also cleaved (10).

In its anticoagulant role, thrombin binds to thrombomodulin (TM), through exosite 1 (22), and activates protein C (23). The thrombin-TM complex enhances the generation of activated protein C (APC) and TAFIa by approximately 1000 fold, compared to free thrombin (22,24).

1.3. Platelets

Vascular damage also exposes subendothelial components, which mediate platelet adhesion and activation. Initial platelet adhesion is mediated by vWF (25). vWF, anchored to collagen, interacts with platelet receptor GPIb-V-IX establishing initial contacts. This slows down the flow of platelets and initiates formation of the platelet plug. Platelet activation is initiated when platelet receptor GPVI binds to collagen (26). Activation of platelets is characterized by platelet shape change, aggregation, and release of contents from α- and dense granules (27). This further propagates platelet thrombus formation.

Activated platelets express phosphatidylserine (PS), a negatively charged phospholipid, through a "flip flop" reaction (27). PS moves from the inner platelet membrane to the outer membrane, providing a surface for coagulation complex assembly. Vitamin-K (VK) dependent proteins are synthesized in the liver and have an affinity for the negatively charged membrane. This is facilitated by the exposure of a membrane-binding site by interaction of Ca^{2+} with γ-carboxylated glutamic acid residues (Gla domain) on these proteins (28).

GPIIbIIIa is the most abundant platelet receptor, with approximately 60,000 to 80,000 copies on the platelet surface (29). It mediates platelet aggregation through vWF and fibrinogen (30). Unstimulated platelets do not bind fibrinogen; however, upon activation by platelet agonists, GPIIbIIIa moves from a resting to an active state. Activation of GPIIbIIIa through "inside-out" signaling, results in high affinity binding of fibrinogen and platelet aggregation (26,29).

1.4. Regulation of Hemostasis

The coagulation process is regulated by the antithrombotic properties of the endothelium, endogenous anticoagulant mechanisms, and the fibrinolytic system. The vascular endothelium, a confluent monolayer of cells, maintains vascular patency (1). Endothelial cells (ECs) prevent platelet adherence and induce vasodilation by synthesizing prostacyclin and nitric oxide (1). tPA is also released and converts plasminogen to plasmin, the key component of the fibrinolytic system. ECs further express heparan sulfate (HS), a glycosaminoglycan (GAG), TM, and endothelial cell

protein C receptor (EPCR). TM and EPCR are major components of the protein C pathway (31).

AT is a potent inhibitor of thrombin, FXa, and other coagulation proteases (11). AT is a serine protease inhibitor (serpin) and inhibits its target enzymes by forming a 1:1 stoichiometric covalent complex. This induces a conformational change in AT, and the specific protease is "trapped" and inactivated. HS catalyzes the inhibition of AT, which is relatively slow under physiological conditions (31). Thrombin is also specifically inhibited by the serpin, heparin cofactor II (HCII). Dermatan sulfate is a cofactor for the inactivation of thrombin by HCII (32).

The protein C pathway inhibits cofactors Va and VIIIa (33). The thrombin-TM complex on the EC surface rapidly forms APC (34). When protein C is bound to EPCR, APC generation is enhanced approximately 20-fold, due to close association between protein C and the thrombin-TM complex (23). APC dissociates from the complex and, with its cofactor Protein S, inactivates FVa and FVIIIa (34), thereby suppressing thrombin generation.

TFPI inhibits the TF-FVIIa complex through an FXa-dependent mechanism to prevent further production of FXa and FIXa (11). TFPI first binds to and inactivates FXa, forming a 1:1 stoichiometric complex, which then inhibits the TF-FVIIa complex (35).

The fibrinolytic system prevents excessive fibrin formation and degrades the fibrin clot. Plasminogen is a single chain GP with fibrin and α_2-AP binding sites. Plasminogen is activated by tPA and urokinase plasminogen activator (uPA) to plasmin. Plasmin

dissolves the fibrin clot by cleaving fibrin and generating fibrin degradation products. Additionally, plasmin cleaves plasminogen, producing truncated versions with a higher affinity for tPA and uPA. Plasminogen and tPA can form a ternary complex with fibrin that enhances plasminogen's rate of activation by approximately 1000 fold (36). Plasminogen activator inhibitor (PAI)-1 complexes with and inhibits tPA and uPA. The tPA-PAI-1 complex competes with free tPA for fibrin binding sites (37). 90% of PAI-1 is stored in platelet α-granules and is released upon platelet activation. Fibrinolysis is also regulated by TAFI, which prevents plasminogen binding to fibrin (38), and α_2-AP and α_2-macroglobulin (α_2-MG), which inhibit plasmin (39). α_2-MG additionally inhibits thrombin (40) and down regulates its generation by inhibiting protein S (41).

1.4.1. α_2-Antiplasmin

α_2-AP is the primary inhibitor of plasmin-mediated fibrinolysis (42). It belongs to the α_1-proteinase inhibitor class of serpins. α_2-AP rapidly inactivates plasmin by forming a 1:1 molar irreversible complex with plasmin. The serpin competitively inhibits fibrin binding, which prevents localization of plasmin (41). α_2-AP inhibits fibrin-bound plasmin at a rate 10-fold slower than free plasmin (43), as plasmin(ogen) binds to fibrin and α_2-AP at the same binding site (44). Additionally, α_2-AP is an efficient substrate of FXIIIa (45). FXIIIa cross-links α_2-AP to fibrin and fibrinogen, which further increases the resistance of the clot to lysis (43).

1.5. Venous Thromboembolism

Venous thromboembolism (VTE) presents as deep vein thrombosis (DVT) and pulmonary embolism (PE), and is the third leading cause of cardiovascular-related death after myocardial infarction and stroke (46). VTE affects approximately one to three in every 1000 persons (47). Venous thrombosis results when natural anticoagulant mechanisms are overwhelmed by thrombogenic stimuli, disrupting the hemostatic balance (48) and generating excessive thrombin. The disease pathology of VTE remains largely undefined, except through Virchow's triad, which was postulated over 150 years ago. Virchow's triad relates the development of venous thrombosis to three risk factors: vascular injury, venous stasis, and hypercoagulability (49).

The endothelium undergoes a phenotypic switch, following vascular damage, and becomes procoagulant (50). Thrombus formation might also be triggered by the exposure of subendothelial components: TF initiates the coagulation cascade, while either collagen or thrombin can predominate platelet activation depending on the pathological setting (51). Systemic factors of immobility and increased blood viscosity, and local factors of vessel dilatation and venous obstruction, lead to venous stasis (52). These factors result in localization and concentration of coagulation proteins, and generate a hypoxic, inflammatory environment that predisposes to thrombosis. An imbalance between procoagulant and anticoagulant mechanisms can produce a hypercoagulable state (53). Typically, natural anticoagulant pathways are compromised, resulting in excessive thrombin generation. Hypercoagulability can further stem from elevated coagulation factor levels and impaired fibrinolysis.

1.5.1. Risk Factors

Risk factors for VTE are either acquired or inherited. 80% of VTE patients present with at least one risk factor that affect at least one of the mechanisms of Virchow's triad (27). Multiple risk factors usually contribute to VTE development: approximately 50% of patients present with both an inherited and acquired risk factor (54) and over 56% patients, in a population-based study, had three or more acquired risk factors present at the time of VTE (55). Combinations of acquired and inherited risk factors influence VTE incidence in a synergistic manner (56).

Acquired risk factors of VTE include immobilization, surgery, cancer, and aging. 15% of patients who were confined to bed for more than one week had venous thrombosis at autopsy, a number that increased to 80% with more prolonged bed rest time (57). Surgery and trauma are associated with a strong risk for VTE development, although manifestation depends on the type of surgery performed. The incidence of VTE in general medical and surgical patients is 10–40%, and 40–60% in orthopedic surgery patients (58). VTE is a frequent complication of cancer and its treatment (59). Patients with cancer, who develop VTE, have a threefold higher risk of death than patients with VTE in the absence of cancer (60). It is uncommon for patients younger than 20 years to develop VTE. However, the incidence of VTE increases with age – the incidence doubles with each additional decade after the age of 40 years (58).

Inherited risk factors can result in a hypercoagulable state. The most prevalent are Factor V Leiden (FVL) and the prothrombin gene mutation, which occur in 50-60%

patients with inherited thrombophilia. FVL confers APC resistance by substitution of glutamine for arginine at amino acid 506, a key site of FVa cleavage for inhibition by APC (61). The prothrombin gene mutation causes a guanine to adenine transition at nucleotide 20210 (49), and is associated with a 2.8 fold increase in thrombosis (62). However, these gene mutations are not considered strong risk factors for VTE. Deficiencies in AT, protein C, and protein S are strong risk factors for VTE development; yet occur infrequently (57). Elevated levels of coagulation factors and chemokines are also associated with venous thrombosis.

1.5.2. Deep Vein Thrombosis and Pulmonary Embolism

VTE is a dynamic disease process, and manifests as two separate entities: DVT and PE (63). Currently, the primary blood test to assess for thrombosis is plasma D-dimer levels; the primary imaging test for DVT is venous ultrasonography; and the primary diagnostic test for PE is chest computed tomography (CT) with intravenous contrast. DVT is characterized by thrombus formation in the deep veins, typically in the lower extremities (58). DVT is classified as distal when the thrombus is located in the calf veins, and proximal when the thrombus forms in the popliteal vein or a more proximal vein (64). Venous thrombi mainly consist of interspersed red blood cells (RBCs), fibrin and platelets (50,65). Venous valves are areas prone to stasis and hypoxia, and are typical sites of DVT formation (66).

A frequent complication of DVT is post-thrombotic syndrome (PTS). PTS presents as chronic, persistent pain, and swelling in the affected limb (67). Approximately 20–

50% of patients with symptomatic DVT develop PTS, with severe PTS occurring in 5-10% (67).

PE is the major complication of DVT and develops when the thrombus, or part of the thrombus, embolizes and obstructs the pulmonary artery circulation (58). Over 90% of acute PE cases arise from proximal DVT (68). Additionally, silent PE occurs in approximately one third of proximal DVT patients (69). Symptomatic PE patients typically present with dyspnea, syncope, pleuritic pain, and hemoptysis. While the risk of PE varies greatly, it can be potentially fatal. The International Cooperative Pulmonary Embolism Registry found the three-month mortality rate of acute PE to be greater than 15% (70). Early death among symptomatic PE patients is 18-fold higher compared to patients presenting with only DVT. Therefore, while DVT and PE are classified under the same disease state, and are generally treated as one disease, survival following PE is much worse than after DVT alone (48). However, patients with fatal PE often have underlying chronic illnesses that can cause and contribute to mortality (71). Moreover, risk of PE is dependent upon the risk factor setting, which could influence DVT stability.

1.6. DVT Stability

The structure of fibrin associated with the clot directly affects clot stability through its fibrinolytic properties (72). Fibrin clot formation is diverse and dependent on hemostatic conditions. Clots with a tight network are less susceptible to lysis than clots with a loosely formed fibrin meshwork (73). Fibrin also regulates fibrinolysis through opposing mechanisms, as it both increases plasminogen activation and complexes with

α_2-AP (73). Plasmin bound to fibrin is relatively protected from inactivation, and facilitates fibrinolysis. However, α_2-AP cross-linked to fibrin inactivates free plasmin within the thrombus environment (43).

The main role of FXIIIa is to enhance the mechanical strength of the clot and increase its resistance to fibrinolysis (15). This is achieved by cross-linking the α- and γ-chains of fibrin, in addition to cross-linking α_2-AP to the α-chain of fibrin and fibrinogen (15). The effect of FXIIIa-mediated fibrin cross-linking on clot stability is debatable. While it has been shown that both α_2-AP cross-linking and α-chain polymerization are involved in fibrinolysis regulation, Fraser et al. have conversely concluded that the antifibrinolytic function of FXIIIa is expressed principally through α_2-AP cross-linking (17). In addition, cross-linking of fibrin by FXIIIa *in vitro* has been shown to down-regulate platelet accumulation on the fibrin surface (18). Therefore, FXIIIa could also have an antithrombotic role in thrombus formation.

Platelet aggregation is primarily mediated through GPIIbIIIa (74). Therefore, thrombus stability could also be reliant on signaling between aggregated platelets, resulting in clot retraction and subsequent protection from fibrinolysis.

1.7. Anticoagulant Treatment

Anticoagulants are administered as the standard of care for DVT. The objective of anticoagulant treatment is to prevent clot extension, recurrence of thrombosis, and progression of DVT to PE (75). Therefore, one of the main goals of anticoagulation is

thrombus stabilization. Thrombus propagation and PE are indicators of anticoagulation failure.

For many decades, the mainstay of anticoagulant therapy has been parenteral administration of unfractionated heparin (UFH) followed by an oral vitamin K antagonist, typically warfarin (76). This treatment course decreases the risk of DVT complications to approximately 5% (77). Throughout the years, the intent of streamlining VTE treatment has led to the development of low molecular weight heparins (LMWHs), direct thrombin inhibitors (DTIs) and FXa inhibitors (78) (Table 1). This objective could be realized with the recent approval of an oral FXa inhibitor for treatment of acute DVT.

1.7.1. Unfractionated heparin

UFH binds to AT and induces a conformational change that promotes the serpin's ability to inhibit thrombin, FXa, FIXa, and FXIIa (79). UFH is a heterogeneous mixture of carbohydrate chains with a mean molecular weight of 15,000 Daltons (79). Only one third of UFH molecules possess the high-affinity AT-binding pentasaccharide, which alone is sufficient to promote the inactivation of FXa by AT. However, to inactivate thrombin, the formation of a ternary complex between AT, UFH and thrombin is necessary, which requires at least 13 additional saccharide units. Formation of this complex enhances thrombin inhibition by greater than 1000 fold (10). However, clot-bound thrombin is protected from rapid inhibition by AT in the presence of heparin (80,81).

As UFH is administered parenterally, it is not suitable for long-term anticoagulant therapy. It has a variable anticoagulant response as it binds various plasma proteins other than AT (82). UFH is cleared through both saturable and nonsaturable mechanisms, and has a dose-dependent half-life (82). In addition, UFH has well-known bleeding complications and is associated with heparin-induced osteoporosis, as well as heparin-induced thrombocytopenia (HIT) (83).

Effectiveness of UFH in the treatment of VTE was established following Barritt and Jordan's landmark trial (84), where treatment with UFH was found to prevent mortality in a patient population of clinically diagnosed PE. Early anticoagulation with UFH has also been shown to reduce mortality in patients with acute PE (85).

1.7.2. Warfarin

Warfarin, a VK antagonist, inhibits the VK conversion cycle and prevents γ-carboxylation of VK-dependent coagulation factors (FII, FVII, FIX, and FX), thereby reducing their procoagulant activity (86). Warfarin simultaneously prevents γ-carboxylation of protein C and protein S (86), additionally acting as a procoagulant.

While warfarin is an effective oral anticoagulant, and is hence approved for long-term therapeutic use, it has many associated limitations: delayed onset of action, necessitating overlap with heparin; various food and drug interactions; bleeding complications; and a narrow therapeutic range (87). To improve the consistency and predictability of the anticoagulant response was the impetus for the development of new oral anticoagulants.

1.7.3. Direct Thrombin Inhibitors

Thrombin is an attractive anticoagulant target due to its central role in the coagulation cascade. Unlike UFH and warfarin, which target multiple coagulation factors, DTIs specifically inhibit thrombin (88). As AT is not required as a cofactor, DTIs can inactivate thrombin bound to fibrin or fibrin degradation products (88). Univalent DTIs bind only to thrombin's active site, whereas bivalent inhibitors target thrombin's exosite 1 as well. Dabigatran and argatroban are examples of univalent DTIs, whereas native hirudin and its recombinant forms are bivalent inhibitors. In comparison to heparins, DTIs are advantageous as they do not bind other plasma proteins, and they have an anti-platelet effect through thrombin inhibition (89).

Lepirudin

Hirudin, a natural occurring anticoagulant, is isolated from the salivary glands of the medicinal leech, *Hirudo medicinalis* (90). It has a characteristic structure of a single polypeptide chain consisting of 65 amino acids with a compact hydrophobic N-terminal core, containing three disulfide bridges, and a sulfated Tyr residue at its C-terminal (91).

Lepirudin, a recombinant hirudin (r-hirudin), is expressed in transfected yeast cells. It lacks a sulfate group on Tyr[63], which reduces its affinity for thrombin by approximately 10-fold compared to native hirudin (92). Lepirudin has a molecular weight of approximately 7 kDa (93). As a DTI, lepirudin binds specifically and irreversibly to free and clot-bound thrombin (80,93). It directly inhibits thrombin via a bivalent mechanism resulting in a non-covalent 1:1 stoichiometric complex (93). Lepirudin binds to exosite 1

of thrombin, preventing interaction with fibrinogen. It also binds to thrombin's apolar binding site, preventing access of other substrates to thrombin's active site (93).

Based on two prospective studies, Heparin-Associated Thrombocytopenia (HAT)-1 and HAT-2, lepirudin is indicated for treatment of patients with immune heparin-induced thrombocytopenia (HIT) (94). Its efficacy in treatment of HIT patients with thromboembolic complications was further confirmed by the HAT-3 trial.

In comparing subcutaneous r-hirudin with intravenous sodium heparin administration in patients with acute lower limb DVT, there were significantly fewer new ventilation/perfusion abnormalities in the r-hirudin treatment group (95). While lepirudin is not approved for this clinical indication, desirudin is administered as prophylaxis for VTE in patients undergoing hip replacement (96).

1.7.4. FXa Inhibition

FXa is also an attractive target for an anticoagulant, as it is situated at the convergence of the intrinsic and extrinsic pathways of coagulation. In addition, it is central to the amplification phase of coagulation as one FXa molecule can produce approximately 1000 thrombin molecules (97). Therefore, FXa inhibitors attenuate thrombin formation (98). Direct FXa inhibitors bind directly to FXa and may inhibit free and prothrombinase-bound FXa. Indirect inhibitors catalyze AT's anticoagulant ability, and only affect free FXa (98).

Fondaparinux

Fondparinux is a synthetic version of the UFH pentasaccharide that binds to AT with high-affinity (99). It induces a conformational change in AT that increases the inhibition rate of FXa. Following FXa inhibition, fondaparinux then dissociates from AT and can be reutilized (99). Fondaparinux has high bioavailability, a 17-hour half-life, and is excreted unchanged in the urine (100). The MATISSE studies have shown that treatment with fondaparinux is at least as effective and safe as LMWH for the initial treatment of symptomatic DVT and as UFH in the initial treatment of PE (101,102).

Rivaroxaban

Rivaroxaban is an oral, direct, competitive inhibitor of FXa (103). As a small molecule, it reversibly inhibits free FXa and has the ability to inhibit prothrombinase- and clot-bound FXa (104). Rivaroxaban limits thrombin generation by both the intrinsic and extrinsic coagulation pathways. Compared to other serine proteases, rivaroxaban selectively binds FXa by greater than 10,000 fold (105). Rivaroxaban has a rapid onset of action (2-4 hours), high bioavailability (80%), and a short half-life (approximately 9 hours). It has a dual mode of elimination, where two-thirds is metabolized in the liver and the remainder is excreted unchanged in urine (106). The EINSTEIN program demonstrated non-inferiority of rivaroxaban alone compared to LMWH followed by VKA in treating acute, symptomatic DVT and PE (107,108). Based on these studies, rivaroxaban is approved for treatment of DVT in the acute setting.

1.7.5. ATH

The antithrombin-heparin complex (ATH) was produced to address associated limitations of UFH therapy. It is generated by prolonged incubation of unmodified human AT with UFH, which results in a covalent complex and the inability of heparin to dissociate from AT (109). ATH inhibits free and fibrin-bound thrombin (110,111), as well as free and prothrombinase-associated FXa (112). In addition, it can catalyze AT's inhibition of free thrombin and FXa. ATH has been shown to have a longer half-life than UFH, and higher anti-FXa and anti-thrombin activity compared to non-covalent mixtures of AT and UFH *in vivo* (110). However, while rigorously tested in several *in vivo* models, ATH is not currently approved for use in any clinical setting.

1.7.6. Abciximab

Abciximab is a human-murine chimeric monoclonal antibody fragment designed to target the activated GPIIbIIIa receptor and attenuate platelet aggregation (113). However, abciximab binds non-selectively, as its structure corresponds to the binding domain of GPIIbIIIa, as well as other integrin receptors (113). In the plasma, abciximab is cleared within minutes through the reticuloendothelial system; however once platelet-bound, the drug can persist for up to one week (114). Abciximab was the first GPIIbIIIa inhibitor approved for clinical use. It is currently clinically indicated for treatment of high-risk patients undergoing percutaneous coronary intervention (PCI) and in patient settings requiring rapid platelet inhibition (114). It is intended for concomitant use with aspirin and heparin, as clinical studies have only investigated its use in those treatment settings (113).

1.8. Anticoagulants and DVT Thrombus Stability

Anticoagulants are administered to stabilize the deep vein thrombus with the goal of preventing PE-associated mortality. However, limited research has been conducted into the role of thrombus stability in the progression of DVT to PE. In a comparison of acute DVT to chronic DVT using ultrasonic tissue characterization, it was concluded that greater thrombus instability was associated with acute DVT, possibly related to thrombi composition (115). Additionally, assessment of acute DVT, using serial venous duplex scans, found higher than expected levels of thrombus extension following anticoagulant treatment (116). This could suggest that acute DVT might be associated with early thrombus instability, which acute administration of anticoagulants could initially perpetuate.

1.9. Mouse Models of DVT and PE

A better understanding of VTE disease mechanisms and relevant treatments has been achieved through the development of various animal models. Murine models are often used to study thrombosis, as mice are easy to breed, cost effective, and genetic manipulations are technically feasible (117). While only small amounts of experimental agents are needed to test their effect *in vivo*, the mouse's tiny vascular system can be challenging to manipulate (117). Additionally, the clinical nature of human thrombotic disorders is difficult to replicate in mice, as mice do not spontaneously develop DVT. An ideal mouse model of thrombosis should simulate clinically relevant thrombus formation

in an anatomically comparable vessel; produce consistent quantitative data; and characterize thrombosis dynamics (118).

As mice do not develop spontaneous DVT, various mechanisms are used to induce thrombus formation, usually through manipulating an aspect of Virchow's triad. Common murine models of large vein thrombosis are the inferior vena cava (IVC) ligation model, IVC stenosis model, electrolytic model, and ferric chloride ($FeCl_3$) injury model.

In the IVC ligation model, side branches of the IVC are ligated and posterior branches are cauterized (119). Ligation produces a hemostatic environment of complete stasis, resulting in vessel wall damage and increased TF expression. While reproducible thrombi are produced, they are completely occlusive (120). The lack of blood flow in this model would prevent systemically injected agents from reaching the occluded segment (120) and thrombus embolization cannot occur.

The stenosis model involves external compression of the IVC to reduce blood flow, which induces thrombus formation (121). This model is currently used to study acute and chronic DVT; however, there is large variation in thrombus size (120).

The electrolytic vein model uses an electric current to generate venous thrombosis. A needle attached to a silver-coated copper wire is inserted into the subcutaneous tissue and IVC and a current is applied (122). This results in EC damage and activation, and produces thrombi of a consistent size that are non-occlusive in nature (122). Studying the effect of experimental agents is possible using this model.

However, initial insertion of the needle can damage the vein wall and the operation time is much longer compared to other models (120).

The $FeCl_3$-injury model was first used to simulate thrombus formation in the IVC of rabbits (123), and then adapted by Kurz et al. to induce arterial thrombosis in rats (124). This model has since been applied to induce DVT in large murine veins. While thrombi reliably form minutes after injury, the speed of formation and resultant thrombus size is dependent on the concentration and exposure time of $FeCl_3$. A disadvantage of this model is that $FeCl_3$ induces transmural damage to the vessel wall, a scenario that is rarely seen in humans with DVT (120). Topical application of $FeCl_3$ causes generation of free radicals and lipid peroxidation (125), resulting in EC denudation and thrombus formation (126). There is a time-dependent increase in EC damage following $FeCl_3$ application (125). However, the mechanism and extent of EC denudation remains unclear (127). Endothelial-derived spheres containing $FeCl_3$ have been detected in the lumen and observed to interact with platelets and fibrin fibers. This could be a possible mechanism of thrombus initiation (125). $FeCl_3$ has also been shown to penetrate the internal elastic lamina though an endocytic/exocytic mechanism (128). Additionally, an *ex vivo* model demonstrated RBC lysis and hemoglobin oxidation following $FeCl_3$-injury that could potentially perpetuate EC denudation (129). While typically thought to induce platelet-rich thrombi, it has been shown that application of $FeCl_3$ to the femoral vein also results in fibrin-rich thrombus formation (130), which is characteristic of clinical venous thrombosis.

2.0 EXPERIMENTAL OBJECTIVES AND HYPOTHESIS

2.1. Rationale

The effect of antithrombotic treatment on venous thrombus stability remains largely undefined. As the standard of care of DVT, anticoagulants are administered to limit thrombus extension (99), prevent reoccurrence of thrombosis (131), and decrease mortality associated with PE (132). If untreated, PE is estimated to occur in approximately 50% of patients with symptomatic proximal DVT, often within a few days or week (133,134). Therefore, anticoagulant treatment should stabilize the preexisting thrombus by reducing embolization, and potential PE.

While acute DVT has been examined a few days after anticoagulant treatment (116,135,136), thrombus embolization has not been studied in the same setting. Examination of deep vein thrombus stability, during the acute phase of therapy, reported higher than expected levels of asymptomatic thrombus extension (116). This suggests that anticoagulant treatment, in the acute setting, might initially impair thrombus stabilization. However, early anticoagulation of patients with acute, symptomatic PE has been shown to be associated with reduced mortality (85).

Thrombin, as the central effector of coagulation, is a logical anticoagulant target (137). As DTIs have been shown to effectively inhibit clot-bound thrombin (80), the resulting decrease in clot-bound thrombin concentration and activity could potentiate thrombus instability, which could manifest as increased embolization. While studies have explored the administration of anticoagulants following arterial thrombus formation

(138) and IVC ligation induced thrombus formation (139), the effect of direct thrombin inhibition on an existing deep vein thrombus has not been examined. This could provide crucial insight into the DVT to PE relationship.

The goal of this project is to evaluate the impact of an acutely administered DTI, specifically lepirudin, on a mouse model of DVT stability in the acute setting. The impact of other antithrombotic treatments on thrombus stability can then be explored.

2.2. Hypothesis

We hypothesize that acute administration of a DTI will decrease the stability of the thrombus in the acute DVT setting. We further hypothesize that a decrease in thrombus stability will result in increased embolization, and potential PE.

2.3. Primary Objectives

2.1.1. Develop and characterize a novel mouse model that can assess DVT stability.

2.1.2. Investigate the effect of direct thrombin inhibition on thrombus stability in this model.

2.4. Secondary Objective

2.3.1. Investigate the effect of other antithrombotic treatments on thrombus stability in our DVT model.

3.0 MATERIALS AND METHODS

3.1 Animal Handling

McMaster University Research Ethics Board approved all animal procedures (AUP #10-05-37). Female C57BL/6 mice (Charles River, Sherbrooke, Quebec, Canada), approximately 20g, were used because of availability and to possibly assess the effect of estrogen later. Mice were anaesthetized with an intraperitoneal injection of ketamine (0.125mg/g mouse body weight (mbw)), xylazine (0.0125mg/g mbw), and atropine sulfate (0.0025mg/g mbw) mixture.

3.2 Fluorescent Labels

3.2.1. Labeling Platelets

Using Pierce Fab Preparation Kit #44985 (Thermo Scientific, Waltham, MA, USA), Fab fragments were prepared from rat anti-mouse integrin αIIbβ3 clone: MWReg30 (CD41) (Emfret Analytics GmbH & Co. KG, Eibelstadt, Germamy), a monoclonal antibody directed against platelet-specific receptor GPIIbIIIa. Generated CD41 Fab fragments were then fluorescently labeled using either Molecular Probes Alexa Fluor (AF) 488 Labeling Kit (Invitrogen, Grand Island, USA) or Molecular Probes AF 647 Labeling Kit (Invitrogen, Grand Island, USA).

To label platelets *in vivo*, prepared CD41 Fab fragments conjugated to AF 488 were injected at a concentration of 1μg/g mbw, and CD41 Fab fragments conjugated to Alex Fluor 647 were injected at a concentration of 0.5μg/g mbw (140).

3.2.2. Labeling Fibrin

Synthesized anti-fibrin peptide (CGLIIQKNEC) (141) was conjugated to fluorescein isothiocyanate (FITC) (LifeTein, NJ, USA) and reconstituted with 0.05M carbonate buffer to a 2mg/mL stock solution. To label fibrin *in vivo*, 50µg of prepared FITC-labeled anti-fibrin peptide, diluted in saline, was administered.

3.3 Testing Fibrin Antibody Specificity

3.3.1. Carotid Artery Blood Collection

The mouse was anaesthetized as described, and its fore limbs were taped on a heating pad, maintained at 40°C. A patch of skin, approximately 1cm in diameter, was removed from the neck. The carotid artery was exposed through blunt dissection and blood flow occluded by placement of an artery clip proximal to the body. The carotid artery was then cannulated using PE 10 polyethylene tubing. The cannulus was stabilized using a 5-0 silk surgical suture and the artery clip removed so blood flow could resume. The cannulus was used to draw approximately 0.6mL of whole blood from the mouse carotid artery into 10% sodium citrate (BD, Franklin Lakes, NJ, USA), 1:10 dilution. Platelet rich plasma (PRP) was obtained by spinning the collected blood at 150 x g for 6 minutes (x 2). The platelet rich supernatants were collected and combined.

3.3.2. PRP Clots To Test Fibrin Peptide Specificity

Blood was drawn through the carotid artery blood collection method outlined (N = 1). Two Eppendorf tubes of 100µL PRP were incubated with 40µg FITC-labeled anti-fibrin peptide. Background fluorescence of the FITC-labeled anti-fibrin peptide was assessed using the Typhoon™ 9400 laser scanner (GE Healthcare, Cooksville, ON,

Canada). The following parameters were used: 50μm resolution, with normal sensitivity, and a 488nm laser. A 16-bit per channel image was generated. Clotting was then initiated in one tube with 1M $CaCl_2$ (final concentration, 20mM $CaCl_2$). The resultant clot was washed extensively with PBS and imaged, and then washed extensively a second time and imaged again. Fluorescence of control and clot tubes was then assessed. Fluorescence of the FITC-labeled anti-fibrin peptide should be confined within the PRP clot if specific (Fig. 2).

3.4. Mouse Model Surgical Preparation

3.4.1. Femoral Vein Isolation

The mouse was anaesthetized as described, and its hind limbs were taped on a heating pad, maintained at 40°C. A patch of skin, approximately 1 cm in diameter, was removed from the right pelvic region. The femoral vein was exposed by blunt dissection and isolated using a 5-0 silk surgical suture (Surgical Specialties Corporation, Reading, PA, USA).

3.4.2. Tracheotomy

Following isolation of the femoral vein, the mouse was rotated 180°, and its front limbs taped on the heating pad. A patch of skin, approximately 1 cm in diameter, was removed from the neck. The trachea was exposed by blunt dissection and cannulated with PE 100 polyethylene tubing (VWR, Mississauga, ON, Canada). The catheter was stabilized with a 5-0 silk surgical suture and assisted the mouse's breathing for the duration of the experiment.

3.4.3. Jugular Vein Cannulation

The jugular vein was exposed through blunt dissection and cannulated using PE 10 polyethylene tubing (VWR, Mississauga, ON, Canada). It was similarly stabilized using a 5-0 silk suture. The cannulus was used to inject sodium pentobarbital (0.05mg/g mbw, Ceva Sante Animale, Rutherford, NJ, USA) - to maintain sedation - and experimental reagents.

3.5. Mouse Model of DVT Stability

3.5.1. $FeCl_3$-Induced Femoral Vein Thrombosis

To induce thrombus formation, a 1 x 2 mm strip of Whatman filter paper (VWR, Mississauga, ON, Canada), soaked in freshly diluted 4% $FeCl_3$ solution from a stock solution of 45% $FeCl_3$ (Sigma-Alridch, St. Louis, MO, USA), was applied to the medial side of the right femoral vein for 5 minutes. Following filter paper removal, the vein was washed twice with sterile saline.

3.5.2. Femoral Vein Thrombus Histology

Tissue Excision and Dehydration

Paraffin sections:

Femoral vein thrombosis was induced as described previously. After 10 minutes, one hour and two hours (N = 3 per group), the femoral vein was ligated, using a 5-0 silk surgical suture on either side of the formed thrombus, excised and fixed in 10% formalin (Sigma-Aldrich, St. Louis, MO, USA), in a 24 well plate, for > 48 hours.

To prevent loss of the femoral vein thrombus, tissue samples were dehydrated manually following fixation in 10% formalin: 30 minutes in 70% ethanol (x 3), 30 minutes in 85% ethanol (x 3), 30 minutes in 100% ethanol (x 3), 45 minutes in xylene (x 3), and stored overnight in paraffin. Samples were embedded in paraffin blocks the following day.

Frozen sections:

Femoral vein thrombosis was induced by $FeCl_3$-injury as described. After one hour and two hours (N = 3 per group), the femoral vein was ligated on either side of the formed thrombus, excised, embedded in cyro-embedding media (OCT), snap-frozen in liquid nitrogen, and stored at -80°C.

Sectioning

For paraffin sections:

Paraffin blocks were sectioned to 5µm thickness using a Leica RM 2125RT Microtome (Leica Microsystems Inc., Concord, ON, Canada). Hematoxylin and Eosin (H&E) stain kit (Sigma-Aldrich, St. Louis, MO, USA) and Carstairs' stain kit (Electron Microscopy Sciences, Hatfield, PA, USA).

For frozen sections:

Frozen tissue blocks were sectioned using a Leica CM 1900 cryostat. Frozen sections, 10µm thick, were obtained for immunohistochemistry (IHC). Slides were stored at -80°C.

Staining

For paraffin sections:

H & E Staining

Paraffin sections were hydrated to water. Sections were stained with Mayer's hematoxylin for 5 minutes, rinsed in tap water, and stained with eosin for 2 minutes, and rinsed in tap water. Slides were then dehydrated, cleared and mounted for visualization using an Olympus series upright microscope with a 10X 0.3 NA dry objective.

Carstairs' Staining

A modified version of the Carstairs' stain method(142) to detect fibrin (red), platelets (navy blue) and RBCs (yellow-brown) was used. Paraffin sections were hydrated to water. Sections were stained with 5% ferric alum for 5 minutes, washed in tap water; Mayer's hematoxylin for 5 minutes and washed in tap water; picric acid-orange G solution (20mL saturated aqueous picric acid, 80mL saturated picric acid in isopropanol, 0.2g orange G) for 1 hour and rinsed in distilled water; ponceau-fuchsin solution (0.5g acid fuchsin, 0.5g ponceau 2R, 1mL acetic acid, distilled water, final volume 100mL) for 5 minutes and rinsed in distilled water; 1% phosphotungstic acid for 5 minutes and rinsed once in distilled water; and aniline blue solution (1g aniline blue in 100mL 1% acetic acid) for 10 minutes, followed by several changes of distilled water. Slides were dehydrated, cleared, and coverslipped. The exact colour of fibrin and platelets is dependent on fixation time (143). Slides were visualized using an Olympus series upright microscope with a 10X 0.3 NA dry objective.

For frozen sections:

H&E Staining

Frozen tissue slides were thawed at RT and fixed in ice-cold methanol (pre-cooled at -20°C for 30 minutes) for 10 minutes. Slides were rehydrated in PBS (pH 7.4) for 3 minutes (x 4) and rinsed in tap water. Sections were stained with Mayer's hematoxylin for 5 minutes, rinsed in tap water, stained with eosin for 2 minutes and rinsed in tap water. Slides were then washed in PBS for 3 minutes (x 4), and mounted. Slides were visualized using an Olympus series upright microscope with a 10X 0.3 NA dry objective.

IHC for α_2-AP

Frozen tissue slides were thawed at RT and fixed in ice-cold methanol (pre-cooled at -20°C for 30 minutes) for 10 minutes. Slides were rehydrated in PBS (pH 7.4) for 3 minutes (x 4). Using a Dako Pen (Dako, Burlington, Ontario), a hydrophobic barrier was drawn around the sections. Slides were incubated in blocking buffer of 10% goat serum (Jackson ImmunoResearch, West Grove, PA, USA) for 30 minutes at RT to block non-specific staining between the primary antibody and the vein tissue. Sections on the slide were covered with goat anti-mouse serpin F2/α_2-AP antigen affinity-purified polyclonal antibody (5μg/mL, R&D Systems, Minneapolis, MN, USA) diluted in PBS, or with PBS as control, and incubated at 4°C overnight in a humidified chamber. Slides were rinsed in PBS for 3 minutes (x 4). Sections on the slide were covered with AF 488 donkey anti-goat IgG antibody (5μg/mL, Life Technologies Inc., Burlington, ON) or AF 647 donkey anti-goat IgG antibody (5μg/mL, Life Technologies Inc., Burlington, ON),

diluted in PBS, and incubated for 30 minutes at RT. The slides were then rinsed in PBS for 3 minutes (x 4). Diluted DAPI solution was added to each slide and incubated for 2 minutes at RT. Slides were rinsed in PBS for 3 minutes (x 4), and mounted. The slides were visualized using an Olympus series fluorescence microscope with a 10X 0.3 NA dry objective. Analysis of fibrin content in the femoral vein, and α_2-AP content within the thrombus was performed using ImageJ Software (Bethesda, Maryland, USA).

3.5.3. Infusion of Detecting Antibodies

Following surgical preparation of the mouse, fluorescently labeled antibodies were infused before $FeCl_3$ injury to visualize the induced thrombus using intravital videomicroscopy (IVM).

3.5.4. Intravital videomicroscopy

The femoral vein thrombus was visualized using IVM on an Olympus BX series microscope. A xenon lamp provided fluorescent illumination, and a DG-4 (Sutter Instrument Company, Novato, CA, USA) with specific excitation filters was used to control the fluorescent excitation beam. Platelets labeled with CD41 Fab fragments conjugated to AF 488 and fibrin labeled with anti-fibrin peptide conjugated to FITC were excited at a 488nm wavelength; and platelets labeled with CD41 Fab fragments conjugated to AF 647 were excited at a 633nm wavelength. Digital images were captured with a 640 X 480 format CCD camera (Hamamatsu Digital Camera C9300-201, NJ, USA). Embolization data was obtained with a 20X 0.5 numerical aperture (NA) water immersion objective, with the camera set to 4 x 4 binning and 10ms exposure

time. Thrombus size data was obtained with a 10X 0.3 NA water immersion objective; the camera was set to 1 x 1 binning and 100ms exposure time. The intensifier gain of the VSI Image Intensifier (Video Scope International, Ltd., Dulles, VA, USA) was set at 43,900-foot lamberts per foot-candle for both objectives. The camera and illumination were controlled, and the images analyzed, using Slidebook 5 (Intelligent Imaging Innovations, Denver, CO, USA).

3.5.5. Quantification of Embolization

Thrombus embolization was established at one hour (N = 12) and at two hours (N = 5) by quantifying the average number of embolic events per minute (EE), the fluorescent intensity of EE, and the average number of large embolic events per minute (large EE, defined below). Embolization was observed in a limited region of interest defined downstream of the thrombus (area measured in pixels) (Fig. 3). The region was captured for a time lapse of 5000 frames, which was equivalent to approximately one minute.

Number of embolic events

An embolic event was defined as visible fluorescence of platelets breaking off from the thrombus, moving downstream, and passing through the region of interest. Visible emboli were manually counted.

Five minutes after thrombus formation, and before treatment was administered, a baseline value of EE was established. Control mice were administered saline to later compare the effect of various antithrombotic treatments. Saline, as control treatment,

was administered 12 minutes after FeCl$_3$-induced thrombus formation. Time of treatment

administration was set to time 0, and embolization was assessed at various time points

afterwards. For the one-hour model, EE were quantified at 3, 18, 33, and 48 minutes

following treatment administration. For the two-hour model, EE were quantified at 3, 18,

33, 48, 63, 78, 93, and 108 minutes following treatment administration.

Fluorescent intensity of embolic events

As a measurement of EE size, the visible fluorescence of embolic events was

quantified in arbitrary units (AU). To standardize this measurement, the quantified

fluorescence was multiplied by area in pixels of the defined region of interest. As

outlined for EE, a baseline value of fluorescent intensity of EE was established at 5

minutes after thrombus formation. For the one-hour model, fluorescent intensity of EE

was quantified at 3, 18, 33, and 48 minutes following treatment. For the two-hour model,

fluorescent intensity of EE was quantified at 3, 18, 33, 48, 63, 78, 93, and 108 minutes

following treatment.

Number of large embolic events

Large embolic events were identified among counted embolic events. An embolic

event was defined as large if its fluorescent intensity was greater than 4 standard

deviations (SD) above the average fluorescent intensity of EE for that time point. For the

one-hour model, large EE were quantified at baseline, and then at 3, 18, 33, and 48

minutes after treatment administration. For the two-hour model, large EE were quantified

at baseline, and then at 3, 18, 33, 48, 63, 78, 93, and 108 minutes following treatment administration.

Outliers

Outliers were identified, by baseline EE, to normalize saline-treated controls and subsequent treatment groups. An outlier was defined as having a baseline EE outside the range of control baseline EE ± 1 SD. Following outlier identification, N = 11 for the one-hour model and N = 5 for the two-hour model in the control group.

3.5.6. Quantification of Thrombus Size

Thrombus size was quantified by the sum of fluorescently labeled platelets within the thrombus in saline-treated mice (Fig. 4). The thrombus was visualized for 500 frames, which was equivalent to approximately one minute. A baseline value of thrombus size was quantified, before treatment administration, at 10 minutes after thrombus formation. Treatment was administered 12 minutes after $FeCl_3$-induced thrombus formation. The time of treatment administration was set to time 0. For the one-hour model (N = 11), thrombus size was quantified at 8, 28, and 38 minutes following treatment administration. For the two-hour model (N = 5), thrombus size was quantified at 8, 28, 38, 58, 68, 88, 98, and 113 minutes following treatment administration (Table 2).

3.5.7. Percentage of Embolizing Thrombus

The percentage of the embolizing thrombus was calculated by subtracting fluorescent intensity of EE from thrombus size in the one-hour and two-hour models. To

normalize IVM parameter differences used to quantify thrombus size and fluorescent intensity of EE in the control group, fluorescent intensity of EE values were divided by 1.6. Normalization was necessary as fluorescent intensity of EE was quantified using 10ms exposure and 4 x 4 binning, whereas thrombus size was measured using 100ms exposure and 1 x 1 binning.

For the one-hour model, these values were multiplied by 60 to determine fluorescent intensity of EE over one hour and averaged. Dividing average fluorescent intensity of EE over one hour by average thrombus size and multiplying by 100 calculated percentage of thrombus embolization.

1) IVM-adjusted fluorescent intensity of EE =

$$\frac{\text{Fluorescent intensity of EE}}{1.6}$$

2) Average (avg) fluorescent intensity of EE over one hour =

IVM adjusted fluorescent intensity of EE x 60

3) Percentage of thrombus embolization =

$$\left[\frac{\text{Avg fluorescent intensity of EE over one hour}}{\text{Avg thrombus size}} \right] \text{x } 100$$

For the two-hour model, the values were multiplied by 120 to determine the fluorescent intensity of EE over two hours, and then averaged. Dividing average

fluorescent intensity of EE over two hours by average thrombus size and multiplying by 100, calculated the percentage of the embolizing thrombus.

3.5.8. Fibrin Content in Large Emboli

To assess fibrin content in large emboli over two hours, fibrin and platelets were both fluorescently labeled. The defined region of interest was captured for 1000 frames, equivalent to approximately one minute, and the camera set to 4 x 4 binning. 633nm and 488nm wavelengths were alternated for fluorescence excitation, with an exposure time of 10ms. As previously outlined, an embolic event was defined as large if its fluorescent intensity was greater than 4SD above the average fluorescent intensity of EE for that time point. Large embolic events containing fibrin were manually counted at 3, 18, 33, 48, 63, 78, 93, and 108 minutes following treatment.

3.5.9. Lung Histology

Femoral vein thrombosis was induced as described previously. After two hours (N = 3), the mouse was euthanized and the left and right lungs were excised separately and fixed in 10% formalin, in 24 well plates, for >48 hours. Lung tissue was dehydrated using a Tissue Tek VIP Vacuum Infiltration Processor (Sakura Finetek USA Inc., CA, USA) and embedded in paraffin.

As previously described, paraffin blocks were sectioned to 5µm thickness, rehydrated and stained using H & E and Carstairs' stain. Slides were then dehydrated, coverslipped, and visualized using an Olympus series upright microscope with a 10X 0.3 NA dry objective.

3.6. Effect of Lepirudin on Thrombin Generation Over Time

3.6.1. Thrombin Generation Assay (TGA) of Lepirudin

Lepirudin, 8U/g mbw, was administered to the mouse via a jugular vein catheter, and blood collected immediately, 1 hour, and 2 hours after injection (N = 3 per group). 40µL of citrated PRP was added to a clear round-bottom plate, and clotting initiated with 50µL HBS, 141nM fluorogenic thrombin substrate, SN-20 (Haematologic Technologies, Inc., Vermont, USA), and 20mM $CaCl_2$ was added for a final volume of 90µL. The 470nm wavelength emission was read at one minute intervals for one hour at 37°C.

3.7. Effect of Lepirudin on DVT Stability

Lepirudin was administered, at 8U/g mbw (144), via the jugular vein cannulus in 50uL of sterile saline, 12 minutes after $FeCl_3$-induced injury.

3.7.1. Effect on Femoral Vein Thrombus Histology

Following administration of lepirudin the femoral vein was excised for paraffin sections after one hour and after two hours (N = 3 per group), and for frozen sections after one hour and after two hours (N = 3 per group). As previously described, femoral vein sections were stained and visualized.

3.7.2. Effect on Embolization

In the lepirudin-treated group, the EE, fluorescent intensity of EE, and large EE were quantified as outlined previously in the control group. Following outlier identification, N = 11 for the one-hour model, and N = 5 for the two-hour model.

3.7.3. Effect of Delayed Treatment on Embolization

Lepirudin was administered 72 minutes after thrombus formation (N = 5). EE, fluorescent intensity of EE, and large EE were then quantified (as outlined previously) at 3, 18, 33 and 48 minutes following treatment administration.

3.7.4. Effect on Thrombus Size

Thrombus size was quantified as previously outlined in lepirudin-treated mice over one hour (N = 11) and two hours (N = 5).

3.7.5. Effect on Percentage of Embolizing Thrombus

As previously outlined, the percentage of embolizing thrombus was calculated in lepirudin-treated mice over one and two hours.

3.7.6. Effect of Lepirudin on Fibrin Content in Large Emboli

After lepirudin administration, fibrin content in large emboli was assessed over two hours as previously described.

3.7.7. Effect on Lung Histology

Two hours after lepirudin administration the lungs were excised for paraffin sections (N = 3). As previously described, the lungs were dehydrated, sectioned and stained.

3.8. Effect of Rivaroxaban on Thrombin Generation Over Time

3.8.1. TGA of Rivaroxaban

Rivaroxaban, $3\mu g/g$ mbw, was administered to the mouse via a jugular vein catheter, and blood collected immediately and 1 hour after injection. TGA, as outlined above, was performed on citrated PRP.

3.9. Effects of Other Antithrombotics on Embolization

Antithrombotics were administered via the jugular vein cannulus in 50uL of sterile saline. Rivaroxaban (Suzhou Howsine Biological Technology Co., Ltd., Suzhou, China) was given as a dose of 3μg/g mbw (145). Fondaparinux (GlaxoSmithKline, Mississauga, ON, Canada) was given at 0.1μg/g mbw. Heparin (LEO Pharma A/S, Ballerup, Denmark) was administered at a dose of 0.1U/g mbw (146). ATH, a kind gift from Dr. Anthony Chan, was given at a dose of 0.08U/g mbw, which was equivalent to anti-FXa activity of UFH dose. Anti-GPIIbIIIa (clone Leo.H4, Emfret Analytics GmbH & Co. KG, Eibelstadt, Germany) was administered at a dose of 1.46μg/g mbw (147).

These compounds were administered 12 minutes following $FeCl_3$-induced injury. The time of treatment administration was set to time 0, and EE and large EE assessed at baseline, and then at 3, 18, 33, and 48 minutes following treatment administration (N = 12 per group).

Following outlier identification, N = 9 for the rivaroxaban, fondaparinux and anti-GPIIbIIIa groups, and N = 11 for the UFH and ATH groups.

3.10. Statistical Analysis

Statistical analysis was performed using GraphPad Prism 5.0 (GraphPad Software Inc.; La Jolla, CA), except for the power calculation for fibrin in large EE, which was performed using G*Power 3.1.3 (Institut Für Experimentelle Psychologie, Düsseldorf, Germany). Only EE and large EE over time in control and lepirudin-treated groups were analyzed using a Kruskal-Wallis test; only fluorescent over time in control

and lepirudin-treated groups were analyzed using one-way ANOVA. Only changes in embolization and percentage of embolizing thrombus, over two hours, were assessed by repeated measures ANOVA. Only fibrin in large emboli in control and lepirudin-treated groups were analyzed using Fischer's exact test. All remaining data was analyzed using Student's *t* tests (parametric) and Mann-Whitney tests (non-parametric). Identified outliers were excluded from data analysis. A *P* value less than 0.05 ($p < 0.05$) was considered significant. Values are expressed as mean ± standard error of the mean (SEM).

4.0 RESULTS

4.1 Establishment Of A Novel Mouse Model Of DVT Stability

4.1.1. FeCl$_3$-Induced Thrombi Composition

Following a pilot study, application of 4% FeCl$_3$ for 5 minutes on the medial side of the femoral vein was determined to be optimal to induce consistent, non-occlusive thrombus formation in our model (data not shown).

To determine general tissue morphology, H & E stain was used (data not shown). To characterize the composition of FeCl$_3$-induced thrombi, and to determine the contribution of fibrin and platelets, Carstairs' stain was used. At 10 minutes, dense fibrin formation was observed with few interspersed platelets (Fig. 5A and 5B); following one hour and up to two hours, it appeared that there was a substantial increase in platelets within the thrombus (Fig. 5C and 5D; Fig. 5E and 5F). There was no significant difference between fibrin content in the femoral vein at one and two hours (one hour = 18.3 ± 6.3%; two hours = 21.7 ± 4.3%; p = 0.69; N = 3 per group). Quantification of α_2-AP *in vivo* and *in* vitro has been well established as a measurement of FXIIIa activity (17,148,149). Therefore, to measure FXIIIa activity, IHC staining was used to determine α_2-AP content in the femoral vein thrombus at one hour (Fig. 6A). 56.3 ± 3.6% of the thrombus contained α_2-AP at one hour. These results indicate that FeCl$_3$-injury results in a thrombus that is characteristic of DVT and contains α_2-AP.

4.1.2. Embolization Decreases Over One Hour

To assess thrombus stability, embolization was visualized and quantified over the time period of one hour. Thrombus embolization was observed as early as it was sought i.e. 5 minutes after injury. Over the next hour, EE gradually decreased (p = 0.55, Fig. 7A), while fluorescent intensity of EE peaked shortly after thrombus formation, and then decreased (p = 0.46, Fig. 7B). Large EE was greatest very early after thrombus formation (baseline), and then a statistically significant decrease in events was observed (Fig. 7C). To allow for comparisons with future antithrombotic treatments, times after saline injection were pooled. When analyzed this way, there was a non-significant decrease in EE (p = 0.18, Fig. 7D) and fluorescent EE (p = 0.46, Fig. 7E), and a statistically significant decrease in large EE (Fig. 7F). These data have shown that embolization decreases over time, which could indicate an increase in thrombus stability.

4.1.3. Embolization Decreases in the 2nd Hour compared to the 1st Hour

To confirm the decrease in embolization observed over one hour, we extended the duration of the model to two hours. Compared to the 1st hour, there was a statistically significant decrease in EE (Fig. 8A) and in the fluorescent intensity of these events (Fig. 8B) in the 2nd hour. There was also an observed decrease in large EE occurring in the 2nd hour compared to the 1st hour (p = 0.39, Fig. 8C), although not statistically significant. These data confirm the observation of decreased embolization over one hour, and indicate increased thrombus stability over the time period of two hours.

4.1.4. Dynamic Thrombus Formation

To assess thrombus dynamics, thrombus size and percentage of thrombus embolization were quantified at specific time points following injury. Over one hour, even though 3.7% ± 0.4% of the thrombus embolized, a statistically significant increase in thrombus size was observed (Fig. 9A). 8.9 ± 2.8% of the thrombus embolized over two hours, and thrombus size significantly decreased in the 2nd hour compared to the 1st hour (Fig. 9B). Between the 1st and 2nd hours, there was a statistically significant decrease in thrombus embolization from 14.7 ± 3.7% to 3.1 ± 0.4%. As continued and non-consistent changes in thrombus size and embolization were observed over two hours, these data indicate the dynamic nature of the formed thrombus *in vivo*.

4.1.5. Fibrin in Large Emboli

To determine fibrin presence in large emboli, fibrin was labeled fluorescently and large EE were visualized using IVM. 42.1 ± 11.7% of large EE were observed to contain fibrin.

4.1.6. Emboli in Lungs

To determine if DVT emboli progressed to the pulmonary artery circulation, as is characteristic of the clinical setting, representative sections of lung tissue were histologically examined for fibrin, platelets and RBCs using Carstairs' stain. After two hours, we observed emboli in the pulmonary arteries of one out of three mice. These emboli contained platelets and RBCs (Fig. 10A and 10B); however fibrin was not

detected (N = 3). Additionally, infarction and inflammation of the lung tissue was observed (Fig. 10C), which was not present in lungs from mice without DVT (Fig. 10D).

4.2. Direct Thrombin Inhibition Decreases Thrombin Generation Over Time

To assess the effect of administered lepirudin on thrombin generation over time, PRP was collected from control mice and from lepirudin-treated mice at different time points (0 hours, one hour and two hours). The area under the curve (AUC), as a measurement of thrombin generation, was compared between groups. Compared to the control group, there was a significant decrease in the AUC at 0 hours and 1 hour after lepirudin administration (Fig. 11). At two hours, while there was a decrease in AUC compared to the control group, it was not statistically significant ($p = 0.21$, Fig. 8). These data indicate continued suppression of thrombin generation up to two hours after direct thrombin inhibition.

4.3. Direct Thrombin Inhibition Decreases DVT Stability

4.3.1. $FeCl_3$-Induced Thrombi Composition

To assess the impact of direct thrombin inhibition on thrombus composition, Carstairs' stain was used on representative paraffin sections following lepirudin treatment at one and two hours (Fig. 12A and 12B; and Fig. 12C and 12D). Compared to the control group, there was no difference in the percentage of fibrin in one-hour old thrombi (Control group = 18.3 ± 6.3%; Lepirudin group = 16.8 ± 7.6%; $p = 0.89$; N = 3 per group, Fig. 13A). At two hours, there was a decrease in the percentage of fibrin in the femoral vein of the lepirudin group compared to the control group, however this was

not statistically significant (Control group = 21.7 ± 4.3%; Lepirudin group = 9.8 ± 5.7%; p = 0.19; N = 3 per group; Fig. 13B).

To assess the effect of direct thrombin inhibition on FXIIIa activity after one hour, α_2–AP in lepirudin-treated thrombi was detected using IHC (Fig. 14A). The percentage of α_2–AP was 17.8 ± 8.8% after one hour (Fig. 15). Treatment with lepirudin resulted in a decease of α_2–AP content within the thrombus compared to the control group at one hour (p = 0.056, Fig. 15). This finding could indicate decreased cross-linking of α_2–AP by FXIIIa following lepirudin administration.

4.3.2. Embolization Increases Over One Hour After Lepirudin Treatment

To assess the effect of direct thrombin inhibition on thrombus stability, embolization was observed over one hour. Early embolization of the thrombus was also observed at baseline. Over the next hour, following lepirudin administration, there were gradual non-significant increases in EE (p = 0.52, Fig. 16A) and fluorescent intensity of EE (p = 0.47, Fig. 16B). Large EE gradually increased and peaked at 33 minutes after treatment administration, after which there was a decrease (p = 0.64, Fig. 16C). Embolic events occurring after treatment administration were pooled and compared to events occurring before treatment. When analyzed this way, there were non-significant increases in EE (p = 0.35, Fig. 16D), fluorescent intensity of EE (p = 0.08, Fig. 16E), and large EE (p = 0.23, Fig. 16F).

To assess the effect of direct thrombin inhibition compared to the control group, embolic events were pooled after treatment administration. In the lepirudin-treated group

there was an increase in EE (p = 0.18, Fig. 17A) and fluorescent intensity of EE compared to the control group (p = 0.062, Fig. 17B), although not significant. However, there was a statistically significant increase in large EE occurring in the lepirudin group compared to the control group (Fig. 17C). Collectively, these data indicate a decrease in thrombus stability after lepirudin treatment over one hour.

4.3.3. Embolization Increases Over Two Hours After Lepirudin Treatment

To confirm the observed increase in embolization following direct thrombin inhibition over one hour, the duration of the model was extended to two hours. The events occurring in the 1st and 2nd hour were pooled and compared. There was a statistically significant increase in EE in the 2nd hour compared to the 1st hour after lepirudin treatment (Fig. 18A). In addition, there was a trend of increasing fluorescent intensity of EE and large EE in the 2nd hour compared to the 1st hour (p = 0.47, Fig. 18B and p = 0.34, Fig. 18C).

To determine the effect of DTI treatment versus no treatment over two hours, the embolic events occurring in the 1st and 2nd hour of the control and lepirudin-treated groups were compared. In the control group there was a decrease in EE (Fig. 19A), fluorescent intensity of EE (Fig. 19B), and large EE (Fig. 19C) between the 1st and 2nd hour. The opposite was observed in the lepirudin-treated group. Analysis using repeated measures ANOVA confirmed that the control and lepirudin groups were significantly different for EE, fluorescent intensity of EE, and large EE (Fig. 19A, 19B, and 19C).

4.3.4. Embolization Increases After Delayed Lepirudin Treatment

To confirm the increase in embolization observed after direct thrombin inhibition, lepirudin was administered one hour after thrombus formation. Following delayed lepirudin treatment, there was a statistically significant increase in EE compared to the control group (Fig. 20A). There was also an increase in the fluorescent intensity of EE (p = 0.073, Fig. 20B) and in large EE (p = 0.64, Fig. 20C) compared to the control group, although not statistically significant. These data are consistent with increased embolization observed over one hour and two hours in the lepirudin-treated group.

4.3.5. Dynamic Thrombus Formation

To assess the impact of direct thrombin inhibition on thrombus dynamics, the percentage of thrombus embolization and thrombus size were quantified before and after lepirudin administration. $34.6 \pm 5.5\%$ and $35.2 \pm 7.0\%$ of the thrombus embolized over one and two hours, respectively (Fig. 21A and 21B). Compared to the control group there was a statistically significant increase in the percentage of the thrombus embolizing over one and two hours (Fig. 21A and 21B). While there was a decrease in the percentage of the thrombus embolizing between the 1st and 2nd hour of the control group, there was an increase in thrombus embolization from $28.0 \pm 9.8\%$ to $42.4 \pm 10.0\%$ in the 2nd hour in the lepirudin group. Therefore, as a result of treatment, both groups were significantly different, when comparing the 1st and 2nd hour of percentage of thrombus embolization (Fig. 21C).

There was a significant increase in thrombus size observed over one hour following lepirudin treatment (Fig. 22A). An increase in thrombus size was also seen

when comparing the 1st and 2nd hour after lepirudin treatment in the two-hour group (p = 0.12, Fig. 22B). These data indicate that the dynamic nature of the thrombus is exacerbated by direct inhibition of thrombin.

4.3.6. Fibrin in Large Emboli

To determine fibrin presence in large emboli, fibrin was labeled fluorescently and large EE were visualized using IVM following lepirudin administration. 33.1 ± 2.6% of large EE were observed to contain fibrin compared to 42.1 ± 11.7% in the control group (Fig. 23). Use of Fisher's exact test to compare the control and lepirudin-treated group showed no difference in the percentage of large EE observed to contain fibrin (p = 1.00). Using a power calculation, it was determined that a sample size of 1322 large embolic events would be needed to reach significance of this parameter.

4.3.7. Emboli in Lungs

After two hours, emboli consisting of platelets and RBCs were also observed in representative sections of all mouse lungs in the lepirudin group (Fig. 24A and 24B, N = 3). Infarction and inflammation of the lung tissue was also observed (Fig. 24C), compared to lung tissue from mice with no DVT (Fig. 24D).

4.4. Direct FXa Inhibition Decreases Thrombin Generation Over Time

To assess the effect of administered rivaroxaban on thrombin generation over time, PRP was collected from control and rivaroxaban-treated mice at 0 hours and one hour after administration. Compared to the control group there was a significant decrease in AUC at 0 hours and 1 hour after rivaroxaban treatment (Fig. 25). This data

indicates that direct FXa inhibition by this dose of rivaroxaban can suppress thrombin generation over one hour.

4.5. Other Antithrombotics affect DVT Stability

4.5.1. Embolization Increases after Direct FXa Inhibition and Decreases after Indirect FXa Inhibition

To assess the impact of direct and indirect FXa inhibition on embolization, rivaroxaban and fondaparinux were administered respectively. Embolic events occurring after treatment administration were pooled and compared to the control group. There was no observed difference between the control and rivaroxaban-treated group in EE ($p = 0.66$, Fig. 26A); however there was a statistically significant decrease in EE following fondaparinux treatment compared to the control group (Fig. 26A). On the other hand, there was a statistically significant increase in large EE in the rivaroxaban group, while no difference was observed in the fondaparinux group when compared to the control group (Fig. 26B). These data could indicate that indirect FXa inhibition could result in greater thrombus stability over time through decreased embolization.

4.5.2. Embolization Increases after UFH and ATH

UFH and ATH were administered in our model to assess the effect of simultaneous thrombin and FXa inhibition. Compared to the control group, there was an increase in EE following treatment with UFH ($p = 0.95$, Fig. 27A) and an even greater increase after ATH treatment ($p = 0.22$, Fig. 27A), although non-significant. However, in both groups there was a statistically significant increase in large EE compared to the

control group (Fig. 27B). It would appear that inhibition of both thrombin and FXa could decrease thrombus stability through increased large embolic events.

4.5.3. Embolization Decreases after GPIIbIIIa Inhibition

To assess the impact of GPIIbIIIa inhibition, given the central role of the receptor in platelet aggregation, Leo.H4 was administered. Following treatment with the GPIIbIIIa-antagonist, there was a statistically significant decrease in EE compared to the control group (Fig. 28A). However, there was no statistically significant difference between the anti-GPIIbIIIa group and the control group in large EE ($p = 0.47$, Fig. 28B). This observed decrease in embolization over time was unexpected and could indicate that Leo.H4 competes with the fluorescently labeled CD41 Fab fragments to bind GPIIbIIIa.

5.0 DISCUSSION

As the effect of antithrombotic therapy on venous thrombus stability remains poorly defined, we established an acute DVT stability model to better understand this relationship. Our mouse model was characterized by early embolization and spontaneous thrombus stabilization over time. While similar to other $FeCl_3$-injury murine models (130,150,151), we used a novel approach by administering treatment *after* thrombus formation to assess the effect on thrombus stability. DTI treatment increased embolization and large embolic events, which suggested significant disruption of DVT stability. Less α_2–AP was found within the lepirudin-treated thrombi compared to controls, suggestive of decreased FXIIIa activity, and emboli rich in platelets and RBCs were found in the pulmonary artery circulation of both groups. The effect of direct and indirect FXa inhibitors, and indirect FXa and thrombin inhibition was also examined. Therefore, using *in vivo* imaging we have assessed the effect of early DTI treatment on acute DVT stability in a model representative of the clinical nature of VTE, and set the stage for further characterization of thrombin and FXa inhibition on this relationship.

5.1. Characterizing a Novel Mouse Model of DVT Stability

5.1.1. Quantifying Thrombus Stability

Thrombus stability was related to the amount of embolization per minute and visualized in real time using IVM. This allowed us to quantify EE, fluorescent intensity of EE, and large EE as measurements of thrombus stability. We expected an increase in thrombus stability to be indicated by a decrease in EE, fluorescent intensity of EE, and

large EE. We rationalized that reduced embolization (i.e. decreases in EE and large EE) and emboli size (i.e. decreases in fluorescent intensity of EE and large EE) should be consistent with greater DVT stability, and decreased potential for PE over time. Assessment of thrombus stability was confined to the stability of the venous thrombus, and not the clot's interaction with the vessel wall. All thrombi were adherent to the vessel wall for the duration of the model; no thrombi were observed to entirely embolize.

5.1.2. $FeCl_3$-induced Thrombi Contain Fibrin, Platelets, and α_2-AP

Thrombus formation was induced in the femoral vein by topical application of 4% $FeCl_3$. Use of $FeCl_3$ is traditionally thought to induce platelet-rich thrombi (152). However, histological examination has shown $FeCl_3$-induced thrombi to be rich in fibrin, platelets and RBCs (129,130,153,154). We examined the composition of formed thrombi in our model using Carstairs' stain. This confirmed the presence of fibrin, platelets, and RBCs at 10 minutes, one hour, and two hours after thrombus formation. As alternating layers of fibrin, RBCs and platelets typically characterize venous thrombi (50,65) we determined the composition of thrombi in our model to be representative of DVT. We also found a substantial presence of α_2-AP within one-hour old thrombi, which could be representative of FXIIIa activity.

5.1.3. Early Embolization and Increasing Thrombus Stability

Embolization was observed immediately after thrombus formation, which implied early thrombus instability. However, over one hour there was a decrease in embolization, which was also observed in the 2nd hour compared to the 1st hour. A

decrease in the percentage turnover of the thrombus over two hours was also observed. As spontaneous embolization gradually decreased, as well as the size of embolic events, these data collectively indicate increased thrombus stability over time. This could imply that PE risk is greatest during early stages of thrombus formation, when the thrombus is least stable. Older thrombi have been shown to be more resistant to lysis both *in vitro* and *in vivo* (155). Therefore, as the thrombus matures PE risk could decrease due to various stabilizing mechanisms. However, the duration of our model was only two hours, and thrombus embolization remains unknown beyond this time point.

FXIIIa primarily expresses its antifibrinolytic function through cross-linking α_2-AP to fibrin and fibrinogen (17). Therefore, the finding of substantial α_2-AP within thrombi could imply that FXIIIa promotes thrombus stability in our model. Mechanical stabilization of the clot by FXIIIa and the protective effect of localized α_2-AP against lysis (151) could potentially result in the observed increase in thrombus stability over time. This is consistent with the finding that FXIIIa-mediated cross-linking of α_2-AP to fibrin and fibrin chains reduced endogenous and tPA-induced fibrinolysis in an experimental model of pulmonary emboli (156). This reasoning could be confirmed by administering an FXIIIa inhibitor after thrombus formation.

Fibrin structure and platelet stabilizing mechanisms likely also contribute to thrombus stability over time. The contribution of these mechanisms towards DVT stability in our model could be ascertained in the future.

5.1.4. Dynamic Thrombus Formation

We observed thrombus formation to be a dynamic process. Over one hour there was a significant increase in thrombus size despite continuous thrombus embolization. However, over two hours we observed a significant decrease in thrombus size, which was consistent with a greater overall percentage turnover of the thrombus. Conversely, over two hours there was also a significant decrease in the percentage of thrombus embolization. This dynamic nature of the thrombus is consistent with the clinical setting (157-159). The growth and dissolution of the venous thrombus could be influenced by a complex interplay of prothrombotic stimuli and natural anticoagulant mechanisms (160).

The sustained growth of the thrombus observed in our model could be attributed to continuous vascular damage perpetuated by $FeCl_3$ application. Lysed RBCs were observed in histological slides of control thrombi, which could imply that the RBC hemolysis/Hb oxidation cycle could cause continued EC damage and expose subendothelial molecules (129). This could perpetuate platelet aggregation and fibrin formation. However, this mechanism of action has not been demonstrated *in vivo*. Accumulation of Fe^{3+}-rich endocytic-exocytic particles in the vascular lumen (128) and formation of $FeCl_3$-filled spheres, which facilitate platelet and fibrin fiber adherence (125), could also contribute to continued vascular damage. The eventual decrease in thrombus size, observed in the 2nd hour, could result from contact-dependent interactions between platelets that facilitate clot retraction and prevent the fibrinolytic action of plasmin (161).

5.1.5. Pulmonary Emboli

It is estimated that 40–50% of proximal DVT patients develop PE (162). Therefore, a clinically relevant mouse model of DVT should imitate the clinical nature of the disease, and emboli should be detectable in the pulmonary artery circulation.

The principal diagnostic method to evaluate suspected PE is chest CT with intravenous contrast (163). Therefore, we first used micro-CT imaging to detect pulmonary artery thrombi, induced by injection of thromboplastin into the jugular vein, through contrast filling deficits. Unfortunately, desired resolution to visualize induced thrombi conclusively and consistently was difficult to achieve (data not shown). Using histology, we were able to detect emboli in the mouse's pulmonary artery circulation after two hours. Infarction and inflammation of the pulmonary tissue was also observed, which is often clinically associated with PE (164). These findings suggest the clinical relevance of our DVT stability model, as it is representative of the clinical nature of VTE.

Observed emboli were rich in platelets and RBCs, with no fibrin visualized using our staining techniques. The lack of discernable fibrin presence was an unexpected result given the composition of $FeCl_3$-induced thrombi and the ability to fluorescently label fibrin within the thrombus *in vivo*. Determination of emboli composition was dependent on visualization of representative lung sections; therefore, it is not possible to discount fibrin content within emboli. While we have shown that femoral vein thrombi embolize into the pulmonary artery circulation, we have yet to correlate DVT stability with PE. This would be integral in determining potential PE risk.

5.1.6. Mouse Model Limitations

While animal models have advanced our understanding of venous thrombosis under various parameters, it is challenging to mimic the spontaneous development of DVT as seen in humans (120). Animal models are unable to imitate certain physical aspects of humans, such as the spontaneous onset of DVT, upright posture and the calf muscle pump, which play an important role in the dynamics of venous blood flow (165). Therefore, developed animal models will have associated limitations.

Firstly, in our mouse model, a potential limitation is the use of $FeCl_3$ to induce thrombus formation. Human venous thrombi are rarely initiated by vein injury, unless associated with surgery or trauma. Vessel damage is a hallmark of several DVT mouse models, and can result in formed thrombi that differ from most human venous thrombi (66). While the $FeCl_3$ model is technically simple and results in a thrombus of reliable size, it does not parallel the initiation of most clinical thrombi (118). Alternatively, DVT could be initiated using a transient direct-current electrical injury. This is a well-characterized model, which has been shown to induce non-occlusive fibrin-rich thrombus formation in the femoral vein (166). Use of an IVC ligation model of venous stasis could also be explored; however, thrombus formation could be less consistent and more characteristic of DVT in a chronic setting. IVC branches could determine the flow dynamic within the IVC, and possibly limit thrombus size (120). The main disadvantage of this model is the lack of blood flow (167), which could limit the effect of

systemically administered treatments on thrombus stability, as well as the ability to measure emboli.

Secondly, DVT was initiated in a proximal vein in our model. Clinical DVT usually initiate distally and extend proximally (133). However, certain clinical settings, such as pregnancy (168) and hip arthroplasty (169) are often complicated by DVT initiated proximally. Most clinically significant PE manifest from proximal DVTs (170), as embolization is more common (171). Therefore, inducing femoral vein thrombosis in our model is consistent with the finding that most significant DVT are associated with the proximal vein thrombi as opposed to calf vein thrombi (172).

Finally, while our model sought to reflect the clinical setting of DVT's progression to PE, we used a standardized approach of intravenous bolus infusion to administer treatment. Clinically, fondaparinux is administered subcutaneously (173) and rivaroxaban is an oral anticoagulant (174). The impact of these drugs on thrombus stability observed in our model could be influenced by the parenteral mode of administration, as their time to action could be enhanced. Additionally, not all tested drugs are indicated for treatment of VTE. Lepirudin is only approved for treatment of HIT patients (175) and ATH has not been tested or approved in the clinical setting. While aspirin has been shown to be efficacious in the prevention of recurrent VTE (176), GPIIbIIIa inhibitors are currently only indicated for use in high-risk patients, or patients not on $P2Y_{12}$ blockers, undergoing PCI(177). However, the effect of these antithrombotics on acute DVT stability can be used to make mechanistic inferences.

5.2. Direct Thrombin Inhibition

Lepirudin was chosen as the administered DTI, as it is a parenteral anticoagulant that has been extensively studied in other mouse models (144,178). The chosen dose (8U/g mbw) has been shown to block fibrin generation and to impair platelet adherence and aggregation, when administered before thrombus formation *in vivo* (144).

There was a significant suppression of thrombin generation immediately and at one hour after lepirudin administration. At two hours, a decrease in thrombin generation was still observed, although to a lesser extent. This coincided with the half-life of lepirudin, which is approximately 80 minutes in healthy patients (179). This effect on thrombin generation could result in the significant increase in thrombus embolization observed after DTI treatment in our model.

As a bivalent inhibitor, lepirudin complexed with thrombin would prevent thrombin's interaction with fibrin (180). This contrasts with univalent inhibitors, such as dabigatran, which only bind to thrombin's catalytic active site and do not interfere with this interaction (181). In addition, dabigatran is a reversible inhibitor (181), whereas lepirudin binds thrombin irreversibly. While we have shown a significant increase in thrombus embolization over time after direct thrombin inhibition, extrapolating these results to other DTIs would have to take into consideration their mechanism of action. This could influence the effect on thrombus stability observed in our model.

5.2.1. Decreased Thrombus Stability after Direct Thrombin Inhibition

Lepirudin administration increased embolization and embolic event size over one hour compared to the control group, which suggested decreased thrombus stability. This effect of lepirudin was confirmed when significant interactions were observed for all parameters between both groups in comparing the 1st and 2nd hour. This implied that DTI treatment decreased thrombus stability, as the control showed decreased embolization between the 1st and 2nd hour. In addition, following delayed lepirudin treatment, increased embolization compared to controls was also observed. Moreover, in comparison to the control group, the lepirudin group had a significant increase in the percentage turnover of the thrombus over two hours as a result of treatment.

Collectively, these results support our hypothesis that acute administration of DTIs could decrease acute DVT stability through increased embolization. DTI treatment could, therefore, be associated with an increase in PE over time in our model. Since thrombin is integral to the promotion and stabilization of thrombi under venous shear rates (161), the increase in embolization could result from impaired thrombin activity within the thrombus. Given thrombin's extensive role in coagulation, this could affect various mechanisms that contribute to thrombus stability.

The susceptibility of formed thrombi to fibrinolysis could also result from reduced thrombin-induced FXIIIa activity (182). The substantial decrease in α_2-AP content observed within the DTI-treated thrombi could indicate suppressed FXIIIa antifibrinolytic activity. Use of an FXIII inhibitor (155,183) in our model could confirm our reasoning, and use of a fluorescently labeled substrate peptide based on the N-terminal sequence

of α_2-AP might be useful in further assessing FXIIIa activity real time *in vivo* (184).

Impairment of thrombin generation over time by DTI administration would most likely result in decreased thrombin concentration and activity within the thrombus. The density of the fibrin clot and thickness of associated fibrin fibers are influenced by thrombin concentration (13). Permeable thrombi, consisting of thick, loosely woven fibrin fibers, tend to be characteristic of low thrombin concentration (13). tPA binds more efficiently to thick-stranded fibrin than to thin fibrin fibers (185). Therefore the increased amount of embolization observed could be attributed to the effect of lepirudin on newly formed fibrin within the clot. DTI treatment could result in a more porous thrombus compared to the control group, which would facilitate interactions between fibrin and plasmin. To confirm fibrin structure within the thrombus, we could use scanning electron microscopy. Platelet-platelet interactions within the thrombus could also be affected by DTI treatment, resulting in enhanced clot lysis. This would be consistent with the increase in observed embolization.

Hirudin competitively binds to exosite 1 on thrombin, releasing it from the thrombin-TM complex (186), which could affect both APC and TAFIa activation. Direct thrombin inhibition has also been shown to impair EC-mediated APC generation (187). This would decrease APC-dependent inactivation of FVa and FVIIIa, which are important cofactors in amplifying thrombin generation. However, clinically, the anticoagulant effect of lepirudin has been shown to override the prothrombotic effect of APC suppression (186). Clot-bound thrombin is thought to have an important role in

fibrinolysis, through localization of TAFIa production (188). Use of heparin to enhance clot lysis through TAFIa suppression was unsuccessful; however use of hirudin in the same setting increased fibrinolysis (188). Since hirudin has been shown to inhibit TAFIa functionality (189) a reduction in TAFIa activity could contribute to the increased embolization observed in our model.

5.2.2. Dynamic Thrombus Formation

Lepirudin treatment resulted in a significant increase in thrombus embolization compared to the control group. The percentage turnover lepirudin-treated thrombi significantly increased over the course of two hours, implying decreased thrombus stability. This was significantly different to the control group, which demonstrated decreased thrombus embolization over time. Despite increased percentage turnover of the thrombus, consistent growth of lepirudin-treated thrombi was also observed. Therefore, administration of a DTI appeared to perpetuate the dynamic nature of thrombus formation.

This result was unexpected as a decrease in thrombus formation and clot size with lepirudin treatment has been demonstrated in other animal models (144,190,191). Agnelli et al. found decreased fibrin accretion on a pre-existing jugular vein thrombus in rabbits after infusion of hirudin over three hours (185,186). Dubois et al. administered lepirudin before thrombus induction and observed a decrease in platelet accumulation and fibrin generation (137). However, in previous models lepirudin was administered before thrombus formation. With the exception of our murine model, the influence of

direct thrombin inhibition on size and embolization of a pre-formed clot has not been examined in the acute setting.

The increase in observed thrombus size could be possibly explained by continuous injury from $FeCl_3$ use; release of soluble agonists from activated platelets within the thrombus that could perpetuate platelet aggregation; and release of fibrin-bound thrombin upon lysis (13). The contribution of various factors towards the dynamic nature of the thrombus is difficult to ascertain, and remains to be further explored. However, our finding is congruent with demonstrated thrombus extension in the acute phase of treatment (116), and increased recurrent VTE observed initially following DTI treatment compared to LMWH treatment observed by the THRIVE Study Investigators (192).

5.2.3. Pulmonary Emboli

Emboli were likewise observed in the pulmonary artery circulation two hours after lepirudin treatment. These emboli also consisted of platelets and RBCs, with no visible fibrin. However, unlike the control group, emboli were found in all of the lepirudin-treated mice. Pulmonary emboli were expected to be more extensive and larger in size, compared to those in the control group, as large EE increased after DTI treatment. In contrast, emboli appeared to be smaller in size, although this observation is presently inconclusive. Identifying the correlation between direct thrombin inhibition and PE would be useful in determining the associated risk.

Interestingly, in a two-hour model of PE, there was decreased mortality in α_2-AP

deficient mice compared to wild type mice (193). As we observed a substantial decrease in α_2-AP in the lepirudin-treated group compared to the control group, this could have a protective effect in our model and decrease PE risk. Simulating our model of DVT stability in α_2-AP deficient mice could provide a better understanding of the plasmin inhibitor's role in relation to emboli development.

5.3. Other Antithrombotics

Having established a reliable mouse model of DVT stability and examined the effect of direct thrombin inhibition, we then decided to explore the effect of FXa inhibition, simultaneous FXa and thrombin inhibition, and GPIIbIIIa inhibition on thrombus stability.

5.3.1. FXa Inhibition and Thrombus Stability

To explore the impact of direct FXa and indirect FXa inhibition, we administered rivaroxaban and fondaparinux, respectively. We have shown that direct inhibition of FXa could decrease thrombus stability possibly by increasing large EE. In contrast, decreased embolization was observed in the fondaparinux treated group, which could indicate increased DVT stability.

As a direct FXa inhibitor, rivaroxaban specifically targets free and clot-bound FXa (194). Thrombin generation is almost completely attenuated at high concentrations of rivaroxaban *in vitro* (195), and we have additionally shown significant suppression of thrombin generation one hour after treatment. Therefore, rivaroxaban could reduce thrombin concentration within the thrombus possibly through inhibition of

prothrombinase-associated FXa.

On the other hand, fondaparinux only targets free FXa. FXa within prothrombinase is protected from inhibition by the AT-pentasaccharide complex (196) - AT is most likely ineffective at competing with prothrombin for FXa's catalytic center (195). Continued thrombin generation within the thrombus, supported by prothrombinase, could contribute to thrombus stabilization.

In comparing rivaroxaban and fondaparinux treatment groups, the contrast in thrombus stability most likely arises from opposing effects on platelet-platelet interactions, FV and FVIII activation, FXIII activation, TAFI activation, and fibrin formation.

5.3.2. FXa and Thrombin Inhibitors and DVT Stability

To explore the impact of simultaneous FXa and thrombin inhibition, UFH and ATH were administered. We have shown that both compounds could decrease thrombus stability, possibly through an increase in large EE.

UFH indirectly inhibits thrombin and FXa through an AT-dependent mechanism (197). However, there are many associated limitations with UFH treatment that prevent attaining therapeutic anticoagulation (79). Non-specific binding of UFH to plasma proteins reduces its anti-FXa activity (198) and results in a variable anti-thrombin response (199). The increase in embolization following UFH administration could result mainly from the indirect inhibition of free thrombin, as indirect inhibition of FXa in our model appears to decrease embolization. A decrease in protein C activation is

associated with heparin administration, as well as a decrease in TAFI activation (188). However, heparin does not inhibit clot-bound thrombin (80) and this could contribute to TAFI activation within the thrombus.

ATH is a covalent compound that inhibits thrombin and FXa through both direct and indirect mechanisms (112,200,201). ATH inhibits free thrombin approximately 4-fold faster than UFH and AT (202). This results in a decrease in thrombin-TM complex formation, and a subsequent down-regulation of protein C activation (202). ATH additionally enhances cleavage of FVa (202). It is thought that the decrease in thrombin-TM would also decrease TAFI activation. In addition, ATH inhibits fibrin-bound thrombin (111), which could decrease thrombin activity within the thrombus. Based on our results, it is thought that ATH effects thrombus stability through direct and indirect thrombin inhibition, as well as direct FXa inhibition. However, the sole impact of indirect thrombin inhibition in our model remains unknown.

While it appears that over one hour both UFH and ATH could decrease thrombus stability, it is difficult to determine whether inhibition of thrombin or FXa had a more significant impact. As both thrombin and FXa are simultaneously inhibited, a synergistic effect on increasing embolization would be expected. However, the interaction of the endogenous anticoagulant and antifibrinolytic mechanisms, in relation to DVT stability in our model, remains unknown.

5.3.3. GPIIbIIIa Inhibition and Thrombus Stability

The GPIIbIIIa inhibitor (Leo.H4) administered in our model mimics the clinical

nature of abciximab and inhibits platelet aggregation (203). Treatment with Leo.H4 decreased embolization indicating a possible increase in thrombus stability. This result was unexpected as the GPIIbIIIa receptor is central to platelet aggregation (204).

Both fluorescently labeled MWReg30 and Leo.H4 bind to the GPIIbIIIa receptor on resting and activated platelets (205,206). Therefore, the observed decrease in EE and large EE could be attributed to competitive inhibition of MWReg30 by the GPIIbIIIa antagonist, which was administered at a higher concentration. This could impair fluorescent visualization of emboli. Injecting Leo.H4 before the fluorescent CD41 platelet marker, or using a fluorescent platelet label directed against GPIb, could confirm this reasoning. Alternatively, emboli could be fibrin-rich in this treatment group, which could decrease embolic event visualization, as platelets are fluorescently labeled. As we have shown fibrin content in approximately one third of large emboli in control and lepirudin groups, this could be confirmed using a specific anti-fibrin compound and the same method of visualization.

5.4. Future Directions

This thesis has outlined the development of a clinically relevant mouse model of acute DVT stability, characterized by early embolization, spontaneous reduction in embolic events over time, and dynamic thrombus formation. Administration of an acute DTI *after* thrombus formation, as a novel approach, was found to decrease proximal DVT stability. To better ascertain the role of thrombus stability in the progression of acute DVT to PE, various parameters of our model can be further delineated. Following

further characterization of our model, it would then be possible to further examine the effect of acute DTI administration on DVT stability, as well as direct and indirect FXa inhibition. In addition, it would be interesting to explore the role of thrombus stability in risk factor settings where the likelihood of PE deviates from the clinical literature.

5.4.1. DVT Stability Model

To better characterize our model, we could assess thrombus stability beyond two hours, determine FXIIIa activity *in vivo*, further examine fibrin content in large emboli, and correlate DVT stability to PE.

Our model implies increased DVT stability over time through a reduction in embolization; however it is uncertain if the thrombus remains stable beyond the time point of two hours. As older thrombi become more resistant to fibrinolysis (149,155), we would expect to observe a continued increase in thrombus stability. Extending the duration of our model would confirm this, and it would be important to ascertain whether there is a corresponding decrease in PE over time as well.

Quantification of α_2-AP has been used as an indicator of FXIIIa activity, both *in vitro* and *in vivo*. However, as we used IHC to determine α_2-AP content within the thrombus, it was only possible to determine the amount of α_2-AP at specific time points *ex vivo*. While thrombi α_2-AP content could represent FXIIIa activity, use of an FXIIIa inhibitor (155,183) and an α_2-AP derived marker (184) could better assess and confirm the antifibrinolytic contribution of real time FXIIIa activity towards DVT stability in our model.

The observation of fibrin in approximately one third of large EE was inconclusive, as the power of our sample size was insufficient. Increasing the sample size of large embolic events would be useful in confirming this observation. Use of a more specific fibrin fluorescent marker could also improve visualization of fibrin content within emboli.

Correlating PE risk to DVT stability, in our model, would be the main future goal. Identifying emboli in the pulmonary artery circulation has demonstrated that our model is representative of the clinical nature of VTE. Therefore, our model of DVT stability is clinically relevant. However, we have not determined the extent of PE risk and emboli size in relation to thrombus stability. Establishing the correlation of PE to proximal DVT stability would be useful in determining PE risk under various treatment settings, and might identify high-risk patient populations.

5.4.2. DVT Stability Model Applications

Embolization of pre-formed thrombi increased after DTI administration, which indicated a decrease in thrombus stability over time. Extending the duration of the model could confirm if this deleterious effect on thrombus stability is prolonged. Assessing the effect of thrombin inhibition on FXIIIa activity *in vivo* and examination of fibrin structure - both *in vitro* and *in vivo* - could provide some mechanistic information related to the possible decrease in thrombus stability. Moreover, as DTI treatment increased large EE, it would be important to determine if DTI treatment resulted in extensive PE in the acute setting.

The central role of FXa in thrombin production also makes it an attractive anticoagulant target. We have shown an increase in embolization following direct FXa inhibition and the opposite outcome after indirect FXa inhibition over one hour. To further characterize the effect of FXa inhibition, we could examine: embolization over an extended period of time; the contribution of FXIIIa; thrombus dynamics; and fibrin clot structure. It would be interesting to determine if direct thrombin and direct FXa inhibition had comparable effects on DVT stability over time.

The progression of DVT to PE is dependent on specific risk factors present in the patient population; certain risk factors augment PE likelihood, while others do not. Factor V Leiden (FVL) confers APC resistance and is paradoxically associated with a higher relative risk for DVT and a similar relative risk for PE compared to individuals without FVL (207). Cancer patients often develop VTE, though the incidence of DVT and PE differs depending on the cancer type; for instance, the incidence of PE is greater in those with liver cancer, compared to stomach cancer patients (208). Additionally, PE is shown to account for a higher percentage of VTE episodes with increasing age, instead of the incidence of DVT and PE increasing proportionately(58). Thrombus stability could be dependent on the risk factor setting, which could possibly lead to the differing likelihood of PE development from DVT. To explore this objective, our model could be simulated in FVL mice, in well-described models of bone and prostate cancer, as well as in aged mice.

5.5. Conclusion

Establishing a mouse model of DVT stability has provided preliminary insight into the effect of anticoagulation on thrombus stability in the acute setting. Real-time assessment of thrombus stability has demonstrated a decrease in embolization and an increase in the stability of the thrombus over time. To address our hypothesis we used a novel approach and intravenously administered a DTI after thrombus formation *in vivo*. The finding of increased embolization and a greater number of large embolic events confirmed our hypothesis of decreased thrombus stability after acute DTI treatment. Increased clot lysis could result from decreased FXIIIa activity, indicated by decreased α_2-AP content within DTI-treated thrombi compared to controls. However, there are several other mechanisms that could contribute to these observations that have yet to be elucidated in our model. The finding of emboli within the pulmonary artery circulation possibly related DVT stability to PE; however this correlation remains to be defined.

Although the exact mechanistic role of DVT stability in our developed mouse model remains to be characterized, this work has set the stage for evaluating the contribution of thrombin and FXa inhibition on thrombus stability over time. This could be beneficial in further defining the effect of acute administration of new, oral anticoagulants on acute DVT, and the impact of different risk factor settings on PE.

6.0. FIGURES
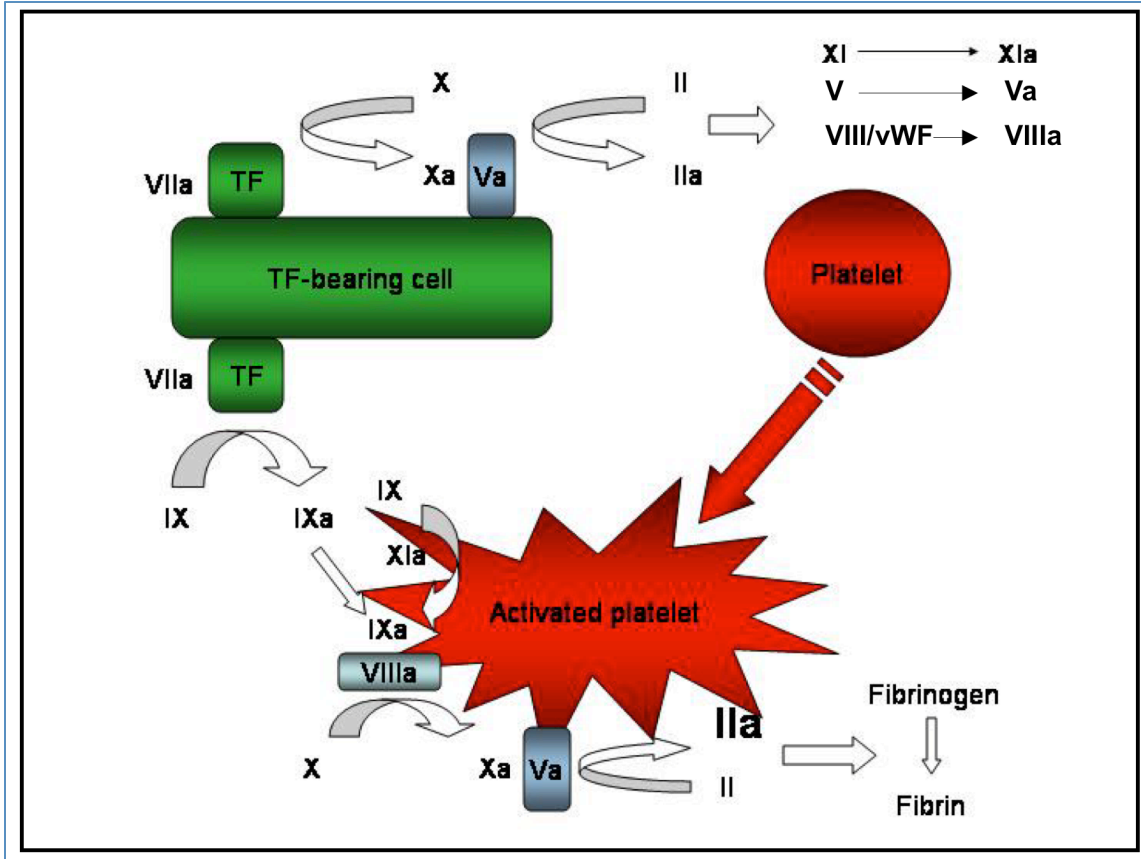
FIGURE 1 - Cell-based Model of Coagulation
Coagulation is initiated on the TF-bearing cell surface. The TF-FVIIa complex activates FX and FIX. FXa forms a complex with FVa – the prothrombinase complex generates a small amount of thrombin to amplify the procoagulant signal. Thrombin activates cofactors V and VIII, FXI, and platelets through PAR cleavage. FIXa forms a complex with FVIIIa to generate FXa on the activated platelet surface. The prothrombinase complex on the activated platelet surface generates a burst of thrombin that cleaves fibrinogen to fibrin. The formation of a fibrin clot that seals the injury site completes the hemostatic process (1).

	LEPIRUDIN	RIVAROXABAN	FONDAPARINUX	UFH	ATH	ABCIXIMAB
Target	Thrombin	FXa	FXa	Thrombin/ FXa	Thrombin/ FXa	GPIIbIIIa
Direct/ Indirect	Direct	Direct	Indirect	Indirect	Both	Direct
Route of administration	IV	Oral	Subcutaneous	IV / Subcutaneous	N/A	IV
Molecular Weight	6,978	436	1,728	≈ 15,000	≈ 76,000	47.6
Bioavailability (%)	≈ 100	≈ 80	≈ 100	≈ 100 / ≈ 30	N/A	≈ 100
Half life (hours)	0.8-1.7	7-11	13-15	1-2	2.6 (in rabbits)	≈ 0.17
Indication in Clinical Setting	HIT	DVT	DVT/PE	DVT/PE	N/A	PCI

TABLE 1: Properties of Antithrombotics Targeting Thrombin, FXa, and GPIIbIIIa in the Clinical Setting
IV = intravenous; HIT = heparin-induced thrombocytopenia; DVT = deep vein thrombosis; PE = pulmonary embolism; N/A = not applicable; PCI = percutaneous coronary intervention
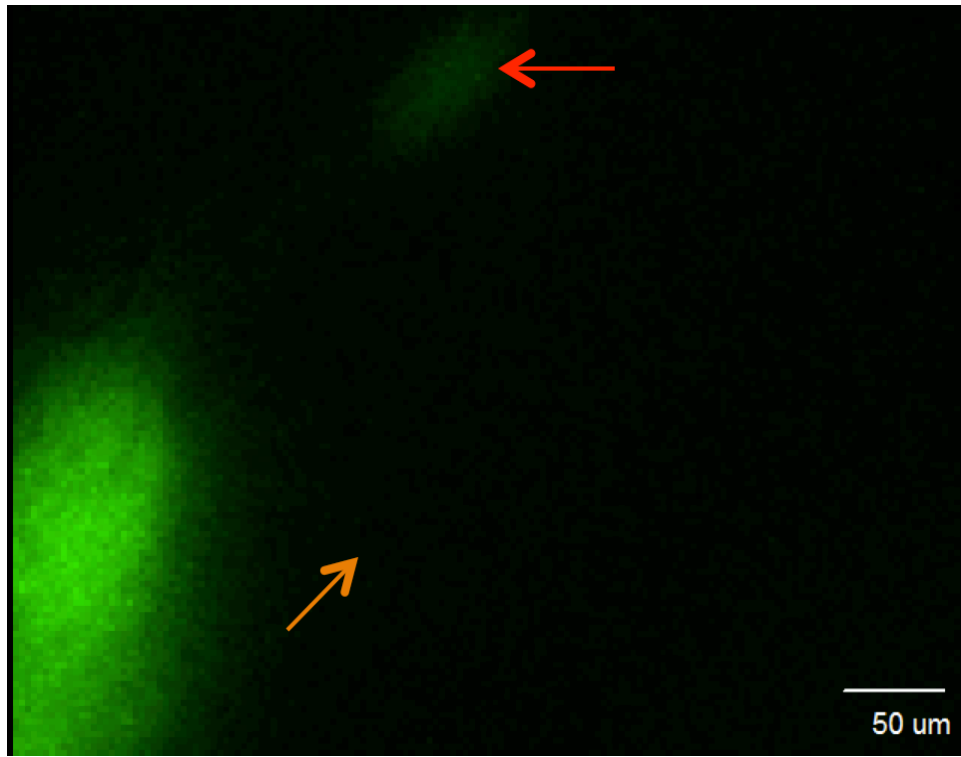
FIGURE 2 - Thrombus Embolization: control group.
Representative image of visibly fluorescent platelets breaking off from the thrombus and moving downstream, defined as an embolic event. Platelets were labeled with prepared CD41 Fab fragments conjugated to Alexa Fluor 488. Embolization was visualized using IVM with a 20X 0.5 NA water immersion objective;the camera set to 4 x 4 binning and 10ms exposure time. Red arrow indicates an embolic event; orange arrow indicates direction of blood flow
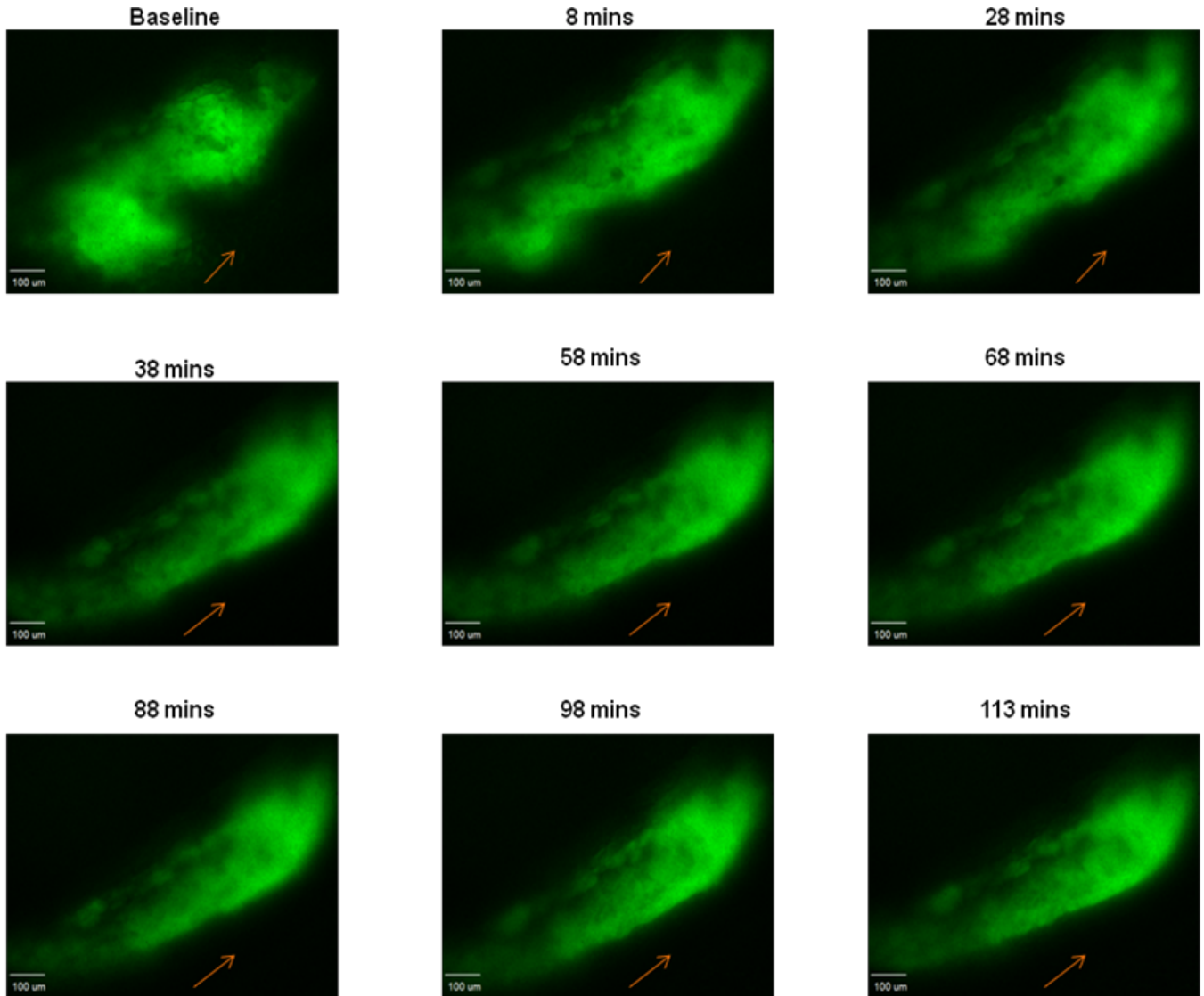
FIGURE 3 - Thrombus Size Over Two Hours: control group
Representative images of a FeCl$_3$-induced thrombus in the femoral vein over two hours. Thrombus size was quantified by the sum of fluorescently labeled platelets. The thrombus was visualized using IVM with a 10X 0.3NA water immersion objective with the camera set to 1 x 1 binning and 100ms exposure. Thrombus size was imaged before (baseline) and at 8, 28, 38, 58, 68, 88, 98, and 113 minutes after saline administration. Saline was given as a control treatment for comparison with future antithrombotic treatments.

No Clot   **Clot**

A

B

C
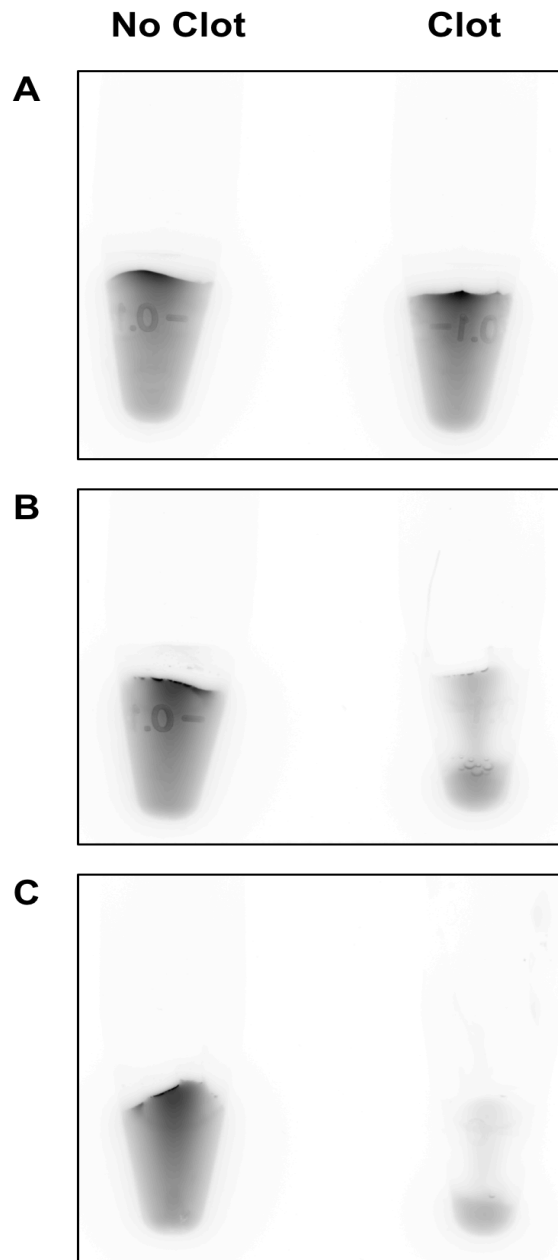
FIGURE 4 – Testing fibrin peptide specificity
(A) Background fluorescence of FITC-labeled fibrin peptide in 100µL PRP. **(B)** Clotting was initiated in the right Eppendorf tube using a final concentration of 20mM $CaCl_2$; the clot was extensively washed with PBS. **(C)** The clot was extensively washed a 2nd time with PBS. Fluorescence was measured using the Typhoon^{TM} 9400 laser scanner set at 50µm resolution, with normal sensitivity, and a 488 laser. N = 1. Images show control (left) and clot (right).
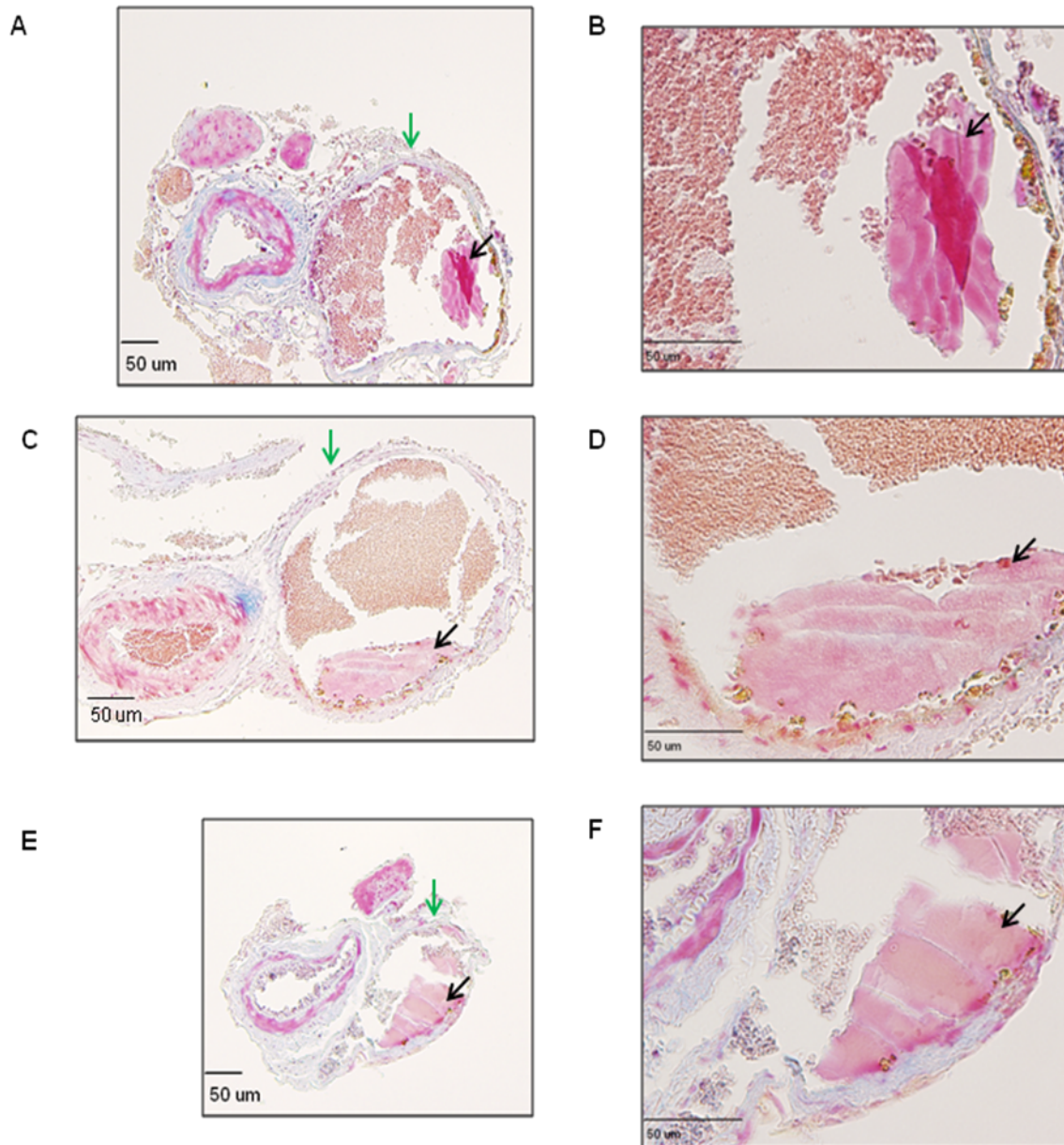
FIGURE 5 – Carstairs' femoral vein thrombus slides at 10 minutes, one hour and two hours: control group

Representative Carstairs' stain for assessment of thrombus composition in control mice at 10 minutes **(A, B)**, 1 hour **(C, D)** and 2 hours **(E, F)** following thrombus formation using a 10X (A, C, E) and 40X (B, D, F) objective, respectively. Fibrin is red, platelets are navy blue, and red blood cells (RBCs) are yellow-red. Black arrows indicate fibrin; green arrows indicate femoral vein. N = 3 per group. Images show the right femoral vein and $FeCl_3$-induced thrombus within.
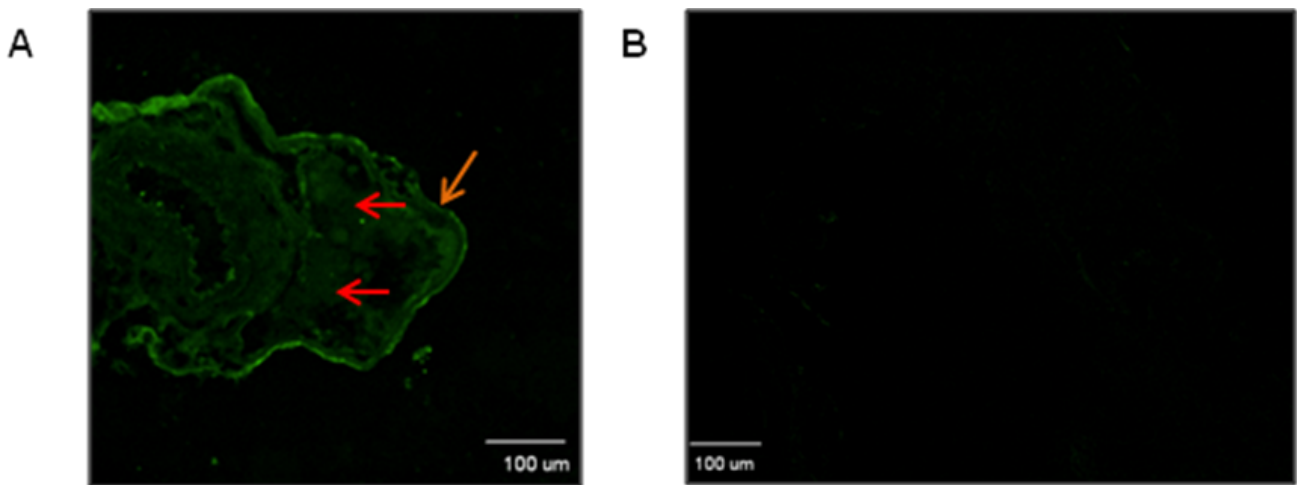
FIGURE 6 – IHC α$_2$–antiplasmin femoral vein thrombus slides at one hour: control group
(A) Representative IHC stain for assessment of α$_2$–AP content in thrombus at one hour in the control group, **(B)** and corresponding negative control. α$_2$–AP was detected with goat anti-mouse serpin F2/α2-AP antigen affinity-purified polyclonal antibody fluorescently labeled with Alexa Fluor 488 donkey anti-goat IgG antibody. Red arrows indicates α$_2$–AP within the thrombus; orange arrow indicates the femoral vein. Representative of three experiments. Images show the right femoral artery and femoral vein, and FeCl$_3$-induced venous thrombus within.
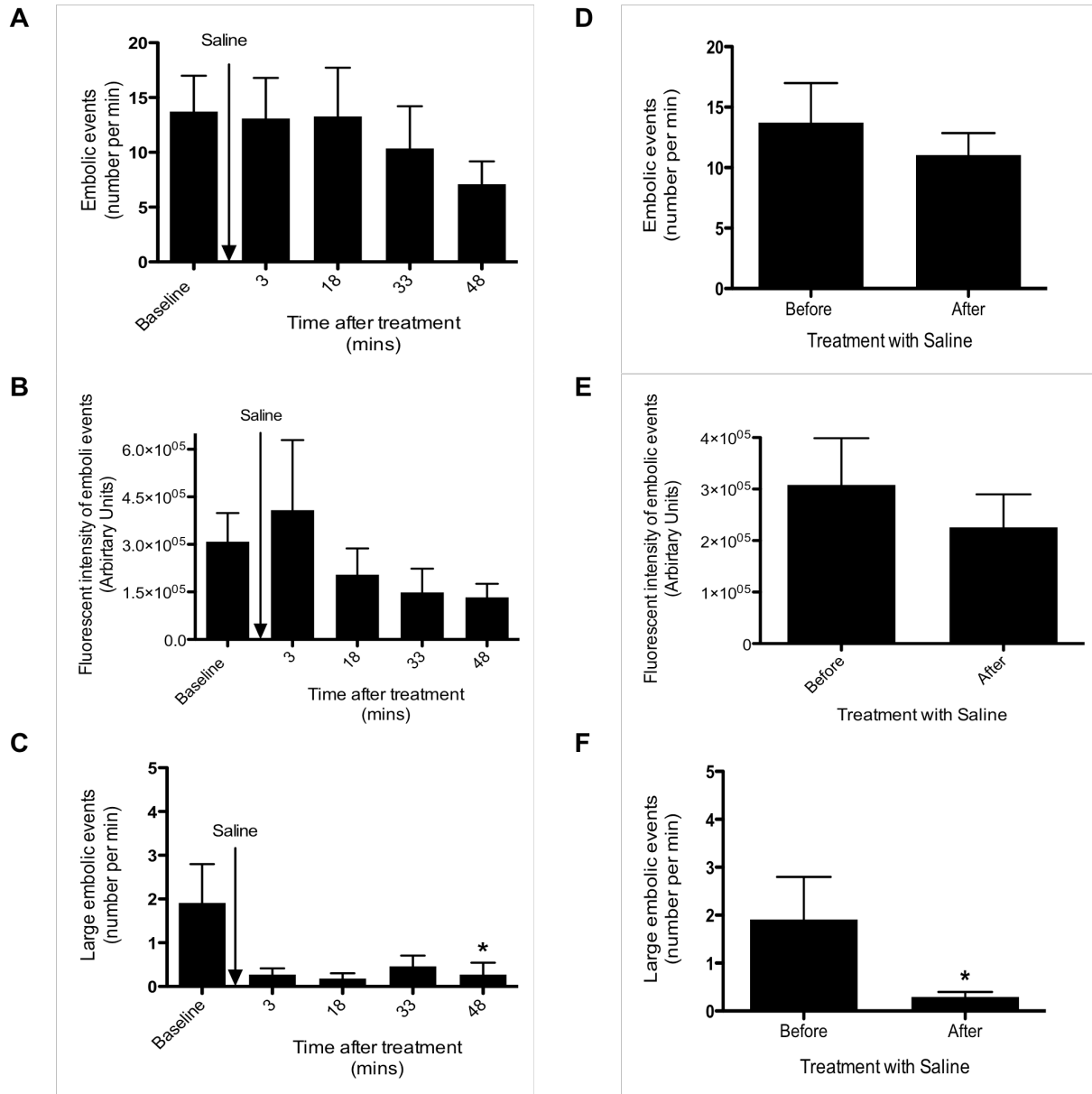
FIGURE 7 – Changes in embolization over one hour: control group
(A) Average number of embolic events occurring per minute (EE), **(B)** fluorescent intensity of EE, expressed as arbitrary units (AU), and **(C)** average number of large embolic events occurring per minute (large EE) observed over one hour at 3, 18, 33, and 48 minutes following saline administration as control treatment. **(D)** EE, **(E)** fluorescent intensity of EE, and **(F)** large EE before and after saline treatment. EE and large EE values are expressed as number per minute (min). Fluorescent intensity values are expressed as arbitrary units (AU). All values are expressed as mean ± SEM and data was analyzed using one-way ANOVA (A-C) with Dunnett's post-hoc test (C) and Student's t-test (D-F). N = 11. * Indicates significance versus before or baseline with $p<0.05$.
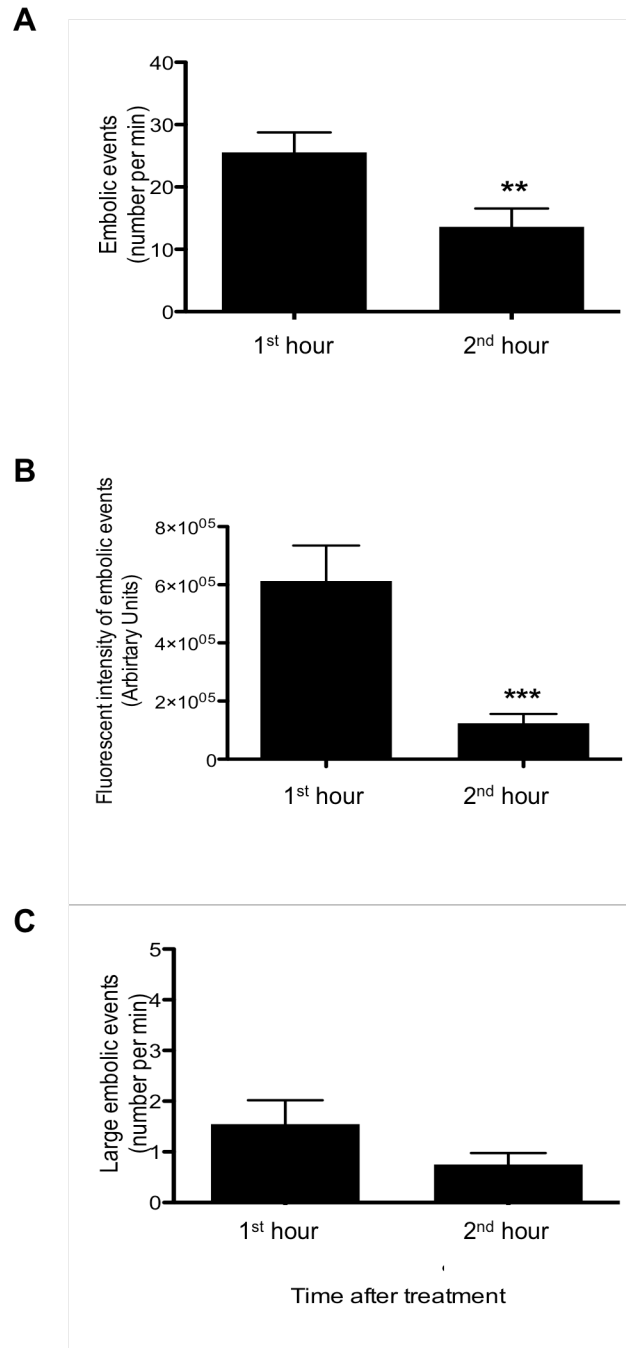
FIGURE 8 – Changes in embolization over two hours: control group
(A) EE, **(B)** fluorescent intensity of the EE, and **(C)** large EE in the 1st and 2nd hour following saline as control treatment. EE and large EE values are expressed as number per min. Fluorescent intensity values are expressed as AU. All values are expressed as mean ± SEM and data was analyzed using Student's t-test. N = 5. ** Indicates significance versus the 1st hour with $p < 0.01$. *** Indicates significance versus the 1st hour with $p < 0.001$.
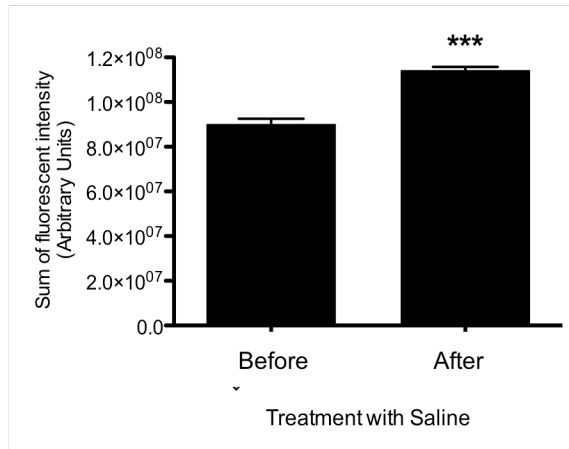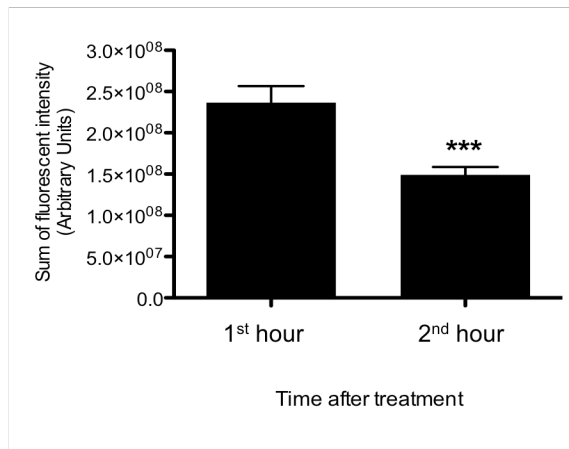
FIGURE 9 – Change in thrombus size over one hour and two hours: control group
(A) Thrombus size, expressed as the sum of fluorescently labeled platelets in AU, before and after saline treatment in the one-hour group. N = 3. **(B)** Thrombus size, expressed as the sum of fluorescently labeled platelets in AU, in the 1st and 2nd hour following saline treatment in the two-hour group. N = 5. All values are expressed as mean ± SEM and data was analyzed using Student's t-test. *** Indicates significance versus before or 1st hour with $p < 0.001$.
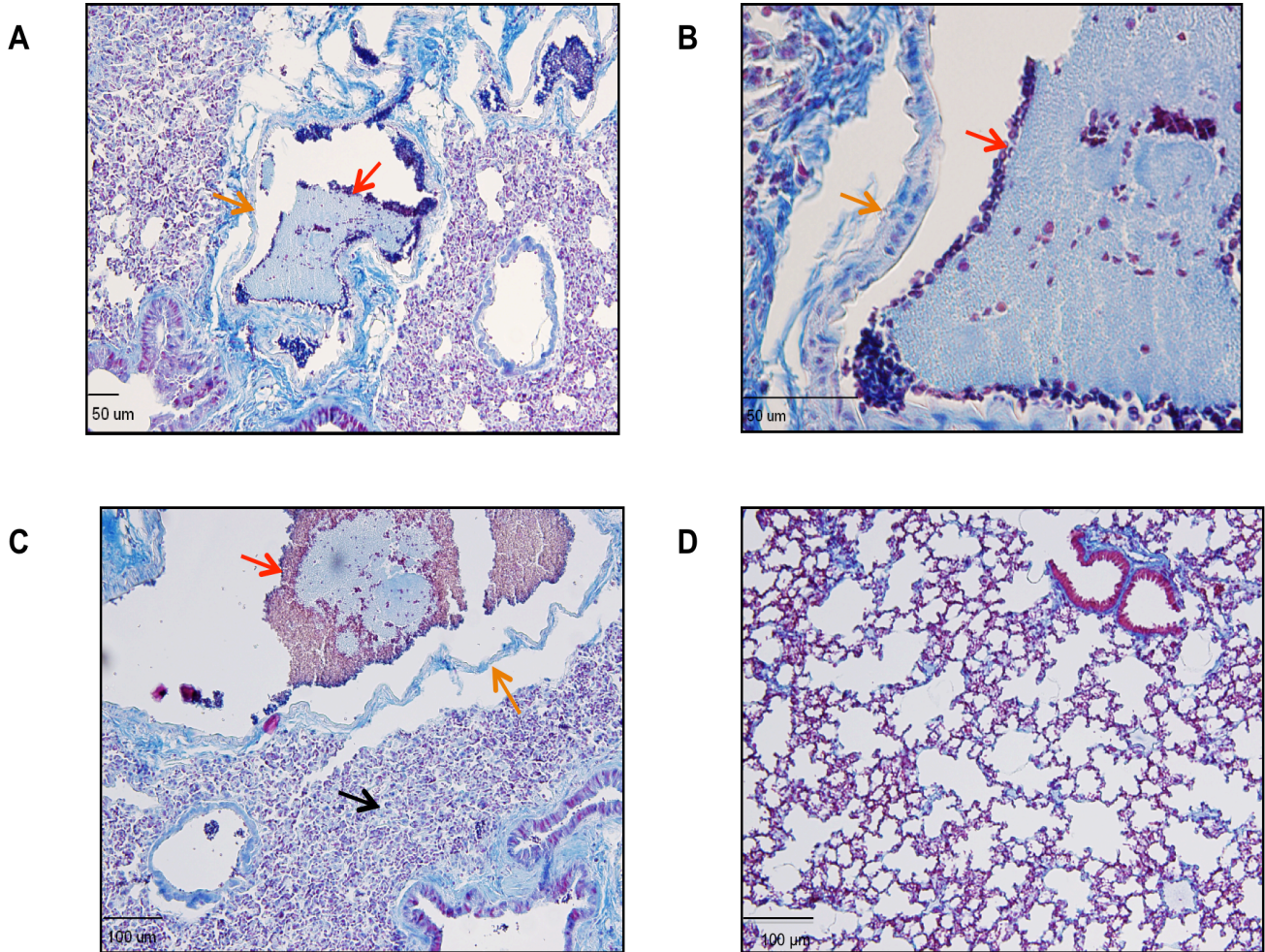
FIGURE 10 – Carstairs' lung slides at two hours: control group
(A, B) Representative Carstairs' stains for assessment of pulmonary emboli within lungs at two hours using a 10X objective (A, C) and a 40X objective (B, D), respectively. **(C)** Representative Carstairs' stains of inflamed lung tissue in the control group at the site of an embolus, and **(D)** lung tissue from a mouse without femoral vein thrombosis. Red arrows indicate embolus; orange arrows indicate the pulmonary artery; black arrow indicates inflamed lung tissue. Representative of three experiments. Images show an embolic event within a pulmonary artery (A, B) and mouse lung tissue (C, D).
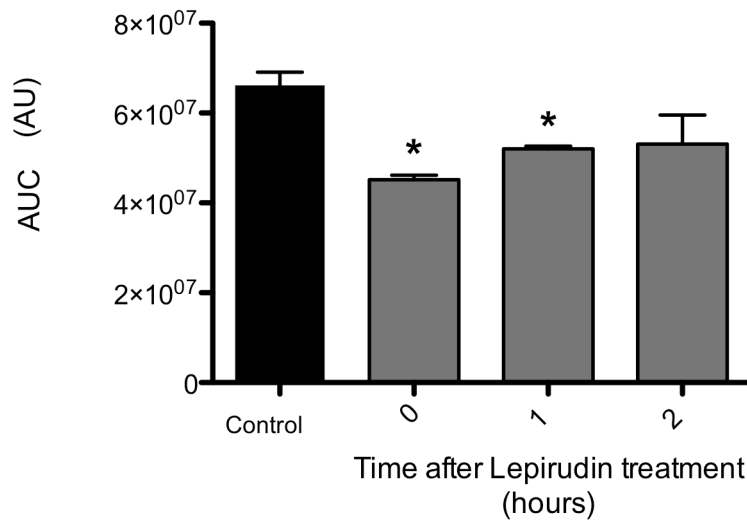
FIGURE 11 – Thrombin generation at zero, one and two hours: lepirudin group
Lepirudin was administered, 8U/g mouse body weight (mbw), and plasma collected at different time points (0 hours; 1 hour; 2 hours) following treatment. Thrombin generation was initiated with $CaCl_2$, assessed at one-minute intervals over one hour in control and lepirudin-treated mouse plasma. Area under the curve (AUC) in control and lepirudin groups was compared as a measurement of thrombin generation. N = 3 per group (in duplicate). Values are expressed as mean ± SEM and data was analyzed using Student's t-test. * Indicates significance versus control with $p < 0.05$.
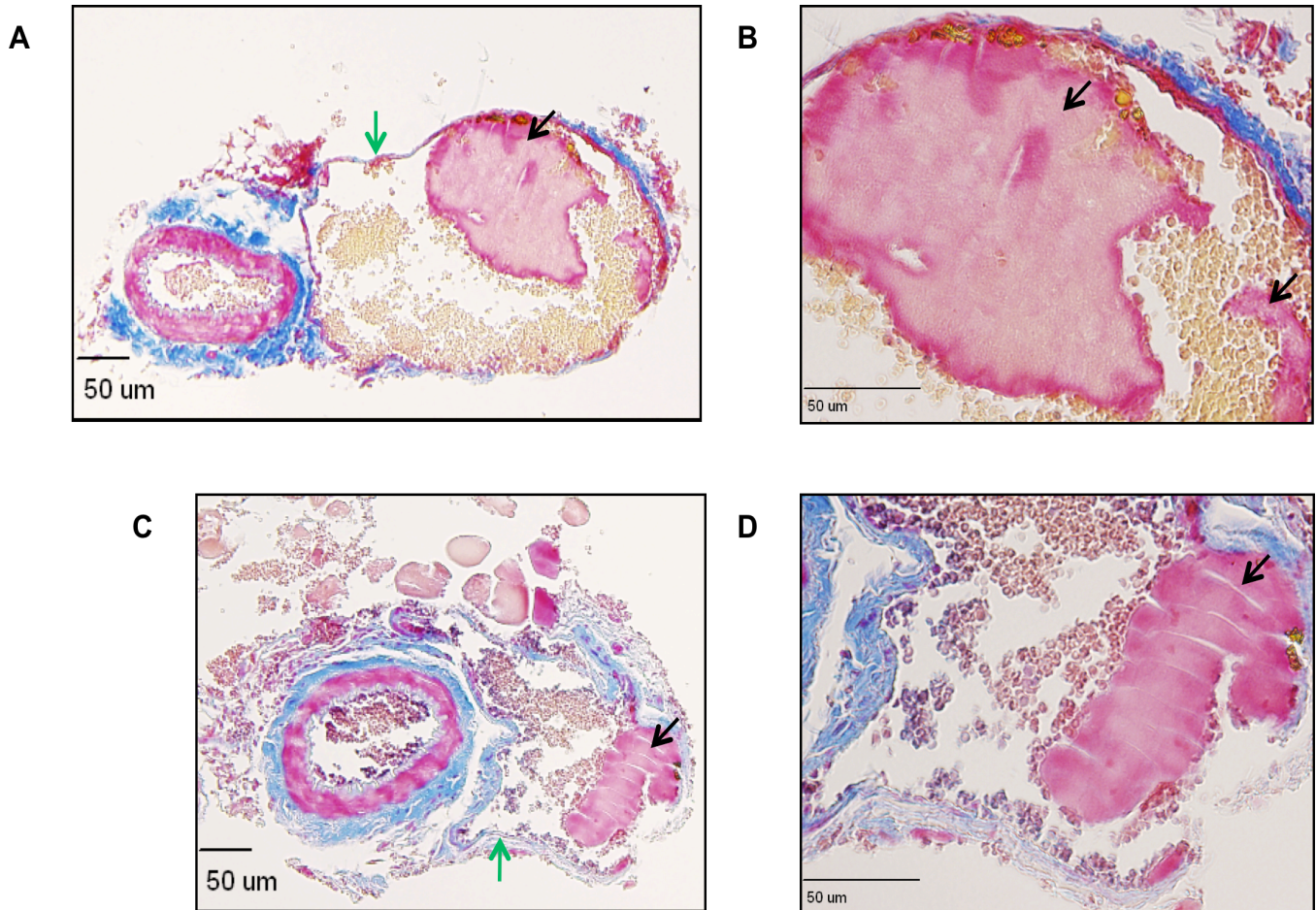
FIGURE 12 – Carstairs' femoral vein thrombus slides at one hour and two hours: lepirudin group
Representative Carstairs' stains for assessment of thrombus composition in lepirudin treated (8U/g mbw) mice at one hour **(A, B)** and two hours **(C, D)** following treatment administration using a 10X (A, C) and 40X (B, D) objective, respectively. Fibrin is red, platelets are navy blue, and RBCs are yellow-brown. Black arrows indicate fibrin; green arrows indicate the femoral vein. N = 3 per group. Images show the right femoral vein and $FeCl_3$-induced thrombus within.
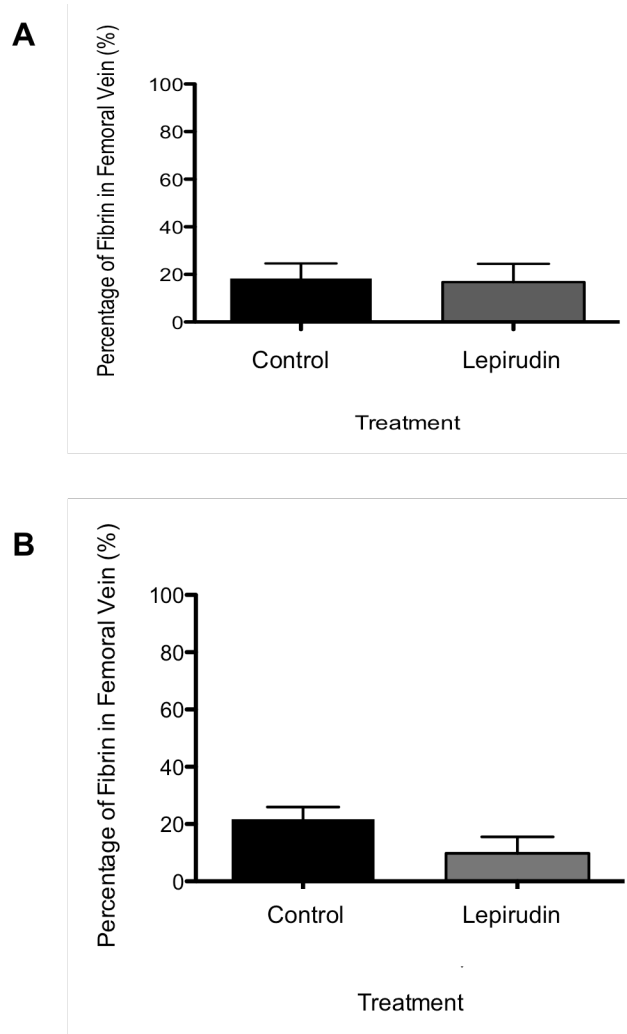
FIGURE 13 – Percentage of fibrin in femoral vein: control versus lepirudin group
(A) Percentage of fibrin in femoral vein one hour after thrombus formation in control and lepirudin-treated (8U/g mbw) groups. **(B)** Percentage of fibrin in the femoral vein two hours after thrombus formation in control and lepirudin-treated groups. All values are expressed as mean percentages ± SEM and data was analyzed using Student's t-test. N = 3 per group.
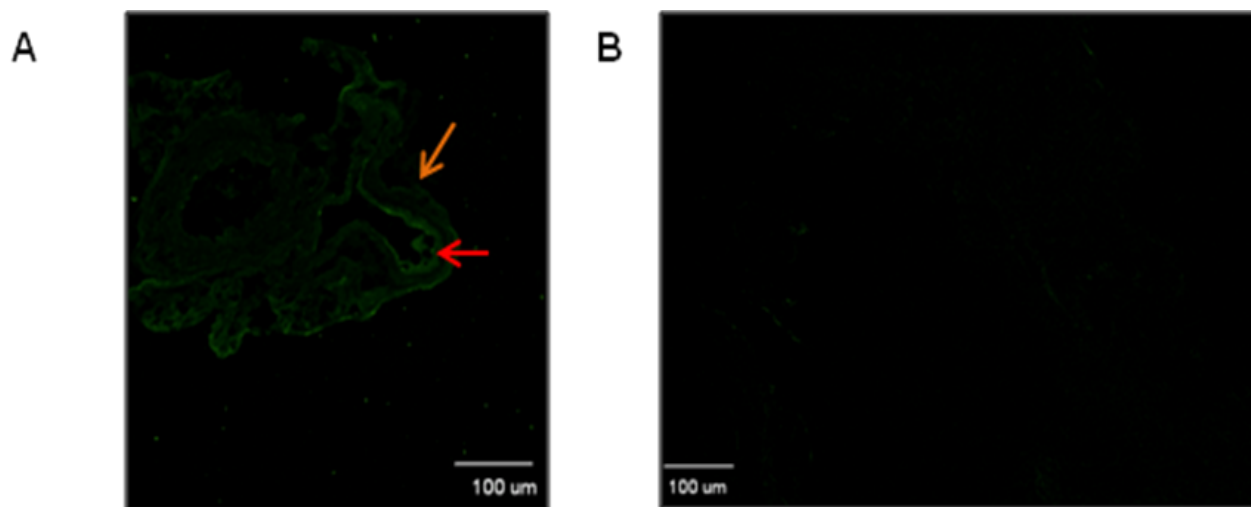
FIGURE 14 – IHC α$_2$–Antiplasmin femoral vein thrombus slides: lepirudin group
(A) Representative IHC stains for assessment of α$_2$–AP content in thrombus at one-hour in lepirudin-treated (8U/g mbw) group, **(B)** and corresponding negative control. α$_2$–AP was detected with goat anti-mouse serpin F2/α2-AP antigen affinity-purified polyclonal antibody fluorescently labeled with Alexa Fluor 488 donkey anti-goat IgG antibody. Red arrow indicates α$_2$–antiplasmin within thrombus; orange arrow indicates femoral vein. Representative of three images. Images show the right femoral vein and artery, and FeCl$_3$-induced thrombus within.
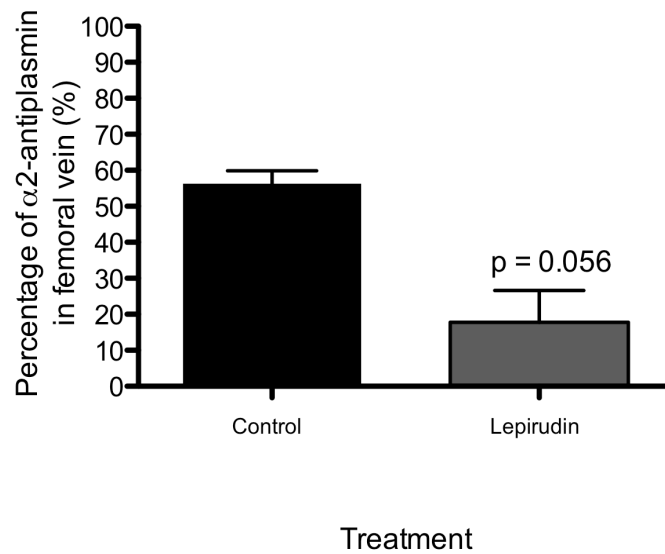
FIGURE 15 – Percentage of α₂–APin thrombus: control versus lepirudin-treated group
Percentage of α_2–AP within thrombus at one hour in control and lepirudin-treated (8U/g mbw) groups. α_2–AP was detected with goat anti-mouse serpin F2/α2-AP antigen affinity-purified polyclonal antibody fluorescently labeled with Alexa Fluor 488 donkey anti-goat IgG antibody. All values are expressed as mean percentages ± SEM and data was analyzed using Student's t-test. N = 3.
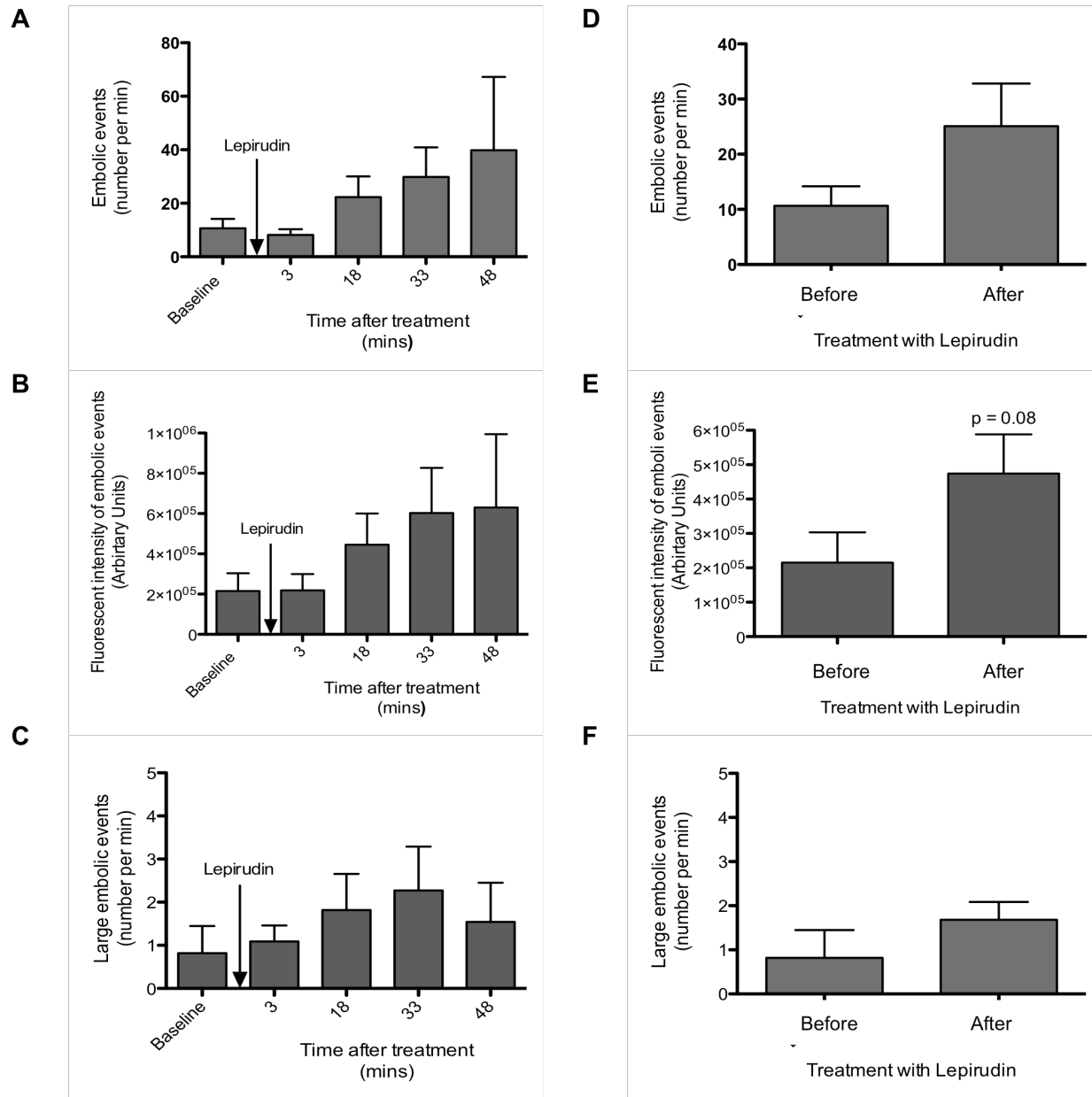
FIGURE 16 – Changes in embolization over one hour: lepirudin group
(A) EE, **(B)** fluorescent intensity of EE, and **(C)** large EE observed over one hour at 3, 18, 33, and 48 minutes following lepirudin (8U/g mbw) administration. **(D)** EE, **(E)** fluorescent intensity of the EE, and **(F)** large EE before and after treatment with 8U/g mbw lepirudin. EE and large EE values are expressed as number per min. Fluorescent intensity values are expressed as AU. All values are expressed as mean ± SEM and data was analyzed using one-way ANOVA (A-C) and Student's t-test (D-F). N = 11.
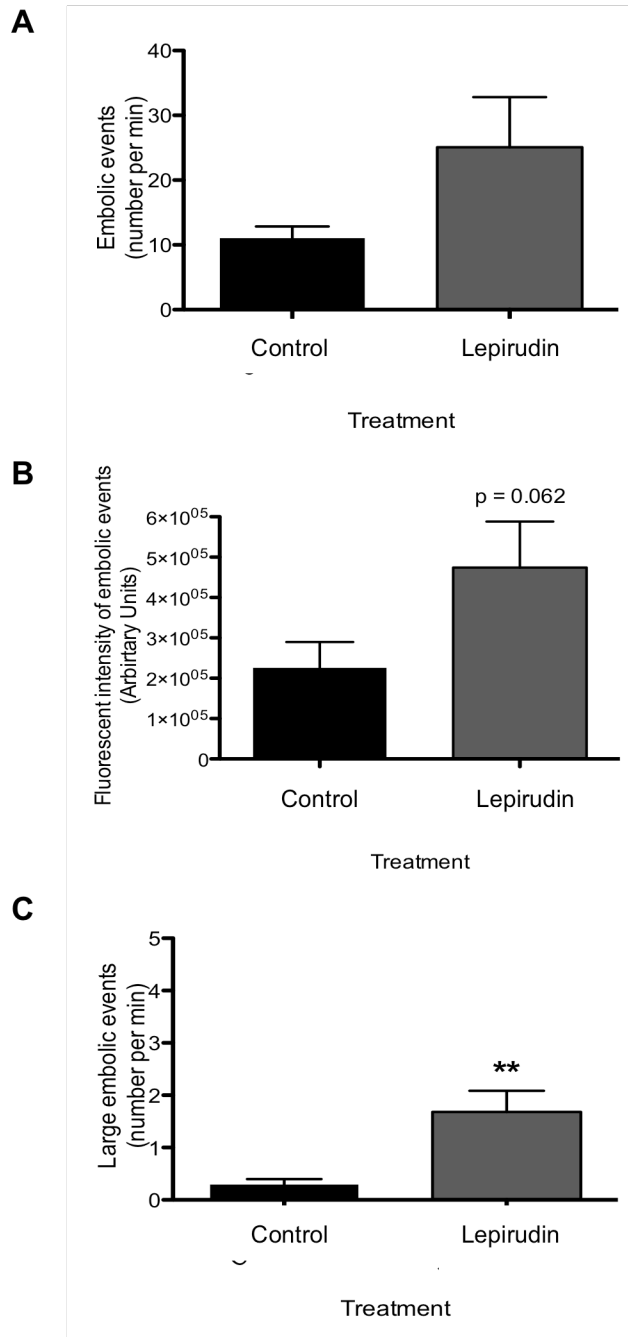
FIGURE 17 – Changes in embolization over one hour: control versus lepirudin group
(A) EE, (B) fluorescent intensity of EE, and **(C)** large EE in control group versus lepirudin treated (8U/g mbw) group. EE and large EE values are expressed as number per min. Fluorescent intensity values are expressed as AU. All values are expressed as mean ± SEM and data was analyzed using Student's t-test. N = 11 per group. ** Indicates significance versus control with p < 0.01.
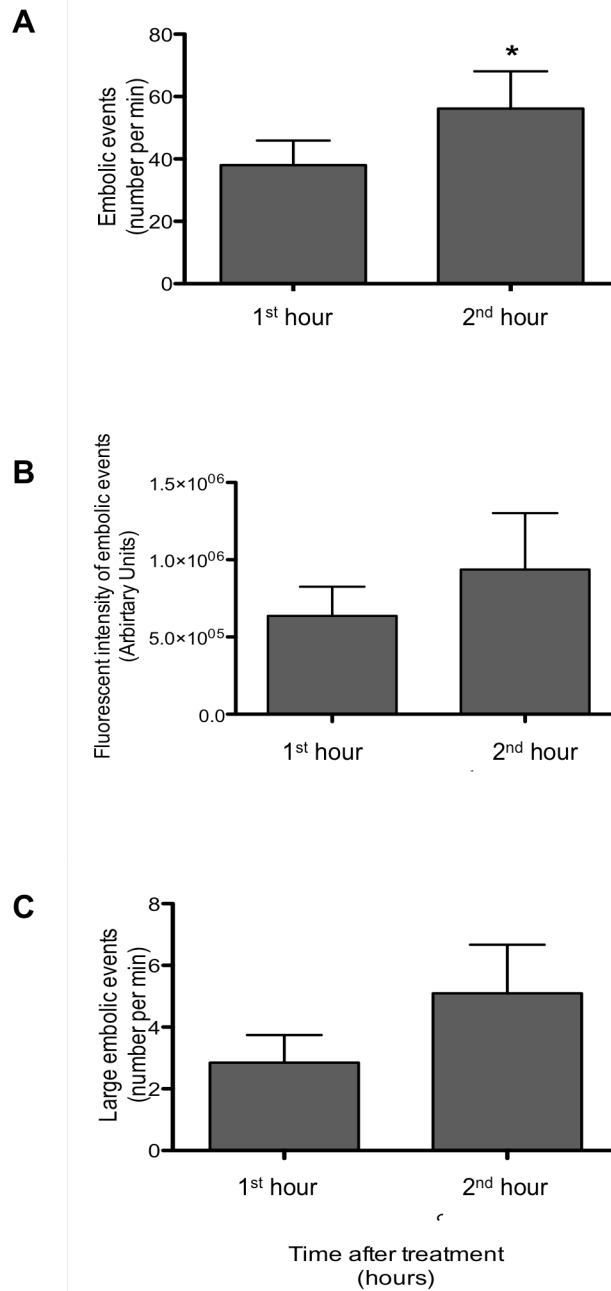
FIGURE 18 – Changes in embolization over two hours: comparing the 1st and 2nd hour in lepirudin group

(A) EE, **(B)** fluorescent intensity of the EE, **(C)** large EE in the 1st and 2nd hour following lepirudin (8U/g mbw) treatment. EE and large EE values are expressed as number per min. Fluorescent intensity values are expressed as AU. All values are expressed as mean ± SEM and data was analyzed using Student's t-test. N = 5. * Indicates significance versus 1st hour with $p < 0.05$.
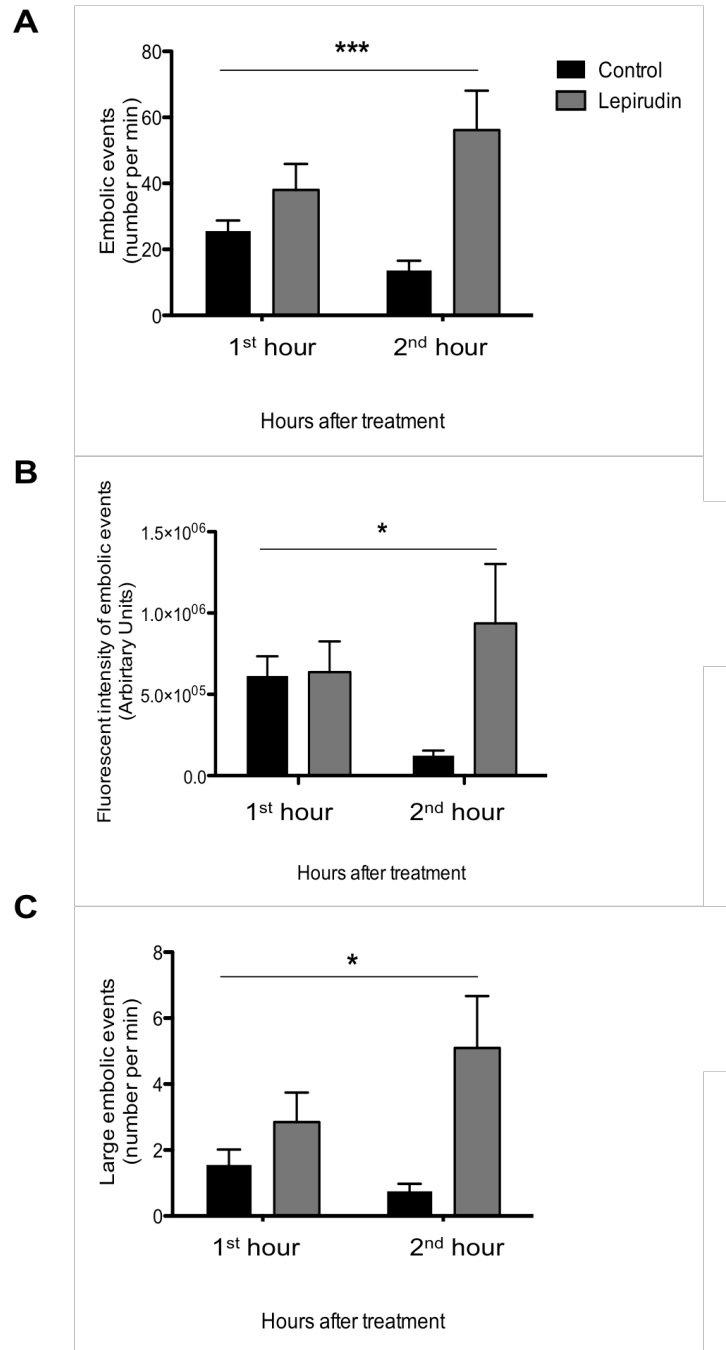
FIGURE 19 – Changes in embolization over two hours: comparing the 1st and 2nd hour in control and lepirudin groups
(A) EE, **(B)** fluorescent intensity of EE, **(C)** large EE in the 1st and 2nd hour in control and lepirudin-treated (8U/g mbw) groups. EE and large EE values are expressed as number per min. Fluorescent intensity values are expressed as AU. All values are expressed as mean ± SEM and data was analyzed using repeated measures ANOVA. N = 5. * Indicates a significant interaction with $p < 0.05$; *** Indicates a significant interaction with $p < 0.0001$.
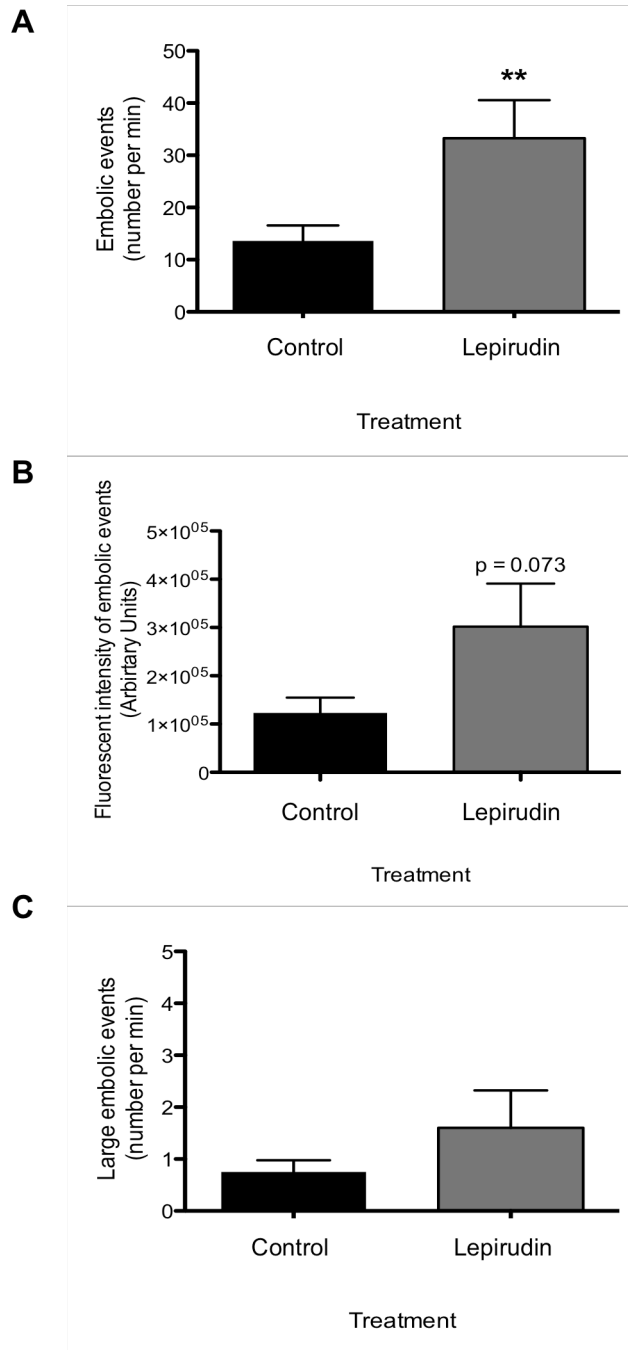
FIGURE 20 – Changes in embolization following delayed lepirudin treatment: control versus lepirudin group
Comparison of the 2nd hour in control mice and mice treated with lepirudin (8U/g mbw) one hour after thrombus formation: **(A)** EE, **(B)** fluorescent intensity of EE, **(C)** large EE. EE and large EE values are expressed as number per min. Fluorescent intensity values are expressed as AU. All values are expressed as mean ± SEM and data was analyzed using Student's t-test. N = 5 per group. ** Indicates significance versus control with $p < 0.01$.
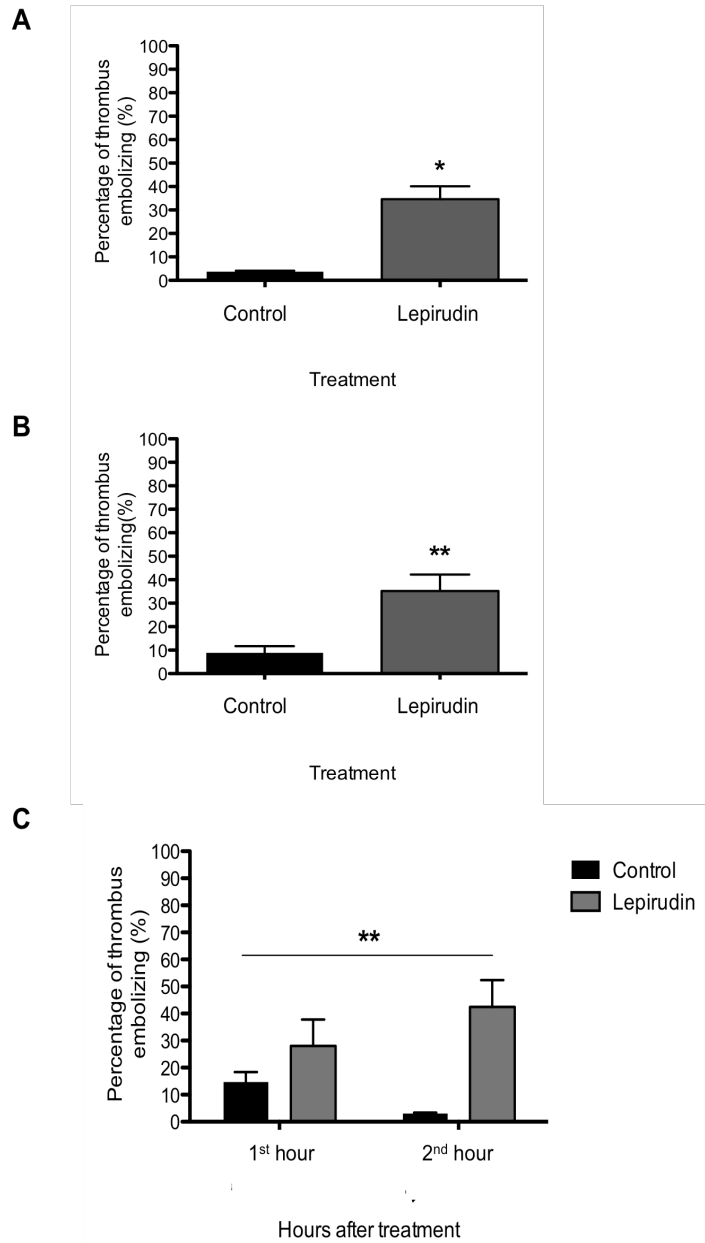
FIGURE 21 – Percentage of embolizing thrombus over one hour and two hours: control versus lepirudin group
(A) Percentage of thrombus embolization in control and lepirudin-treated (8U/g mbw) mice over one hour. N = 4 per group. **(B)** Percentage of thrombus embolization in control and lepirudin-treated mice over two hours. N = 5 per group. **(C)** Comparison of percentage of thrombus embolization in the 1st and 2nd hour of control and lepirudin-treated groups. All values are expressed as mean percentages ± SEM and data was analyzed using Student's t-test (A, B) and repeated measures ANOVA (C). * Indicates significance versus control with $p < 0.05$; ** Indicates significance versus control with $p < 0.01$ (B) and significance of treatment with $p < 0.01$ (C).
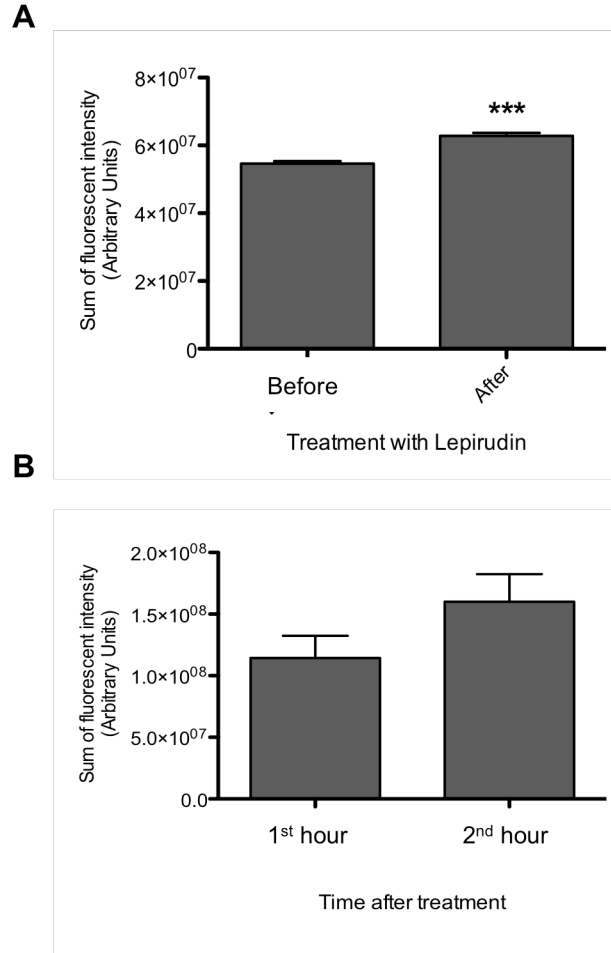
FIGURE 22 – Change in thrombus size over one hour and two hours: lepirudin group
(A) Thrombus size, expressed as the sum of fluorescently labeled platelets in AU, before and after lepirudin (8U/g mbw) treatment in the one-hour group. N = 4. **(B)** Thrombus size, expressed as the sum of fluorescently labeled platelets in AU, in the 1st and 2nd hour following lepirudin treatment in the two-hour group. N = 5. All values are expressed as mean ± SEM and data was analyzed using Student's t-test. *** Indicates significance versus before with $p < 0.0001$.
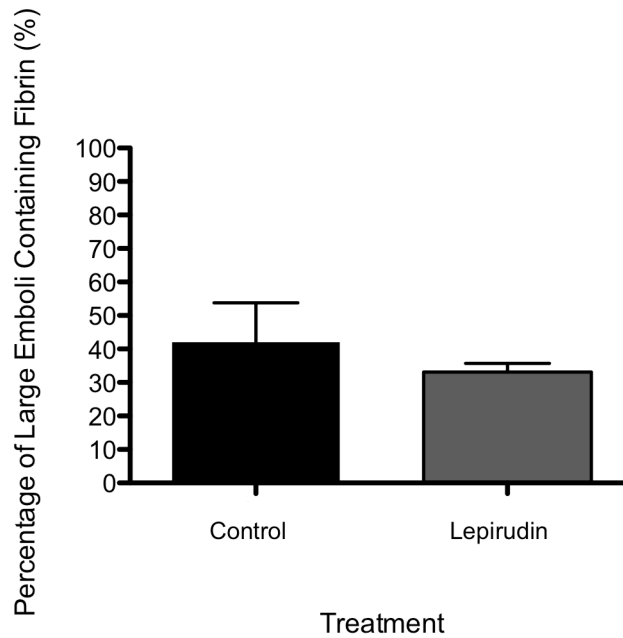
FIGURE 23 – Percentage of large emboli containing fibrin over two hours: control versus lepirudin group

The percentage of large EE containing fibrin, in control and lepirudin-treated (8U/g mbw) mice, over two hours. Platelets were labeled with CD41 Fab fragments conjugated to Alexa Fluor 647 and fibrin was labeled with a synthesized anti-fibrin peptide conjugated to FITC. N = 3 per group. All values are expressed as mean percentages ± SEM and data was analyzed using Fisher's exact test.
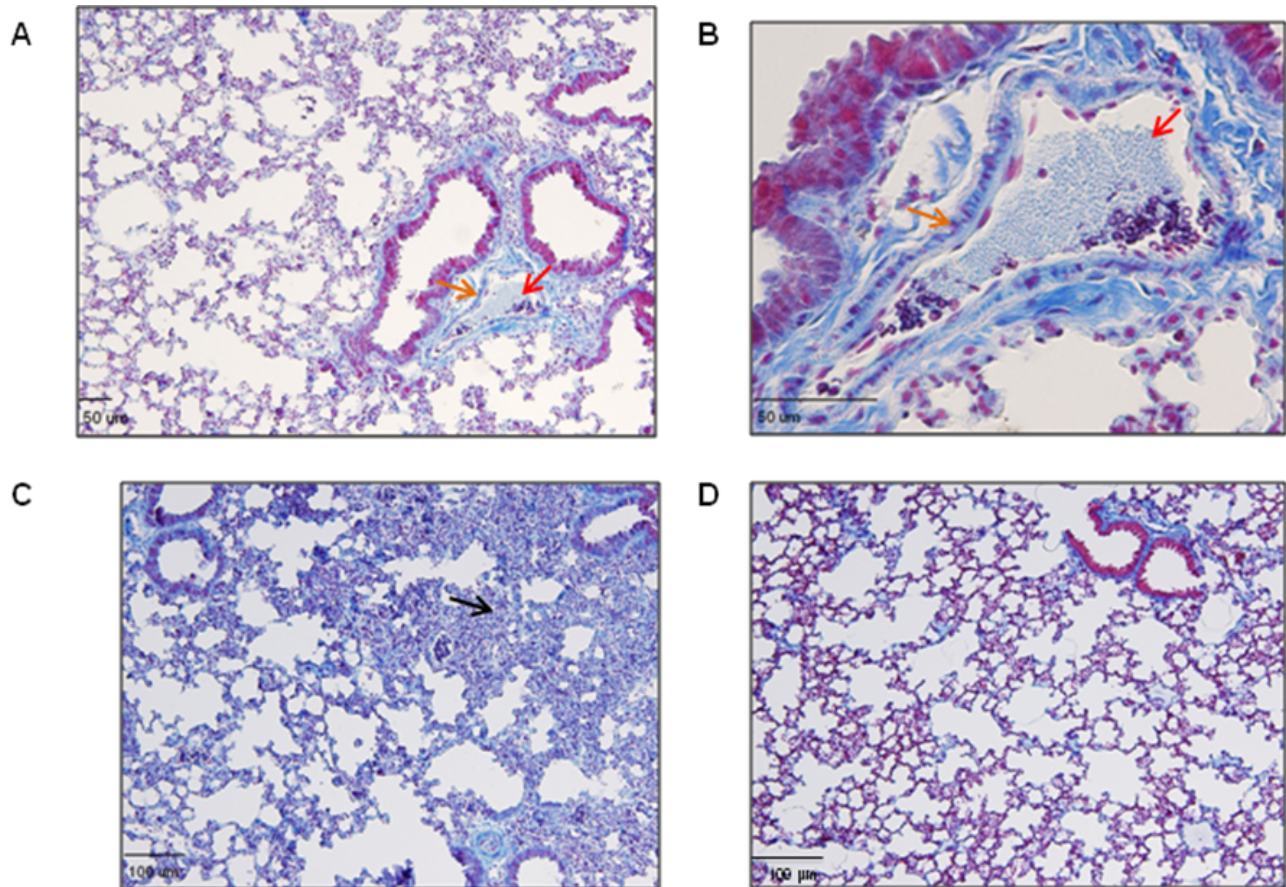
FIGURE 24 – Carstairs' pulmonary emboli slides at two hours: lepirudin group
(A, B) Representative Carstairs' stains for assessment of pulmonary emboli within the pulmonary artery circulation at two hours using a 10X objective and 40X objective, respectively. Images show a representative section of an embolic event within a pulmonary artery. **(C, D)** Representative Carstairs' stains of lung tissue in the lepirudin group at 2 hours and a mouse with no femoral vein thrombus using a 10X objective. Red arrow indicates an embolus; orange arrow indicates pulmonary artery; black arrow indicates lung tissue inflammation. N = 3. Images show an embolic event within a pulmonary artery (A, B) and mouse lung tissue (C, D).
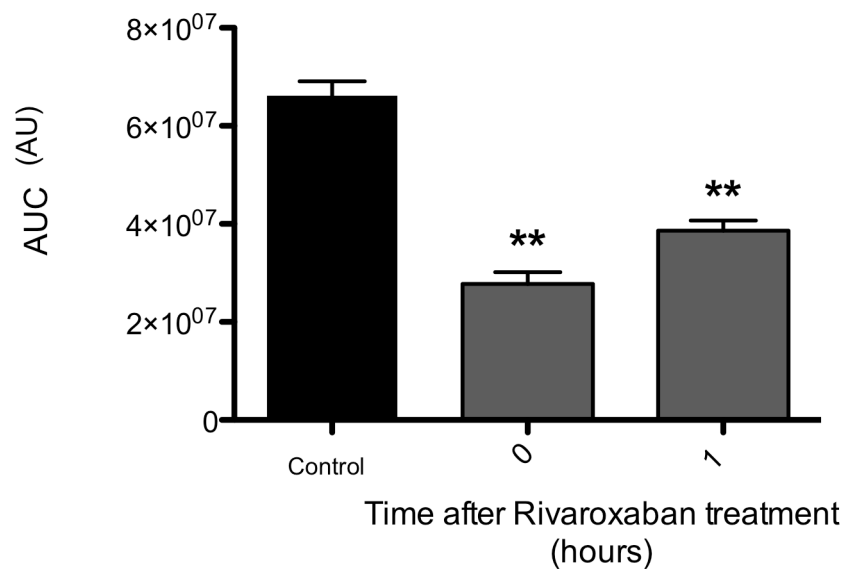
FIGURE 25 – Thrombin generation at zero hours and one hour: rivaroxaban group
Rivaroxaban was administered, 3 µg/g mbw, and plasma collected at different time points (0 hours and 1 hour) following treatment. Thrombin generation was initiated with $CaCl_2$, and assessed at one-minute intervals over one hour in control and lepirudin-treated mouse plasma. AUC in control and rivaroxaban groups was compared as a measurement of thrombin generation. N = 3 per group (in duplicate). Values are expressed as mean percentages ± SEM and data was analyzed using Student's t-test. ** Indicates significance versus control with $p < 0.01$.
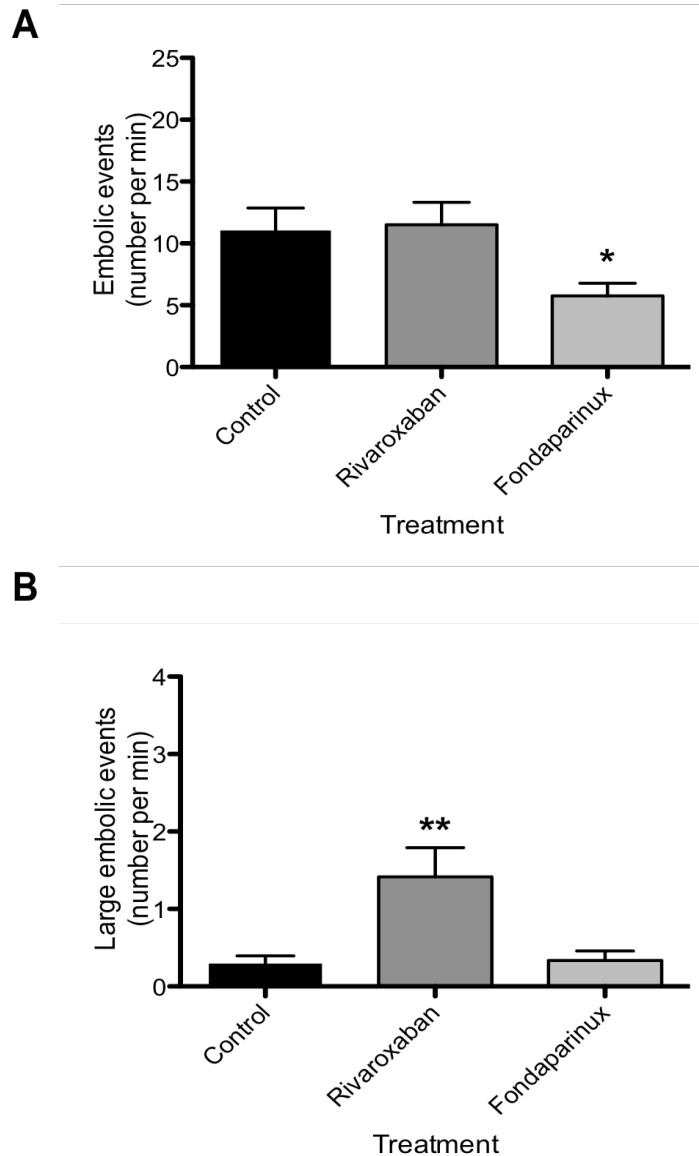
FIGURE 26 – Change in embolization over one hour: control versus rivaroxaban and fondaparinux groups.
(A) EE in control group (N = 11) versus rivaroxaban (3µg/g mbw, N = 9) and fondaparinux (0.1µg/g mbw, N = 9) groups after treatment. **(B)** Large EE in control group versus rivaroxaban and fondaparinux groups after treatment. EE and large EE values are expressed as number per min. All values are expressed as mean ± SEM and data was analyzed using Student's t-test. * Indicates significance versus control with $p < 0.05$; ** Indicates significance versus before and baseline with $p < 0.01$.
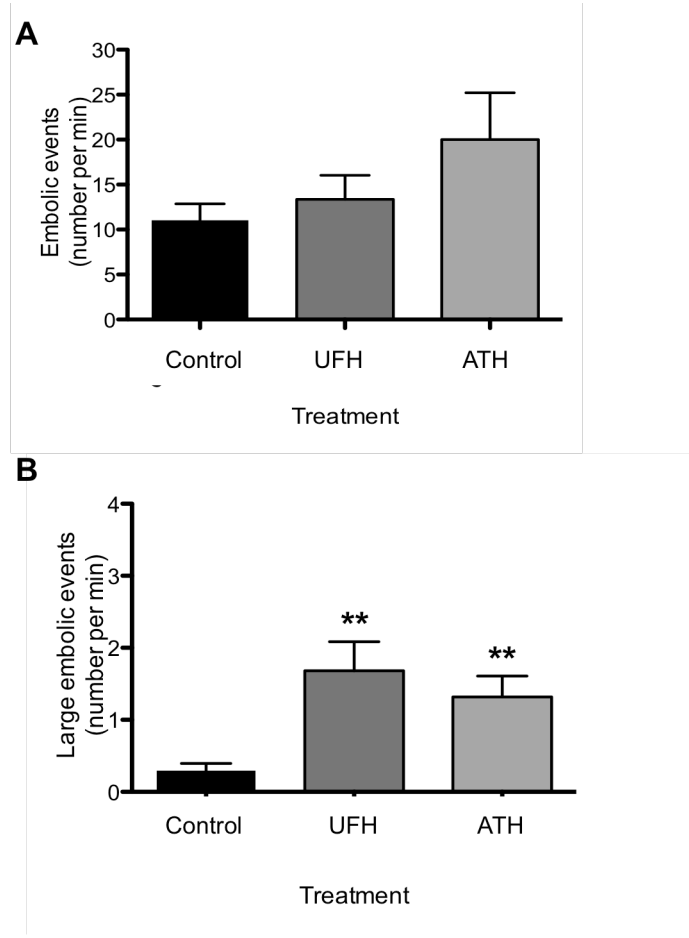
FIGURE 27 – Change in embolization over one hour: control versus UFH and ATH groups
(A) EE in control group (N = 11) versus UFH (N = 11) and ATH (N = 11) groups after treatment. **(B)** Large EE in control group versus UFH and ATH groups after treatment. EE and large EE values are expressed as number per min. All values are expressed as mean ± SEM and data was analyzed using Student's t-test. ** Indicates significance versus control with $p < 0.01$.
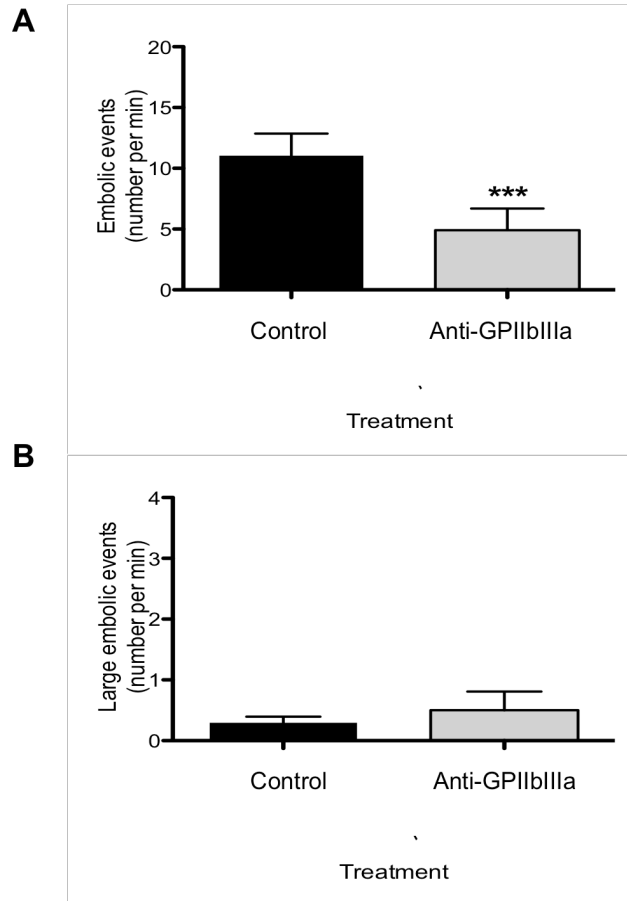
FIGURE 28 – Change in embolization over one hour: control versus anti-GPIIbIIIa group
(A) EE in control group (N = 11) versus anti-GPIIbIIIa group (N = 8) after treatment. **(B)** Large EE in control group versus anti-GPIIbIIIa group after treatment. EE and large EE values are expressed as number per min. All values are expressed as mean ± SEM and data was analyzed using Student's t-test. *** Indicates significance versus control with $p < 0.001$.

7.0. REFERENCES

(1) Furie B, Furie BC. Mechanisms of thrombus formation. N Engl J Med 2008 08/28;359(1533-4406; 0028-4793; 9):938-949.

(2) Monroe DM, Hoffman M, Roberts HR. Platelets and thrombin generation. Arterioscler Thromb Vasc Biol 2002 09/01;22(1524-4636; 1079-5642; 9):1381-1389.

(3) Furie B, Furie BC. Thrombus formation in vivo. J Clin Invest 2005 12;115(0021-9738; 0021-9738; 12):3355-3362.

(4) Chu AJ. Tissue factor, blood coagulation, and beyond: an overview. Int J Inflam 2011;2011:367284.

(5) Monkovic DD, Tracy PB. Activation of human factor V by factor Xa and thrombin. Biochemistry 1990 Feb 6;29(5):1118-1128.

(6) Allen DH, Tracy PB. Human coagulation factor V is activated to the functional cofactor by elastase and cathepsin G expressed at the monocyte surface. J Biol Chem 1995 Jan 20;270(3):1408-1415.

(7) Dormann D, Clemetson KJ, Kehrel BE. The GPIb thrombin-binding site is essential for thrombin-induced platelet procoagulant activity. Blood 2000 Oct 1;96(7):2469-2478.

(8) Saenko EL, Shima M, Gilbert GE, Scandella D. Slowed release of thrombin-cleaved factor VIII from von Willebrand factor by a monoclonal and a human antibody is a novel mechanism for factor VIII inhibition. J Biol Chem 1996 Nov 1;271(44):27424-27431.

(9) Hoffman M. Remodeling the blood coagulation cascade. J Thromb Thrombolysis 2003 Aug-Oct;16(1-2):17-20.

(10) Di Cera E. Thrombin as procoagulant and anticoagulant. J Thromb Haemost 2007 Jul;5 Suppl 1:196-202.

(11) Mann KG, Butenas S, Brummel K. The dynamics of thrombin formation. Arterioscler Thromb Vasc Biol 2003 01/01;23(1524-4636; 1079-5642; 1):17-25.

(12) Crawley JT, Zanardelli S, Chion CK, Lane DA. The central role of thrombin in hemostasis. J Thromb Haemost 2007 Jul;5 Suppl 1:95-101.

(13) Wolberg AS, Campbell RA. Thrombin generation, fibrin clot formation and hemostasis. Transfus Apher Sci 2008 Feb;38(1):15-23.

(14) Bagoly Z, Koncz Z, Harsfalvi J, Muszbek L. Factor XIII, clot structure, thrombosis. Thromb Res 2012 Mar;129(3):382-387.

(15) Bereczky Z, Katona E, Muszbek L. Fibrin stabilization (factor XIII), fibrin structure and thrombosis. Pathophysiol Haemost Thromb 2003 Sep-2004 Dec;33(5-6):430-437.

(16) Sakata Y, Aoki N. Cross-linking of alpha 2-plasmin inhibitor to fibrin by fibrin-stabilizing factor. J Clin Invest 1980 Feb;65(2):290-297.

(17) Fraser SR, Booth NA, Mutch NJ. The antifibrinolytic function of factor XIII is exclusively expressed through alpha(2)-antiplasmin cross-linking. Blood 2011 Jun 9;117(23):6371-6374.

(18) Rubens FD, Perry DW, Hatton MW, Bishop PD, Packham MA, Kinlough-Rathbone RL. Platelet accumulation on fibrin-coated polyethylene: role of platelet activation and factor XIII. Thromb Haemost 1995 May;73(5):850-856.

(19) Kahn ML, Zheng YW, Huang W, Bigornia V, Zeng D, Moff S, et al. A dual thrombin receptor system for platelet activation. Nature 1998 Aug 13;394(6694):690-694.

(20) Coughlin SR. Protease-activated receptors in hemostasis, thrombosis and vascular biology. J Thromb Haemost 2005 Aug;3(8):1800-1814.

(21) Cirino G, Vergnolle N. Proteinase-activated receptors (PARs): crossroads between innate immunity and coagulation. Curr Opin Pharmacol 2006 Aug;6(4):428-434.

(22) Di Cera E. Thrombin interactions. Chest 2003 Sep;124(3 Suppl):11S-7S.

(23) Esmon CT. The protein C pathway. Chest 2003 Sep;124(3 Suppl):26S-32S.

(24) Mosnier LO, Bouma BN. Regulation of fibrinolysis by thrombin activatable fibrinolysis inhibitor, an unstable carboxypeptidase B that unites the pathways of coagulation and fibrinolysis. Arterioscler Thromb Vasc Biol 2006 Nov;26(11):2445-2453.

(25) Varga-Szabo D, Pleines I, Nieswandt B. Cell adhesion mechanisms in platelets. Arterioscler Thromb Vasc Biol 2008 Mar;28(3):403-412.

(26) Brass LF. Thrombin and platelet activation. Chest 2003 Sep;124(3 Suppl):18S-25S.

(27) Lopez JA, Kearon C, Lee AY. Deep venous thrombosis. Hematology Am Soc Hematol Educ Program 2004:439-456.

(28) Furie B, Furie BC. The molecular basis of blood coagulation. Cell 1988 May 20;53(4):505-518.

(29) Topol EJ, Byzova TV, Plow EF. Platelet GPIIb-IIIa blockers. Lancet 1999 Jan 16;353(9148):227-231.

(30) Savage B, Saldivar E, Ruggeri ZM. Initiation of platelet adhesion by arrest onto fibrinogen or translocation on von Willebrand factor. Cell 1996 Jan 26;84(2):289-297.

(31) Wu KK, Thiagarajan P. Role of endothelium in thrombosis and hemostasis. Annu Rev Med 1996;47(0066-4219; 0066-4219):315-331.

(32) Tollefsen DM. Heparin cofactor II modulates the response to vascular injury. Arterioscler Thromb Vasc Biol 2007 Mar;27(3):454-460.

(33) Roberts HR, Hoffman M, Monroe DM. A cell-based model of thrombin generation. Semin Thromb Hemost 2006 04;32 Suppl 1(0094-6176; 0094-6176):32-38.

(34) Van de Wouwer M, Collen D, Conway EM. Thrombomodulin-protein C-EPCR system: integrated to regulate coagulation and inflammation. Arterioscler Thromb Vasc Biol 2004 08;24(1524-4636; 1079-5642; 8):1374-1383.

(35) Lwaleed BA, Bass PS. Tissue factor pathway inhibitor: structure, biology and involvement in disease. J Pathol 2006 Feb;208(3):327-339.

(36) Coughlin PB. Antiplasmin: the forgotten serpin? FEBS J 2005 Oct;272(19):4852-4857.

(37) Dobrovolsky AB, Titaeva EV. The fibrinolysis system: regulation of activity and physiologic functions of its main components. Biochemistry (Mosc) 2002 Jan;67(1):99-108.

(38) Guimaraes AH, Rijken DC. Thrombin activatable fibrinolysis inhibitor (TAFI) affects fibrinolysis in a plasminogen activator concentration-dependent manner. Study of seven

plasminogen activators in an internal clot lysis model. Thromb Haemost 2004 Mar;91(3):473-479.

(39) Lijnen HR. Elements of the fibrinolytic system. Ann N Y Acad Sci 2001;936(0077-8923; 0077-8923):226-236.

(40) Cvirn G, Gallistl S, Muntean W. Effects of alpha(2)-macroglobulin and antithrombin on thrombin generation and inhibition in cord and adult plasma. Thromb Res 2001 Feb 1;101(3):183-191.

(41) Cvirn G, Gallistl S, Koestenberger M, Kutschera J, Leschnik B, Muntean W. Alpha 2-macroglobulin enhances prothrombin activation and thrombin potential by inhibiting the anticoagulant protein C/protein S system in cord and adult plasma. Thromb Res 2002 Mar 1;105(5):433-439.

(42) Schaller J, Gerber SS. The plasmin-antiplasmin system: structural and functional aspects. Cell Mol Life Sci 2011 Mar;68(5):785-801.

(43) Carpenter SL, Mathew P. Alpha2-antiplasmin and its deficiency: fibrinolysis out of balance. Haemophilia 2008 Nov;14(6):1250-1254.

(44) Sasaki T, Morita T, Iwanaga S. Identification of the plasminogen-binding site of human alpha 2-plasmin inhibitor. J Biochem 1986 Jun;99(6):1699-1705.

(45) Lee KN, Lee CS, Tae WC, Jackson KW, Christiansen VJ, McKee PA. Crosslinking of alpha 2-antiplasmin to fibrin. Ann N Y Acad Sci 2001;936:335-339.

(46) Mackman N. Triggers, targets and treatments for thrombosis. Nature 2008 02/21;451(1476-4687; 0028-0836; 7181):914-918.

(47) Rosendaal FR. Venous thrombosis: the role of genes, environment, and behavior. Hematology Am Soc Hematol Educ Program 2005(1520-4383; 1520-4383):1-12.

(48) Heit JA. Venous thromboembolism: disease burden, outcomes and risk factors. J Thromb Haemost 2005 08;3(1538-7933; 1538-7836; 8):1611-1617.

(49) Ageno W, Squizzato A, Garcia D, Imberti D. Epidemiology and risk factors of venous thromboembolism. Semin Thromb Hemost 2006 10;32(0094-6176; 0094-6176; 7):651-658.

(50) Mammen EF. Pathogenesis of venous thrombosis. Chest 1992 12;102(0012-3692; 0012-3692; 6):640S-644S.

(51) Gross PL, Weitz JI. New antithrombotic drugs. Clin Pharmacol Ther 2009 08;86(1532-6535; 0009-9236; 2):139-146.

(52) Dalen.J.E. Venous Thromboembolism. 2003(180).

(53) Dutta TK, Venugopal V. Venous thromboembolism: the intricacies. J Postgrad Med 2009 01;55(0022-3859; 0022-3859; 1):55-64.

(54) Bertina RM. Genetic approach to thrombophilia. Thromb Haemost 2001 Jul;86(1):92-103.

(55) Spencer FA, Emery C, Lessard D, Anderson F, Emani S, Aragam J, et al. The Worcester Venous Thromboembolism study: a population-based study of the clinical epidemiology of venous thromboembolism. J Gen Intern Med 2006 Jul;21(7):722-727.

(56) Samama MM, Dahl OE, Quinlan DJ, Mismetti P, Rosencher N. Quantification of risk factors for venous thromboembolism: a preliminary study for the development of a risk assessment tool. Haematologica 2003 12;88(1592-8721; 0390-6078; 12):1410-1421.

(57) Anderson FA,Jr., Spencer FA. Risk factors for venous thromboembolism. Circulation 2003 06/17;107(1524-4539; 0009-7322; 23):I9-16.

(58) Michota F. Venous thromboembolism: epidemiology, characteristics, and consequences. Clin Cornerstone 2005;7(1098-3597; 4):8-15.

(59) Lee AY, Levine MN. Venous thromboembolism and cancer: risks and outcomes. Circulation 2003 06/17;107(1524-4539; 0009-7322; 23):I17-I21.

(60) Monreal M, Falga C, Valdes M, Suarez C, Gabriel F, Tolosa C, et al. Fatal pulmonary embolism and fatal bleeding in cancer patients with venous thromboembolism: findings from the RIETE registry. J Thromb Haemost 2006 09;4(1538-7933; 1538-7836; 9):1950-1956.

(61) Lentz SR. Another lesson from the factor V Leiden mouse: thrombin generation drives arterial disease. Circulation 2005 04/12;111(1524-4539; 0009-7322; 14):1733-1734.

(62) Poort SR, Rosendaal FR, Reitsma PH, Bertina RM. A common genetic variation in the 3'-untranslated region of the prothrombin gene is associated with elevated plasma prothrombin levels and an increase in venous thrombosis. Blood 1996 Nov 15;88(10):3698-3703.

(63) Kroegel C, Reissig A. Principle mechanisms underlying venous thromboembolism: epidemiology, risk factors, pathophysiology and pathogenesis. Respiration 2003 01;70(0025-7931; 0025-7931; 1):7-30.

(64) Planes A, Vochelle N, Darmon JY, Fagola M, Bellaud M, Huet Y. Risk of deep-venous thrombosis after hospital discharge in patients having undergone total hip replacement: double-blind randomised comparison of enoxaparin versus placebo. Lancet 1996 Jul 27;348(9022):224-228.

(65) Line BR. Pathophysiology and diagnosis of deep venous thrombosis. Semin Nucl Med 2001 Apr;31(2):90-101.

(66) Esmon CT. Basic mechanisms and pathogenesis of venous thrombosis. Blood Rev 2009 09;23(1532-1681; 0268-960; 5):225-229.

(67) Kahn SR, Ginsberg JS. Relationship between deep venous thrombosis and the postthrombotic syndrome. Arch Intern Med 2004 01/12;164(0003-9926; 0003-9926; 1):17-26.

(68) Galanaud JP, Sevestre-Pietri MA, Bosson JL, Laroche JP, Righini M, Brisot D, et al. Comparative study on risk factors and early outcome of symptomatic distal versus proximal deep vein thrombosis: results from the OPTIMEV study. Thromb Haemost 2009 Sep;102(3):493-500.

(69) Tzoran I, Saharov G, Brenner B, Delsart D, Roman P, Visona A, et al. Silent pulmonary embolism in patients with proximal deep vein thrombosis in the lower limbs. J Thromb Haemost 2012 Apr;10(4):564-571.

(70) Goldhaber SZ, Visani L. The International Cooperative Pulmonary Embolism Registry. Chest 1995 Aug;108(2):302-304.

(71) Carson JL, Kelley MA, Duff A, Weg JG, Fulkerson WJ, Palevsky HI, et al. The clinical course of pulmonary embolism. N Engl J Med 1992 May 7;326(19):1240-1245.

(72) Weisel JW. Structure of fibrin: impact on clot stability. J Thromb Haemost 2007 Jul;5 Suppl 1:116-124.

(73) Lord ST. Molecular mechanisms affecting fibrin structure and stability. Arterioscler Thromb Vasc Biol 2011 Mar;31(3):494-499.

(74) Jackson SP, Nesbitt WS, Westein E. Dynamics of platelet thrombus formation. J Thromb Haemost 2009 Jul;7 Suppl 1:17-20.

(75) Ramzi DW, Leeper KV. DVT and pulmonary embolism: Part II. Treatment and prevention. Am Fam Physician 2004 Jun 15;69(12):2841-2848.

(76) Merli G. Anticoagulants in the treatment of deep vein thrombosis. Am J Med 2005 Aug;118 Suppl 8A:13S-20S.

(77) Prandoni P, Lensing AW, Cogo A, Cuppini S, Villalta S, Carta M, et al. The long-term clinical course of acute deep venous thrombosis. Ann Intern Med 1996 Jul 1;125(1):1-7.

(78) Nutescu EA, Shapiro NL, Chevalier A, Amin AN. A pharmacologic overview of current and emerging anticoagulants. Cleveland Clinic Journal of Medicine 2005;72(Supplemental 1):S1-S6.

(79) Krishnaswamy A, Lincoff AM, Cannon CP. The use and limitations of unfractionated heparin. Crit Pathw Cardiol 2010 Mar;9(1):35-40.

(80) Weitz JI, Hudoba M, Massel D, Maraganore J, Hirsh J. Clot-bound thrombin is protected from inhibition by heparin-antithrombin III but is susceptible to inactivation by antithrombin III-independent inhibitors. J Clin Invest 1990 Aug;86(2):385-391.

(81) Becker DL, Fredenburgh JC, Stafford AR, Weitz JI. Exosites 1 and 2 are essential for protection of fibrin-bound thrombin from heparin-catalyzed inhibition by antithrombin and heparin cofactor II. J Biol Chem 1999 Mar 5;274(10):6226-6233.

(82) Garcia DA, Baglin TP, Weitz JI, Samama MM, American College of Chest Physicians. Parenteral anticoagulants: Antithrombotic Therapy and Prevention of Thrombosis, 9th ed: American College of Chest Physicians Evidence-Based Clinical Practice Guidelines. Chest 2012 Feb;141(2 Suppl):e24S-43S.

(83) Hirsh J, O'Donnell M, Eikelboom JW. Beyond unfractionated heparin and warfarin: current and future advances. Circulation 2007 Jul 31;116(5):552-560.

(84) BARRITT DW, JORDAN SC. Anticoagulant drugs in the treatment of pulmonary embolism. A controlled trial. Lancet 1960 Jun 18;1(7138):1309-1312.

(85) Smith SB, Geske JB, Maguire JM, Zane NA, Carter RE, Morgenthaler TI. Early anticoagulation is associated with reduced mortality for acute pulmonary embolism. Chest 2010 Jun;137(6):1382-1390.

(86) Hirsh J, Dalen J, Anderson DR, Poller L, Bussey H, Ansell J, et al. Oral anticoagulants: mechanism of action, clinical effectiveness, and optimal therapeutic range. Chest 2001 Jan;119(1 Suppl):8S-21S.

(87) Lin PJ. Reviewing the reality: why we need to change. Eur Heart J Suppl 2005;7(E):E15-E20.

(88) Di Nisio M, Middeldorp S, Buller HR. Direct thrombin inhibitors. N Engl J Med 2005 Sep 8;353(10):1028-1040.

(89) Lee CJ, Ansell JE. Direct thrombin inhibitors. Br J Clin Pharmacol 2011 Oct;72(4):581-592.

(90) Monreal M, Costa J, Salva P. Pharmacological properties of hirudin and its derivatives. Potential clinical advantages over heparin. Drugs Aging 1996 Mar;8(3):171-182.

(91) Sohn JH, Kang HA, Rao KJ, Kim CH, Choi ES, Chung BH, et al. Current status of the anticoagulant hirudin: its biotechnological production and clinical practice. Appl Microbiol Biotechnol 2001 Dec;57(5-6):606-613.

(92) Rydel TJ, Tulinsky A, Bode W, Huber R. Refined structure of the hirudin-thrombin complex. J Mol Biol 1991 Sep 20;221(2):583-601.

(93) Greinacher A. Lepirudin: a bivalent direct thrombin inhibitor for anticoagulation therapy. Expert Rev Cardiovasc Ther 2004 May;2(3):339-357.

(94) Greinacher A, Lubenow N. Recombinant hirudin in clinical practice: focus on lepirudin. Circulation 2001 Mar 13;103(10):1479-1484.

(95) Schiele F, Lindgaerde F, Eriksson H, Bassand JP, Wallmark A, Hansson PO, et al. Subcutaneous recombinant hirudin (HBW 023) versus intravenous sodium heparin in treatment of established acute deep vein thrombosis of the legs: a multicentre prospective dose-ranging randomized trial. International Multicentre Hirudin Study Group. Thromb Haemost 1997 May;77(5):834-838.

(96) Bergese SD, Minkowitz HS, Arpino PA, Sane DC, Levy JH. Multicenter Trial of Desirudin for the Prophylaxis of Thrombosis: An Alternative to Heparin-Based Anticoagulation (DESIR-ABLE). Clin Appl Thromb Hemost 2012 Jul 15.

(97) Turpie AG. Oral, direct factor Xa inhibitors in development for the prevention and treatment of thromboembolic diseases. Arterioscler Thromb Vasc Biol 2007 Jun;27(6):1238-1247.

(98) Rupprecht HJ, Blank R. Clinical pharmacology of direct and indirect factor Xa inhibitors. Drugs 2010 Nov 12;70(16):2153-2170.

(99) Weitz JI. New anticoagulants for treatment of venous thromboembolism. Circulation 2004 Aug 31;110(9 Suppl 1):I19-26.

(100) Turpie AG, Eriksson BI, Bauer KA, Lassen MR. New pentasaccharides for the prophylaxis of venous thromboembolism: clinical studies. Chest 2003 Dec;124(6 Suppl):371S-378S.

(101) Buller HR, Davidson BL, Decousus H, Gallus A, Gent M, Piovella F, et al. Fondaparinux or enoxaparin for the initial treatment of symptomatic deep venous thrombosis: a randomized trial. Ann Intern Med 2004 Jun 1;140(11):867-873.

(102) Buller HR, Davidson BL, Decousus H, Gallus A, Gent M, Piovella F, et al. Subcutaneous fondaparinux versus intravenous unfractionated heparin in the initial treatment of pulmonary embolism. N Engl J Med 2003 Oct 30;349(18):1695-1702.

(103) Gulseth MP, Michaud J, Nutescu EA. Rivaroxaban: an oral direct inhibitor of factor Xa. Am J Health Syst Pharm 2008 Aug 15;65(16):1520-1529.

(104) Perzborn E, Strassburger J, Wilmen A, Pohlmann J, Roehrig S, Schlemmer KH, et al. In vitro and in vivo studies of the novel antithrombotic agent BAY 59-7939--an oral, direct Factor Xa inhibitor. J Thromb Haemost 2005 Mar;3(3):514-521.

(105) Perzborn E, Kubitza D, Misselwitz F. Rivaroxaban. A novel, oral, direct factor Xa inhibitor in clinical development for the prevention and treatment of thromboembolic disorders. Hamostaseologie 2007 Sep;27(4):282-289.

(106) Eikelboom JW, Weitz JI. New anticoagulants. Circulation 2010 Apr 6;121(13):1523-1532.

(107) The EINSTEIN Investigators. Oral Rivaroxaban for Symptomatic Venous Thromboembolism. N.Engl.J.Med. 2010;363(26):2499-2510.

(108) EINSTEIN-PE Investigators, Buller HR, Prins MH, Lensin AW, Decousus H, Jacobson BF, et al. Oral rivaroxaban for the treatment of symptomatic pulmonary embolism. N Engl J Med 2012 Apr 5;366(14):1287-1297.

(109) Chan AK, Berry L, Klement P, Julian J, Mitchell L, Weitz J, et al. A novel antithrombin-heparin covalent complex: antithrombotic and bleeding studies in rabbits. Blood Coagul Fibrinolysis 1998 Oct;9(7):587-595.

(110) Chan AKC, Berry LR, O'Brodovich H, Klement P, Mitchell L, Baranowski B, et al. Covalent Antithrombin-Heparin Complexes with High Anticoagulant Activity: Intravenous, Subcutaneous, and Intratracheal Administration. The American Society For Biochemistry and Molecular Biology 1997;272(35):22111-22117.

(111) Berry LR, Becker DL, Chan AK. Inhibition of fibrin-bound thrombin by a covalent antithrombin-heparin complex. J Biochem 2002 Aug;132(2):167-176.

(112) Stevic I, Berry LR, Chan AK. Mechanism of inhibition of the prothrombinase complex by a covalent antithrombin-heparin complex. J Biochem 2012 Aug;152(2):139-148.

(113) Hashemzadeh M, Furukawa M, Goldsberry S, Movahed MR. Chemical structures and mode of action of intravenous glycoprotein IIb/IIIa receptor blockers: A review. Exp Clin Cardiol 2008 Winter;13(4):192-197.

(114) Kristensen SD, Wurtz M, Grove EL, De Caterina R, Huber K, Moliterno DJ, et al. Contemporary use of glycoprotein IIb/IIIa inhibitors. Thromb Haemost 2012 Feb;107(2):215-224.

(115) Kolecki RV, Sigel B, Justin J, Feleppa EJ, Parsons RE, Kitamura H, et al. Determining the acuteness and stability of deep venous thrombosis by ultrasonic tissue characterization. J Vasc Surg 1995 Jun;21(6):976-984.

(116) Caps MT, Meissner MH, Tullis MJ, Polissar NL, Manzo RA, Zierler BK, et al. Venous thrombus stability during acute phase of therapy. Vasc Med 1999;4(1):9-14.

(117) Dorffler-Melly J, Schwarte LA, Ince C, Levi M. Mouse models of focal arterial and venous thrombosis. Basic Res Cardiol 2000 12;95(0300-8428; 0300-8428; 6):503-509.

(118) Cooley BC. Murine models of thrombosis. Thromb Res 2012 May;129 Suppl 2:S62-4.

(119) Diaz JA, Ballard-Lipka NE, Farris DM, Hawley AE, Wrobleski SK, Myers DD, et al. Impaired fibrinolytic system in ApoE gene-deleted mice with hyperlipidemia augments deep vein thrombosis. J Vasc Surg 2012 Mar;55(3):815-822.

(120) Diaz JA, Obi AT, Myers DD,Jr, Wrobleski SK, Henke PK, Mackman N, et al. Critical review of mouse models of venous thrombosis. Arterioscler Thromb Vasc Biol 2012 Mar;32(3):556-562.

(121) Singh I, Smith A, Vanzieleghem B, Collen D, Burnand K, Saint-Remy JM, et al. Antithrombotic effects of controlled inhibition of factor VIII with a partially inhibitory human monoclonal antibody in a murine vena cava thrombosis model. Blood 2002 May 1;99(9):3235-3240.

(122) Diaz JA, Wrobleski SK, Hawley AE, Lucchesi BR, Wakefield TW, Myers DD,Jr. Electrolytic inferior vena cava model (EIM) of venous thrombosis. J Vis Exp 2011 Jul 12;(53):e2737. doi(53):e2737.

(123) Reinmann-Hunziger G. *Uber experimentelle Thrombose und ihre Behandlung mit Heparin*. Schweizerische Medizinische Wochenschrift 1944;74:66-69.

(124) Kurz KD, Main BW, Sandusky GE. Rat model of arterial thrombosis induced by ferric chloride. Thromb Res 1990 Nov 15;60(4):269-280.

(125) Eckly A, Hechler B, Freund M, Zerr M, Cazenave JP, Lanza F, et al. Mechanisms underlying FeCl3-induced arterial thrombosis. J Thromb Haemost 2011 Apr;9(4):779-789.

(126) Bellido-Martin L, Chen V, Jasuja R, Furie B, Furie BC. Imaging fibrin formation and platelet and endothelial cell activation in vivo. Thromb Haemost 2011 May;105(5):776-782.

(127) Brill A. A ride with ferric chloride. J Thromb Haemost 2011 Apr;9(4):776-778.

(128) Tseng MT, Dozier A, Haribabu B, Graham UM. Transendothelial migration of ferric ion in FeCl3 injured murine common carotid artery. Thromb Res 2006;118(2):275-280.

(129) Woollard KJ, Sturgeon S, Chin-Dusting JP, Salem HH, Jackson SP. Erythrocyte hemolysis and hemoglobin oxidation promote ferric chloride-induced vascular injury. J Biol Chem 2009 May 8;284(19):13110-13118.

(130) Hara T, Bhayana B, Thompson B, Kessinger CW, Khatri A, McCarthy JR, et al. Molecular imaging of fibrin deposition in deep vein thrombosis using fibrin-targeted near-infrared fluorescence. JACC Cardiovasc Imaging 2012 Jun;5(6):607-615.

(131) Gross PL, Weitz JI. New anticoagulants for treatment of venous thromboembolism. Arterioscler Thromb Vasc Biol 2008 Mar;28(3):380-386.

(132) Prasad V, Rho J, Cifu A. The Diagnosis and Treatment of Pulmonary Embolism: A Metaphor for Medicine in the Evidence-Based Medicine Era. Arch Intern Med 2012 Apr 2.

(133) Kearon C. Natural history of venous thromboembolism. Circulation 2003 Jun 17;107(23 Suppl 1):I22-30.

(134) Meignan M, Rosso J, Gauthier H, Brunengo F, Claudel S, Sagnard L, et al. Systematic lung scans reveal a high frequency of silent pulmonary embolism in patients with proximal deep venous thrombosis. Arch Intern Med 2000 Jan 24;160(2):159-164.

(135) Turpie AG, Fisher WD, Bauer KA, Kwong LM, Irwin MW, Kalebo P, et al. BAY 59-7939: an oral, direct factor Xa inhibitor for the prevention of venous thromboembolism in patients after total knee replacement. A phase II dose-ranging study. J Thromb Haemost 2005 Nov;3(11):2479-2486.

(136) Caprini JA, Arcelus JI, Motykie G, Kudrna JC, Mokhtee D, Reyna JJ. The influence of oral anticoagulation therapy on deep vein thrombosis rates four weeks after total hip replacement. J Vasc Surg 1999 Nov;30(5):813-820.

(137) Weitz JI. Factor Xa or thrombin: is thrombin a better target? J Thromb Haemost 2007 Jul;5 Suppl 1:65-67.

(138) Tomaru T, Nakamura F, Aoki N, Sakamoto Y, Omata M, Uchida Y. Local treatment with an antithrombotic drug reduces thrombus size in coronary and peripheral thrombosed arteries. Heart Vessels 1996;11(3):133-144.

(139) Aghourian MN, Lemarie CA, Blostein MD. In vivo monitoring of venous thrombosis in mice. J Thromb Haemost 2012 Mar;10(3):447-452.

(140) Falati S, Gross P, Merrill-Skoloff G, Furie BC, Furie B. Real-time in vivo imaging of platelets, tissue factor and fibrin during arterial thrombus formation in the mouse. Nat Med 2002 Oct;8(10):1175-1181.

(141) Pilch J, Brown DM, Komatsu M, Jarvinen TA, Yang M, Peters D, et al. Peptides selected for binding to clotted plasma accumulate in tumor stroma and wounds. Proc Natl Acad Sci U S A 2006 Feb 21;103(8):2800-2804.

(142) Li D, Weng S, Yang B, Zander DS, Saldeen T, Nichols WW, et al. Inhibition of arterial thrombus formation by ApoA1 Milano. Arterioscler Thromb Vasc Biol 1999 Feb;19(2):378-383.

(143) Carstairs KC. The identification of platelets and platelet antigens in histological sections. J Pathol Bacteriol 1965 Jul;90(1):225-231.

(144) Dubois C, Panicot-Dubois L, Gainor JF, Furie BC, Furie B. Thrombin-initiated platelet activation in vivo is vWF independent during thrombus formation in a laser injury model. J Clin Invest 2007 Apr;117(4):953-960.

(145) Wagner NM, Dressel T, Schafer K, Konstantinides S. Effect of the Factor Xa Inhibitor Rivaroxaban on Arterial Thrombosis in Wild-Type and Apolipoprotein E-Deficient Mice. Thromb Res 2012 Jan 24.

(146) Dolmans DE, Kadambi A, Hill JS, Waters CA, Robinson BC, Walker JP, et al. Vascular accumulation of a novel photosensitizer, MV6401, causes selective thrombosis in tumor vessels after photodynamic therapy. Cancer Res 2002 Apr 1;62(7):2151-2156.

(147) Emfret Analytics. Purified Rat Anti-Mouse Integrin αIIbβ3 (GPIIbIIIa, CD41/61) Monoclonal Antibody. 2003.

(148) Robinson BR, Houng AK, Reed GL. Catalytic life of activated factor XIII in thrombi. Implications for fibrinolytic resistance and thrombus aging. Circulation 2000 Sep 5;102(10):1151-1157.

(149) Jaffer FA, Tung CH, Wykrzykowska JJ, Ho NH, Houng AK, Reed GL, et al. Molecular imaging of factor XIIIa activity in thrombosis using a novel, near-infrared fluorescent contrast agent that covalently links to thrombi. Circulation 2004 Jul 13;110(2):170-176.

(150) Wang X, Smith PL, Hsu MY, Ogletree ML, Schumacher WA. Murine model of ferric chloride-induced vena cava thrombosis: evidence for effect of potato carboxypeptidase inhibitor. J Thromb Haemost 2006 02;4(1538-7933; 1538-7836; 2):403-410.

(151) Jaffer FA, Tung CH, Gerszten RE, Weissleder R. In vivo imaging of thrombin activity in experimental thrombi with thrombin-sensitive near-infrared molecular probe. Arterioscler Thromb Vasc Biol 2002 Nov 1;22(11):1929-1935.

(152) Day SM, Reeve JL, Myers DD, Fay WP. Murine Thrombosis Models. Thromb.Haemost. 2004;92:486-494.

(153) Zhou J, May L, Liao P, Gross PL, Weitz JI. Inferior vena cava ligation rapidly induces tissue factor expression and venous thrombosis in rats. Arterioscler Thromb Vasc Biol 2009 Jun;29(6):863-869.

(154) Marsh Lyle E, Lewis SD, Lehman ED, Gardell SJ, Motzel SL, Lynch JJ,Jr. Assessment of thrombin inhibitor efficacy in a novel rabbit model of simultaneous arterial and venous thrombosis. Thromb Haemost 1998 Mar;79(3):656-662.

(155) Shebuski RJ, Sitko GR, Claremon DA, Baldwin JJ, Remy DC, Stern AM. Inhibition of factor XIIIa in a canine model of coronary thrombosis: effect on reperfusion and acute reocclusion after recombinant tissue-type plasminogen activator. Blood 1990 Apr 1;75(7):1455-1459.

(156) Reed GL, Houng AK. The contribution of activated factor XIII to fibrinolytic resistance in experimental pulmonary embolism. Circulation 1999 Jan 19;99(2):299-304.

(157) Killewich LA, Bedford GR, Beach KW, Strandness DE,Jr. Spontaneous lysis of deep venous thrombi: rate and outcome. J Vasc Surg 1989 Jan;9(1):89-97.

(158) Meissner MH, Manzo RA, Bergelin RO, Markel A, Strandness DE,Jr. Deep venous insufficiency: the relationship between lysis and subsequent reflux. J Vasc Surg 1993 Oct;18(4):596-605; discussion 606-8.

(159) Meissner MH, Caps MT, Bergelin RO, Manzo RA, Strandness DE,Jr. Propagation, rethrombosis and new thrombus formation after acute deep venous thrombosis. J Vasc Surg 1995 Nov;22(5):558-567.

(160) Hirsh J, Hoak J. Management of Deep Vein Thrombosis and Pulmonary Embolism**
**. Circulation 1996;93:2212-2245.

(161) Rivera J, Lozano ML, Navarro-Nunez L, Vicente V. Platelet receptors and signaling in the dynamics of thrombus formation. Haematologica 2009 May;94(5):700-711.

(162) Girard P, Decousus M, Laporte S, Buchmuller A, Herve P, Lamer C, et al. Diagnosis of pulmonary embolism in patients with proximal deep vein thrombosis: specificity of symptoms and perfusion defects at baseline and during anticoagulant therapy. Am J Respir Crit Care Med 2001 Sep 15;164(6):1033-1037.

(163) Piazza G, Goldhaber SZ. Acute pulmonary embolism: part I: epidemiology and diagnosis. Circulation 2006 Jul 11;114(2):e28-32.

(164) Parambil JG, Savci CD, Tazelaar HD, Ryu JH. Causes and presenting features of pulmonary infarctions in 43 cases identified by surgical lung biopsy. Chest 2005 Apr;127(4):1178-1183.

(165) Napoli C, De NF, Pignalosa O, Lerman A, Sica G, Fiorito C, et al. In vivo veritas: thrombosis mechanisms in animal models. Scand J Clin Lab Invest 2006;66(0036-5513; 0036-5513; 5):407-427.

(166) Cooley BC, Szema L, Chen CY, Schwab JP, Schmeling G. A murine model of deep vein thrombosis: characterization and validation in transgenic mice. Thromb Haemost 2005 Sep;94(3):498-503.

(167) Wrobleski SK, Farris DM, Diaz JA, Myers DD,Jr, Wakefield TW. Mouse complete stasis model of inferior vena cava thrombosis. J Vis Exp 2011 Jun 15;(52). pii: 2738. doi(52):10.3791/2738.

(168) Chan WS, Spencer FA, Ginsberg JS. Anatomic distribution of deep vein thrombosis in pregnancy. CMAJ 2010 Apr 20;182(7):657-660.

(169) Dahl OE, Aspelin T, Lyberg T. The role of bone traumatization in the initiation of proximal deep vein thrombosis during cemented hip replacement surgery in pigs. Blood Coagul Fibrinolysis 1995 Dec;6(8):709-717.

(170) Moser KM, LeMoine JR. Is embolic risk conditioned by location of deep venous thrombosis? Ann Intern Med 1981 Apr;94(4 pt 1):439-444.

(171) Kolbel T, Alhadad A, Acosta S, Lindh M, Ivancev K, Gottsater A. Thrombus embolization into IVC filters during catheter-directed thrombolysis for proximal deep venous thrombosis. J Endovasc Ther 2008 Oct;15(5):605-613.

(172) Hill SL, Holtzman GI, Martin D, Evans P, Toler W, Goad K. The origin of lower extremity deep vein thrombi in acute venous thrombosis. Am J Surg 1997 Jun;173(6):485-490.

(173) Bates SM, Jaeschke R, Stevens SM, Goodacre S, Wells PS, Stevenson MD, et al. Diagnosis of DVT: Antithrombotic Therapy and Prevention of Thrombosis, 9th ed: American College of Chest Physicians Evidence-Based Clinical Practice Guidelines. Chest 2012 Feb;141(2 Suppl):e351S-418S.

(174) Kreutz R. Pharmacodynamic and pharmacokinetic basics of rivaroxaban. Fundam Clin Pharmacol 2012 Feb;26(1):27-32.

(175) Warkentin TE. How I diagnose and manage HIT. Hematology Am Soc Hematol Educ Program 2011;2011:143-149.

(176) Becattini C, Agnelli G, Schenone A, Eichinger S, Bucherini E, Silingardi M, et al. Aspirin for preventing the recurrence of venous thromboembolism. N Engl J Med 2012 May 24;366(21):1959-1967.

(177) Armstrong PC, Peter K. GPIIb/IIIa inhibitors: from bench to bedside and back to bench again. Thromb Haemost 2012 May 2;107(5):808-814.

(178) Vandendries ER, Hamilton JR, Coughlin SR, Furie B, Furie BC. Par4 is required for platelet thrombus propagation but not fibrin generation in a mouse model of thrombosis. Proc Natl Acad Sci U S A 2007 Jan 2;104(1):288-292.

(179) Parissis H. Lepirudin as an alternative to "heparin allergy" during cardiopulmonary bypass. J Cardiothorac Surg 2011 Apr 8;6:44.

(180) Kaminski M, McDonagh J. Inhibited thrombins. Interactions with fibrinogen and fibrin. Biochem J 1987 Mar 15;242(3):881-887.

(181) Hankey GJ, Eikelboom JW. Dabigatran etexilate: a new oral thrombin inhibitor. Circulation 2011 Apr 5;123(13):1436-1450.

(182) Shen L, Lorand L. Contribution of fibrin stabilization to clot strength. Supplementation of factor XIII-deficient plasma with the purified zymogen. J Clin Invest 1983 May;71(5):1336-1341.

(183) Leidy EM, Stern AM, Friedman PA, Bush LR. Enhanced thrombolysis by a factor XIIIa inhibitor in a rabbit model of femoral artery thrombosis. Thromb Res 1990 Jul 1;59(1):15-26.

(184) Ali M, Ridger V, Pease R, Howells G, Grant P, Ariens R, et al. Establishment of method and image analysis systems to monitor clot formation and FXIII activity in real time using a murine in vivo model of thrombosis. Journal of thrombosis and haemostasis : JTH 2012;10(6):e10-e24.

(185) Sidelmann JJ, Gram J, Jespersen J, Kluft C. Fibrin clot formation and lysis: basic mechanisms. Semin Thromb Hemost 2000;26(6):605-618.

(186) Mattsson C, Menschik-Lundin A, Nylander S, Gyzander E, Deinum J. Effect of different types of thrombin inhibitors on thrombin/thrombomodulin modulated activation of protein C in vitro. Thromb Res 2001 Dec 15;104(6):475-486.

(187) Linder R, Frebelius S, Jansson K, Swedenborg J. Inhibition of endothelial cell-mediated generation of activated protein C by direct and antithrombin-dependent thrombin inhibitors. Blood Coagul Fibrinolysis 2003 Feb;14(2):139-146.

(188) Colucci M, Pentimone A, Binetti BM, Cramarossa M, Piro D, Semeraro N. Effect of heparin on TAFI-dependent inhibition of fibrinolysis: relative importance of TAFIa generated by clot-bound and fluid phase thrombin. Thromb Haemost 2002 Aug;88(2):282-287.

(189) Florian-Kujawski M, Baltasar F, Neville B, Hoppensteadt D, Fareed J. Relative Inhibition of Thrombin Activatable Fibrinolytic Inhibitor by Newly Developed Thrombin Inhibitors: Impact on Bleeding and Antithrombotic Actions. The FASEB Journal 2006;20:A655.

(190) Agnelli G, Pascucci C, Cosmi B, Nenci GG. The comparative effects of recombinant hirudin (CGP 39393) and standard heparin on thrombus growth in rabbits. Thromb Haemost 1990 Apr 12;63(2):204-207.

(191) Agnelli G, Renga C, Weitz JI, Nenci GG, Hirsh J. Sustained antithrombotic activity of hirudin after its plasma clearance: comparison with heparin. Blood 1992 Aug 15;80(4):960-965.

(192) Fiessinger JN, Huisman MV, Davidson BL, Bounameaux H, Francis CW, Eriksson H, et al. Ximelagatran vs low-molecular-weight heparin and warfarin for the treatment of deep vein thrombosis: a randomized trial. JAMA 2005 Feb 9;293(6):681-689.

(193) Matsuno H, Okada K, Ueshima S, Matsuo O, Kozawa O. Alpha2-antiplasmin plays a significant role in acute pulmonary embolism. J Thromb Haemost 2003 Aug;1(8):1734-1739.

(194) Samama MM. The mechanism of action of rivaroxaban--an oral, direct Factor Xa inhibitor--compared with other anticoagulants. Thromb Res 2011 Jun;127(6):497-504.

(195) Gerotziafas GT, Elalamy I, Depasse F, Perzborn E, Samama MM. In vitro inhibition of thrombin generation, after tissue factor pathway activation, by the oral, direct factor Xa inhibitor rivaroxaban. J Thromb Haemost 2007 Apr;5(4):886-888.

(196) Brufatto N, Ward A, Nesheim ME. Factor Xa is highly protected from antithrombin-fondaparinux and antithrombin-enoxaparin when incorporated into the prothrombinase complex. J Thromb Haemost 2003 Jun;1(6):1258-1263.

(197) Hirsh J, Anand SS, Halperin JL, Fuster V. Mechanism of action and pharmacology of unfractionated heparin. Arterioscler Thromb Vasc Biol 2001 Jul;21(7):1094-1096.

(198) Young E, Cosmi B, Weitz J, Hirsh J. Comparison of the non-specific binding of unfractionated heparin and low molecular weight heparin (Enoxaparin) to plasma proteins. Thromb Haemost 1993 Oct 18;70(4):625-630.

(199) Cosmi B, Fredenburgh JC, Rischke J, Hirsh J, Young E, Weitz JI. Effect of nonspecific binding to plasma proteins on the antithrombin activities of unfractionated heparin, low-molecular-weight heparin, and dermatan sulfate. Circulation 1997 Jan 7;95(1):118-124.

(200) Berry L, Stafford A, Fredenburgh J, O'Brodovich H, Mitchell L, Weitz J, et al. Investigation of the anticoagulant mechanisms of a covalent antithrombin-heparin complex. J Biol Chem 1998 Dec 25;273(52):34730-34736.

(201) Paredes N, Wang A, Berry LR, Smith LJ, Stafford AR, Weitz JI, et al. Mechanisms responsible for catalysis of the inhibition of factor Xa or thrombin by antithrombin using a covalent antithrombin-heparin complex. J Biol Chem 2003 Jun 27;278(26):23398-23409.

(202) Van Walderveen MC, Berry LR, Atkinson HM, Chan AK. Covalent antithrombin-heparin effect on thrombin-thrombomodulin and activated protein C reaction with factor V/Va. Thromb Haemost 2010 May;103(5):910-919.

(203) Sarratt KL, Chen H, Zutter MM, Santoro SA, Hammer DA, Kahn ML. GPVI and alpha2beta1 play independent critical roles during platelet adhesion and aggregate formation to collagen under flow. Blood 2005 Aug 15;106(4):1268-1277.

(204) Coller BS. Platelet GPIIb/IIIa antagonists: the first anti-integrin receptor therapeutics. J Clin Invest 1997 Dec 1;100(11 Suppl):S57-60.

(205) Nieswandt B, Echtenacher B, Wachs FP, Schroder J, Gessner JE, Schmidt RE, et al. Acute systemic reaction and lung alterations induced by an antiplatelet integrin gpIIb/IIIa antibody in mice. Blood 1999 Jul 15;94(2):684-693.

(206) Wannemacher KM, Zhu L, Jiang H, Fong KP, Stalker TJ, Lee D, et al. Diminished contact-dependent reinforcement of Syk activation underlies impaired thrombus growth in mice lacking Semaphorin 4D. Blood 2010 Dec 16;116(25):5707-5715.

(207) Makelburg AB, Veeger NJ, Middeldorp S, Hamulyak K, Prins MH, Buller HR, et al. Different risk of deep vein thrombosis and pulmonary embolism in carriers with factor V Leiden compared with non-carriers, but not in other thrombophilic defects. Results from a large retrospective family cohort study. Haematologica 2010 06;95(1592-8721; 0390-6078; 6):1030-1033.

(208) Stein PD, Beemath A, Meyers FA, Skaf E, Sanchez J, Olson RE. Incidence of venous thromboembolism in patients hospitalized with cancer. Am J Med 2006 01;119(1555-7162; 0002-9343; 1):60-68.